

**CHARACTERIZATION OF A KARST COASTAL ECOSYSTEM IN THE MEXICAN  
CARIBBEAN: ASSESSING THE INFLUENCE OF COASTAL HYDRODYNAMICS  
AND SUBMERGED GROUNDWATER DISCHARGES ON SEAGRASS**

A Dissertation

by

ISRAEL MEDINA

Submitted to the Office of Graduate Studies of  
Texas A&M University  
in partial fulfillment of the requirements for the degree of

DOCTOR OF PHILOSOPHY

May 2011

Major Subject: Oceanography

**CHARACTERIZATION OF A KARST COASTAL ECOSYSTEM IN THE MEXICAN  
CARIBBEAN: ASSESSING THE INFLUENCE OF COASTAL HYDRODYNAMICS  
AND SUBMERGED GROUNDWATER DISCHARGES ON SEAGRASS**

A Dissertation

by

ISRAEL MEDINA

Submitted to the Office of Graduate Studies of  
Texas A&M University  
in partial fulfillment of the requirements for the degree of

DOCTOR OF PHILOSOPHY

Approved by:

Chair of Committee,	Björn Kjerfve
Committee Members,	Stephen Davis
	Steven DiMarco
	William Heyman
Head of Department,	Piers Chapman

May 2011

Major Subject: Oceanography

## ABSTRACT

Characterization of a Karst Coastal Ecosystem in the Mexican Caribbean: Assessing the Influence of Coastal Hydrodynamics and Submerged Groundwater Discharges on Seagrass. (May 2011)

Israel Medina, Bachelor of Biology, Universidad Autónoma de Yucatán;  
M.S., Centro de Investigación y de Estudios Avanzados del Instituto Politécnico  
Nacional

Chair of Advisory Committee: Dr. Björn Kjerfve

Bahia de la Ascension (BA) is a pristine, shallow, karst bay located in the Mexican Caribbean, a region experiencing rapid population growth stimulated by intense tourism development. The overall objective of this study was to address the natural hydrographic variability of this inherently vulnerable ecosystem and assess its influence on a key habitat, the seagrass. The chapters follow the three-branched nature of the study which tackled the connected ecosystem issues of coastal hydrology, physical dynamics of flow and circulation, and the ecological dynamics of the seagrass species *Thalassia testudinum* in BA.

Freshwater input to BA is primarily by submerged groundwater discharges and surface runoff; both sources are derived from fissures in the aquifer but feature distinct water quality due to the interaction with adjacent wetlands. Hurricanes explain 36% of the interannual precipitation variability in the region. The water balance indicates a persistent net outflow from BA to the adjacent shelf, suggesting an intense exchange across inlets. Both diurnal and semidiurnal tidal frequencies are attenuated in the inner bay, where a meteorologically-induced subtidal water level increase may occur during four-day southeasterly winds. A clear SW-NE salinity gradient was established during dry and rainy seasons, with a strong tidally-driven marine influence throughout the central basin, and a perennial mesohaline ambient in the southwestern-most bay, where hydrodynamics are primarily controlled by wind stress.

*Thalassia testudinum* is the dominant seagrass species in BA, occupying ~90% of the substrate, including the freshwater-influenced inner bay. High nutrient inputs, including phosphorus which might have limiting effects in karst environments, along with the wind-driven circulation controlling water residence times are associated with the successful development of *T. testudinum* (up to 1,461.23 g DW m<sup>-2</sup>) within the SW bay. Farthest into the central basin, *Thalassia* consistently exhibited an inverse correlation between abundance and density of shoots. This pattern was enhanced under exceptional precipitation and inputs of denuded organic matter resulting from hurricanes making landfall on this region. The relationship between nutrient distribution and the above/belowground ratio suggested that *Thalassia* growing in BA favors the development of the aerial component as nutrients availability increases.

This study provides a basic understanding of the most important processes molding the patterns of variability exhibited by *T. testudinum* in Bahia de la Ascension. The salinity gradient and external nutrient supply, along with the hydrodynamic component, define the spatial scale at which the connectivity between the adjacent wetland, the bay, and the shelf may occur.

Por otro logro compartido:

A mis padres Guillermo Medina Abad y Margarita Gómez Ramírez, mis hermanas Jericó y Bethel, mi esposa Sonia y mis hijas Adriana y Sofía.

## ACKNOWLEDGEMENTS

Foremost, I would like to thank my committee chair, Dr. Björn Kjerfve, for his sage advice and support throughout my Ph.D studies. I would also like to express my deep gratitude to my committee members, Dr. Stephen Davis, Dr. Steven DiMarco, and Dr. William Heyman who shared their research expertise with me, helping me to improve my conceptual basis, which was fundamental to the development of my doctoral project.

I am indebted to the National Council of Science and Technology in México (CONACYT) for the financial support during the first three years of my Ph.D. program in the U.S.A. I also want to extend my gratitude to The Nature Conservancy (TNC), Peninsula de Yucatan, and to the board and staff in the Reserva de la Biósfera de Sian Ka'an, natural protected area, which provided the funds and necessary logistical support to develop all the field work during this research.

The successful completion of this study has involved the backing of many people. I would like to acknowledge in particular the support and assistance of Dr. Ismael Mariño and Dr. Cecilia Enríquez who first brought me into the world of oceanography and with whom I began to learn about the intriguing nature of hydrodynamic processes in the always amazing coastal environment. Their timely guidance at a very critical stage of this research was decisive for completion of this project. I thank Dr. Jorge Herrera-Silveira for his invaluable suggestions on an early draft of my research proposal and his continued support to complete this project, including the instrumentation utilized and his assistance to obtain the funds for field campaigns. Without the generous help of these individuals, this investigation would not have been possible.

I would like to thank Dr. Susana Enríquez, for her generosity in giving of her time and expertise reviewing and providing thoughtful comments on Chapter-III, which allowed me to be more critical about the outcomes of this research project and improve my perspective not only on this particular chapter, but on the whole dissertation.

I wish to thank also Anne Miller for her thoughtfulness and consideration in assisting with the editing of this document.

Thanks also go to my friends and colleagues and the Department of Oceanography faculty for making my time at Texas A&M University a true learning experience. My sincere appreciation to the staff of the Primary Production Laboratory and the Coastal Processes and Physical Oceanography Laboratory in CINVESTAV for their assistance in field and helpful suggestions during the data analysis stage.

It is difficult to overstate my appreciation to my friends in College Station, Texas with whom I have shared memorable experiences in life, especially to Rosalio Mireles (Ross) and Miguel Rojas, who were willing to assist me during the years I lived in CS, as well as during my many returns to Aggieland.

I cannot conclude without expressing how grateful I am to my mother, father and sisters, because with their own commitment and perseverance throughout their lives, they have provided the cornerstone of my professional and personal development; thank you for sharing with me this project completely all the way down. I also want to thank my wife Sonia for her patience and love and to my two daughters Adriana and Sofia, for being my permanent motivation and making my days worth living.

**NOMENCLATURE**

BA	Bahia de la Ascension
CC	Cayo Culebras
DB	Drainage Basin
GD	Groundwater Discharges
MBRS	Mesoamerican Barrier Reef System
RL	Reef Lagoon
SAV	Submerged Aquatic Vegetation
SGD	Submerged Groundwater Discharges
SKBR	Sian Ka'an Biosphere Reserve
VG	Vigia Grande
WC	Western Caribbean
YP	Yucatan Peninsula



## TABLE OF CONTENTS

	Page
ABSTRACT .....	iii
DEDICATION .....	v
ACKNOWLEDGEMENTS .....	vi
NOMENCLATURE.....	viii
TABLE OF CONTENTS.....	ix
LIST OF FIGURES .....	xi
LIST OF TABLES .....	xiv
 CHAPTER	
I INTRODUCTION: CHARACTERIZATION OF BAHIA DE LA ASCENSION, A COASTAL KARST ECOSYSTEM ALONG THE EASTERN YUCATAN COAST .....	1
Introduction.....	1
Study Site .....	3
Materials and Methods.....	9
Results and Discussion.....	15
Conclusions .....	30
II MODELING OF HYDRODYNAMIC VARIABILITY IN A COASTAL BAY, YUCATAN, MEXICO .....	31
Introduction.....	31
Study Site .....	32
Materials and Methods.....	33
Results and Discussion.....	44
Summary and Conclusion.....	53

CHAPTER	Page	
III	SEASONAL RESPONSES OF <i>THALASSIA TESTUDINUM</i> TO THE PHYSICAL-ENVIRONMENTAL SETTING IN A SHALLOW COASTAL BAY OF THE WESTERN CARIBBEAN.....	56
	Introduction.....	56
	Study Site .....	60
	Materials and Methods.....	61
	Results .....	66
	Discussion .....	79
	Conclusions .....	87
IV	CONCLUSIONS .....	89
	REFERENCES .....	92
	VITA .....	101

## LIST OF FIGURES

		Page
Figure 1.1	Study site: Yucatan Peninsula; Ascension Bay and drainage basin; Ascension Bay with relevant features, barrier reef and bathymetry .	4
Figure 1.2	Freshwater inputs in Ascension Bay .....	5
Figure 1.3	Mean precipitation $\pm$ 1SE and air temperature $\pm$ 1SE in Sian Ka'an Biosphere Reserve, 2000-2007.....	7
Figure 1.4	Prevalent winds in Ascension Bay for the period 2000-2007 and during the year of the field campaigns 2007.....	7
Figure 1.5	Measured and 6-hr low-pass water level in Reef Lagoon and Vigia Grande during dry season.....	21
Figure 1.6	Measured and 6-hr low-pass water level in Reef Lagoon and Vigia Grande during rainy season.....	22
Figure 1.7	Winds in Ascension Bay during field trips: June 2007; October 2007.....	23
Figure 1.8	Spatial distribution of salinity during dry season sampling and rainy season sampling.....	26
Figure 1.9	Temperature and salinity CTD profiles in the bay's inlets cross-sections during dry season and rainy season.....	27
Figure 1.10	Current velocities in the Reef Lagoon during dry season and rainy season .....	29
Figure 2.1	Map of the Gulf of Mexico and Bahia de la Ascension in the Western Caribbean .....	34
Figure 2.2	Adaptive grid of the model domain.....	35
Figure 2.3	Kinetic energy calculated every $\Delta t$ at individual nodes and presented as the integral for the whole system at every semidiurnal cycle .....	39
Figure 2.4	Modeled water discharge across the bay-shelf boundary in the water volume conservation test.....	39
Figure 2.5	Water level series at the Vigia Grande mooring.....	40

	Page
Figure 2.6	Water level and wind velocity time series in Vigia Grande during dry season sampling and rainy season sampling ..... 41
Figure 2.7	Three wind events occurring in 2007 and utilized in combination with tides to force the hydrodynamic model: Trades; north winds; and southeast winds ..... 43
Figure 2.8	Instantaneous water discharge anomaly across the bay-shelf boundary ..... 45
Figure 2.9	Instantaneous water-level and currents when the model is forced with only tides during four instantaneous tidal phases: a) ebb; b) low; c) flood; and d) high ..... 47
Figure 2.10	Modeled water level obtained in both the inner and outer portions of the channel connecting Vigia Grande embayment with the bay's central basin under the spring tides plus southeast winds scenario. 48
Figure 2.11	Instantaneous water level and currents when the model is forced with tides plus a) SE winds in ebb tide; b) "Nortes" in flood tide; c) Trades in low tide; and d) Trades in flood tide ..... 49
Figure 2.12	Seven-day-average water level and residual currents..... 51
Figure 3.1	Map of Bahia de la Ascension in the Western Caribbean..... 58
Figure 3.2	Study site with 62 sampling stations ..... 59
Figure 3.3	Three distinct <i>Thalassia testudinum</i> beds classified according to morphometric, structural, and density attributes from a Landsat ETM <sup>+</sup> image ..... 64
Figure 3.4	Seasonal variability of hydrographic properties in Bahia de la Ascension during the 2006 and 2007 sampling campaigns ..... 67
Figure 3.5	Seasonal variability of inorganic nutrients in Bahia de la Ascension during the 2006 and 2007 sampling campaigns ..... 70
Figure 3.6	Intra-annual variability of seagrass aboveground biomass (a), belowground biomass (b), and aboveground/belowground ratio (c) across <i>T. testudinum</i> vegetation classes in Bahia de la Ascension during 2006..... 74
Figure 3.7	Intra-annual variability of <i>Thalassia</i> leaf morphometry across vegetation classes in Bahia de la Ascension during 2006 ..... 77

	Page
Figure 3.8 Seasonal variability of <i>Thalassia</i> abundance and shoot density across vegetation classes in Bahia de la Ascension during 2006-2007.....	78

## LIST OF TABLES

		Page
Table 1.1	Geomorphologic and hydrologic traits of Bahia de la Ascension. ....	4
Table 1.2	Historic occurrence of hurricanes in the Sian Ka'an Reserve (source: <a href="http://www.nhc.noaa.gov/pastall.shtml">http://www.nhc.noaa.gov/pastall.shtml</a> ). Before 1953 hurricanes were not given names. Categories for hurricanes are provided according to the Saffir-Simpson Hurricane Wind Scale (Marshall 2009). Tropical storm (TS) Dorothy was included because of the substantial damage reported.....	8
Table 1.3	Eight-year average flows for each month ( $\times 10^6 \text{ m}^3 \text{ mo}^{-1}$ ) (2000-2008) were used to compute the water balance in Bahia de la Ascension. Fresh water is the combined surface plus subsurface flows. ....	11
Table 1.4	Summary of the spatial autocorrelation analysis carried out for salinity during both seasons. The parameters shown are: the model fitted to data, range beyond which spatial autocorrelation among sampling units ceases, the proportion of the variance accounted by the fitted model (e.g., take values from 0 to 1), and the agreement between the experimental semivariogram vs. theoretical model accounted for by $r^2$ (i.e., regression coefficient)...	13
Table 1.5	Table showing the mean $\pm$ SD, minimum, and maximum values of temperature and salinity during both samplings in two sites of Bahia de la Ascension (RL: reef lagoon and VG: Vigia Grande embayment).....	25
Table 2.1	The simulations run on the hydrodynamic model including forcing functions and simulation times utilized on the distinct cases. Eight-day long simulations were used for the wind forcing simulations because "Nortes" are characteristically short-lived episodes in the Yucatan Peninsula .....	36
Table 2.2	The summary of statistics of the model performance. RMS = Root Mean Square; RMAE = Relative Mean Absolute Error (a value $< 0.2$ corresponds to an excellent agreement; Sutherland et al. 2004).....	41
Table 3.1	Interpretation of the Braun-Blanquet scores utilized for rapid assessment over the seagrass meadows.....	63

	Page	
Table 3.2	Seasonal water quality parameters (mean values $\pm$ 1 standard deviation) at 3 sites (e.g., supervised classification) across Bahia de la Ascension during 2006-2007: Vigia Grande at the inner bay (VG), bay's central basin (CB), and Cayo Culebras at the seaward boundary (CC). Temperature is given in $^{\circ}$ C and inorganic nutrients concentration in $\mu$ M.....	68
Table 3.3	Seasonal Principal Component Analysis (PCA) in Bahia de la Ascension during 2006-2007 .....	71
Table 3.4	Seasonal structural and demographic parameters (median values and coefficient of variation percent) of <i>Thalassia testudinum</i> at three sites (supervised classification) across Bahia de la Ascension: Vigia Grande at the inner bay (VG), bay's central basin (CB), and Cayo Culebras at the seaward boundary (CC). ab: aboveground and bb: belowground biomasses are given in g DW $m^{-2}$ , A/B is aboveground/belowground ratio, and short shoot (SS) density as individuals $m^{-2}$ .....	73
Table 3.5	Average biomasses (g DW $m^{-2}$ ) and short shoot densities ( $m^{-2}$ ) in shallow ecosystems of the Gulf of Mexico and the Caribbean Sea. Information drawn from CARICOMP - Caribbean Coral Reef, Seagrass and Mangrove Sites (Kjerfve 1998), except for Hall et al. 1999.....	80

## CHAPTER I

### INTRODUCTION: CHARACTERIZATION OF BAHIA DE LA ASCENSION, A COASTAL KARST ECOSYSTEM ALONG THE EASTERN YUCATAN COAST

#### Introduction

The Yucatan Peninsula is a large limestone platform of Tertiary-Holocene carbonates deposited on Jurassic-Cretaceous beds (Back and Hanshaw 1970). The karstic soil of the low relief Yucatan is defined by the proclivity of carbonate bedrock to dissolve, which precludes significant surface water flow and promotes the development of an extensive underground freshwater network (Back et al. 1979; Marin and Perry 1994). Freshwater flow into the coastal ocean comes from both non-point and local submerged groundwater discharges (SGD) or springs. Groundwater discharge from the eastern Yucatan to the coastal ocean has been estimated utilizing a mass-wasting method as  $8.6 \times 10^6 \text{ m}^3$  per year per km of coastline (Hanshaw and Back 1980).

Because of the Yucatan's geohydrological character, increasing development of the tourism industry in the Mexican Caribbean (the eastern YP) represents a potential threat to the integrity of coastal ecosystems. The limestone's high permeability allows rainwater to penetrate rapidly through the base rock into the aquifer. This enhanced infiltration through the soil not only lowers the amount of available fresh water at the surface, but also makes the aquifer particularly susceptible to contamination. Although initiatives designated as "ecotourism" do reduce environmental disturbance, they cannot be regarded as a benign, non-consumptive use of land and biological resources. Indeed in many instances, their introduction has had negative effects on the natural systems (Jackson 1986; Edwards 1989; Tudela 1989).



The Sian Ka'an Biosphere Reserve, which is the third largest protected area in Mexico, is located along the Caribbean coast of the Yucatan Peninsula. Within the Reserve is Bahia de la Ascension (BA; Fig. 1.1), a shallow bay bound at the eastern edge by a semi-continuous barrier reef formation and one of the few pristine coastal ecosystems in the Mexican Caribbean. This bay has high biological diversity and is an important nursery habitat for two shark species (*Charcarinus leucas*, *Negaprion brevirostris*), manatee (*Trichechus manatus*), and spiny lobster (*Panulirus argus*), among others (Vidal and Basurto 2003). Research conducted in this location has focused primarily on the transport of biota (ichthyoplankton, Chiappa-Carrara et al. 2003; zooplankton, Gasca and Suarez 1994), food-web studies (Vidal and Basurto 2003), spiny lobster fishery stock estimations (Lozano-Alvarez et al. 1991), and ontogenetic habitat evaluation for a variety of fishes (Quintal-Lizama and Vasquez-Yeomans 2001) and crustaceans (Lipcius et al. 1998). Despite all of this, the hydrography and water quality of Bahia de la Ascension is poorly known.

The generalized evidence of human-driven increments in nutrient input across the world's coastal zones and the alteration of the ratios of such influx (Jickells 1998) points out the necessity of assessing Bahia de la Ascension's seasonal and spatial patterns of water quality, as well as the main processes involved in its magnitude and variability. Salinity distribution trends are of particular interest because salinity gradients define the spatial heterogeneity across BA, which supports the high biological diversity and productivity characterizing this ecosystem (Lozano-Alvarez et al. 1991; Mazzotti et al. 2005). Furthermore, the conservative behavior of salinity makes it a natural "tracer" for monitoring the input of distinct materials to the system (e.g., nutrients, pollutants), estimating the average flushing time of such constituents, and evaluating the effects of potential water management strategies being carried out several kilometers inland. A common feature in the functioning of shallow coastal ecosystems is the occurrence of time-varying hydrographic gradients and the dominant role of low frequency forcing functions (e.g., intra-annual precipitation-evaporation balance) controlling their fluctuations (Kjerfve 1986; Nuttle et al. 2000). In the short term, wind stress may exert a notable influence on the distribution and variability of water quality parameters in these systems. Additionally, tidal variability may regulate water exchange with the sea as a function of the geomorphologic characteristics of the channel in the inlet zone (Kjerfve 1994; Smith et al. 1994).

Regarding the environmental pressure brought on by high-impact tourism in the region, and the relationship between the health of the system and the socio-economic well-being of its inhabitants, it is the objective of this chapter to analyze the spatial patterns of salinity in Bahia de la Ascension and to determine the dominant factor controlling salinity: SGD or water exchanged across the inlets. It is also my intention to assess what other forces modulate this dynamic (e.g., wind stress), and how this relationship changes between dry and rainy seasons. It is anticipated that understanding the natural fluctuations in the bay's salinity will aid in determining the impact of adjacent coastal development projects on the Sian Ka'an Biosphere Reserve's marine ecosystems.

### **Study Site**

Bahia de la Ascension (19° 40' 32.76" N; 87° 32' 30.87" W) is a flooded karst depression (580 km<sup>2</sup>) bound on the ocean side by a 6-km discontinuous fringing reef and with a 14-km ocean entry between Punta Allen and Punta Hualastok (Fig. 1.1). Maximum width (horizontal distance from the inlets to the reef crest) and average depth of the reef lagoon (RL) are 7 km and 5.5 m, respectively. The mean water depth is 2.2 m, with a 6.8 m maximum depth along the east-west tidal channel, located between Punta Allen and Cayo Culebras, a 5.5 km mangrove cay placed in the middle of the bay-reef lagoon boundary. Tides in the zone are mixed, semidiurnal (Kjerfve 1981) with a maximum range of 33 cm (CICESE 2006). The bay's surrounding drainage basin is 1, 222 km<sup>2</sup>.

Freshwater discharges into BA are due to the geological uplift and low relief on the karst platform, which has developed flooded formations at the intersections with the aquifer (Buterlin 1958; Espejel 1983). This freshwater supply derives from a vast array of fractures in the limestone, mainly in the southwestern bay, as well as from SGD along the western margin (Fig. 1.2). The environmental diversity within the bay spans from rocky bottom, featuring coarse sandy cover in the north-central basin, to fine sand and silt sediment in the southwestern Vigia Grande embayment, a ≈78 km<sup>2</sup> lagoon which hydrologic variability is evidently controlled by the shallow depth (<0.5m) and freshwater inputs from springs (Fig. 1.1).

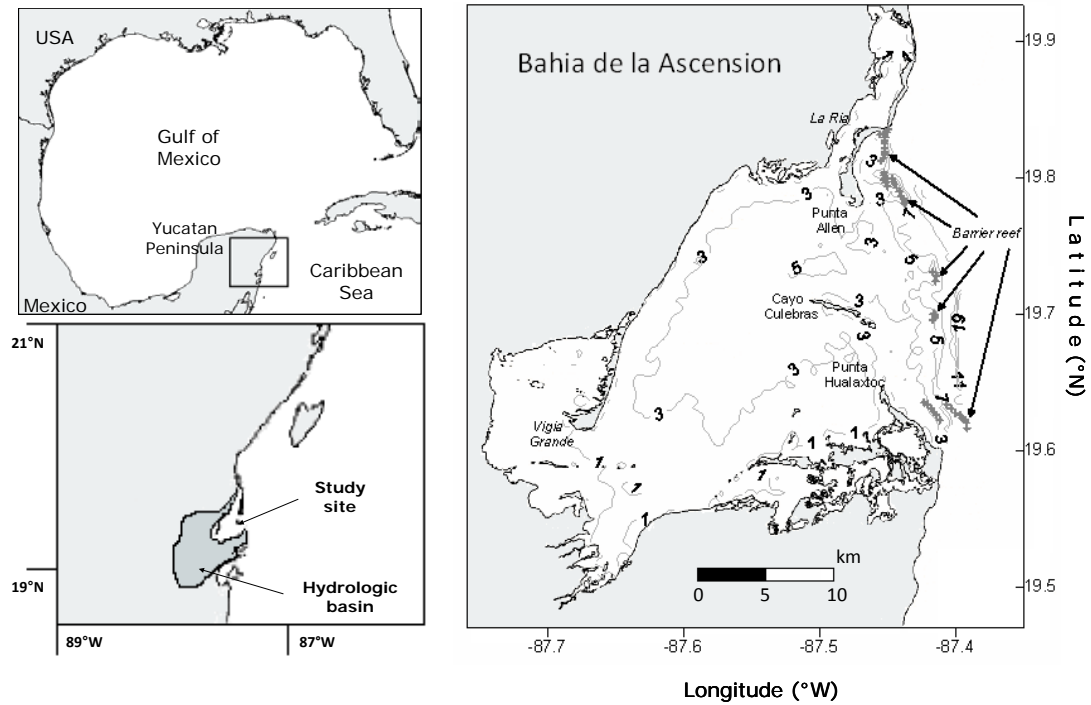


Figure 1.1. Study site: (*upper left*) Yucatan Peninsula; (*lower left*) Ascension Bay and drainage basin; (*right panel*) Ascension Bay with relevant features, barrier reef and bathymetry.

Table 1.1.- Geomorphologic and hydrologic traits of Bahia de la Ascension.

Feature	Estimation
Surface area of lagoon (km <sup>2</sup> )	580
Drainage basin area (km <sup>2</sup> )	1,222
Total mean water volume (x 10 <sup>6</sup> m <sup>3</sup> )	1,422
Mean depth; deepest (m)	2.2; 6.8
Mean tidal range (m)	0.18
Tidal prism (x 10 <sup>6</sup> m <sup>3</sup> )	104.4
Water residence time (days)	86

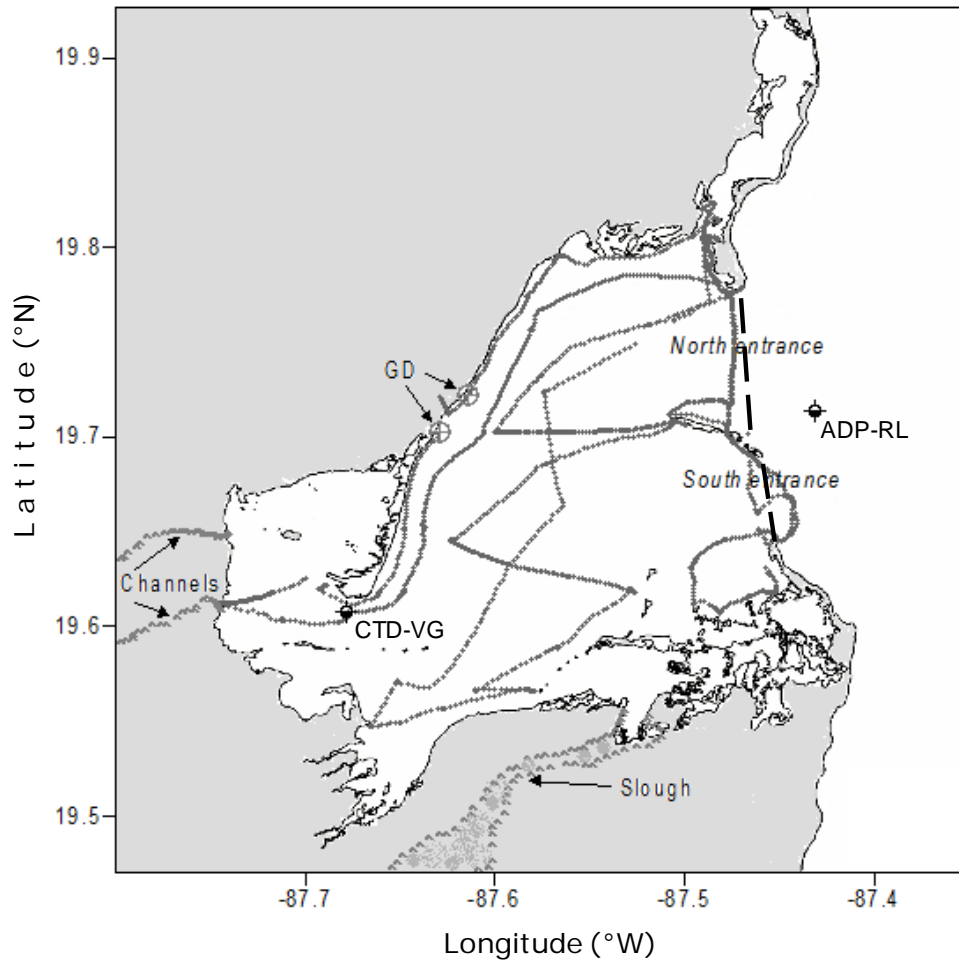


Figure 1.2. Freshwater inputs (surface channels, slough, and groundwater discharges, GD) in Ascension Bay. Anchored instruments during field trips are shown: ADP in the reef lagoon (ADCP-RL) and CTD in Vigia Grande (CTD-VG); as well as location of the cross-section CTD profiling (----), and flow-through continuous sampling across the bay (.....).

### *Weather and climate*

The local climate in the south of the Quintana Roo state is hot, sub-humid with three seasonal periods: rainy, dry, and "Nortes" (see below for description). The mean annual temperature is around 22°C; the average minimum temperature occurs in January and is slightly above 18°C. The mean annual precipitation varies from 1,200 mm to 1,500 mm; March is the driest month with an average 60 mm precipitation. According to the Köppen (1936), the climate of the bay is classified as Aw" (X'), a "savanna" climate, although in the eastern Yucatan the vegetation is a medium sub-perennial tropical forest. The area just south of BA has isothermal conditions with mean annual temperature oscillation less than 5°C, whereas the area north of the bay experiences thermal oscillation of 5-7 °C. The precipitation/temperature (P/T) ratio is ~45 mm/°C south of the bay and exceeds 55 mm/°C north of the bay (Garcia 1988).

Mean monthly rainfall, air temperature, and wind data for the period 2000-2007 in the SKBR was obtained from the National Meteorological Service (SMN 2007) meteorological station located within the Reserve and 35 km north of BA. Wind data were recorded by a Vaisala automatic weather station. The seasonality in the Mexican Caribbean is characterized by rainfall fluctuations rather than temperature variability (Fig. 1.3). There is a distinct dry season (February-May) and a distinct rainy season (June-October). The period from November to January is characterized by slight precipitation and low air temperatures due to boreal winds bringing cold, dry polar air masses to the region (i.e., locally known as *Nortes*). The dominant winds in the region are northeast trades and southeasterly winds (Fig. 1.4). Northeasterlies are characterized by an average speed of 3.2 m s<sup>-1</sup>, with strongest trades typically occurring in June. The southeast winds are prevalent in March, with a mean speed of 3.3 m s<sup>-1</sup>.

The Caribbean coast of the YP exhibits the highest occurrence of hurricanes in Mexico (Blake et al. 2007). The low relief of the YP offers little resistance to hurricanes, which often traverse the entire Peninsula. Despite the existence of historic recordings of hurricanes affecting the Sian Ka'an protected area since the 19<sup>th</sup> Century (Table 1.2), detailed information documenting the impacts over the zone is scarce. Obviously, the substantial precipitation, wind stress, and storm surge associated with hurricanes will have an impact on the environment.

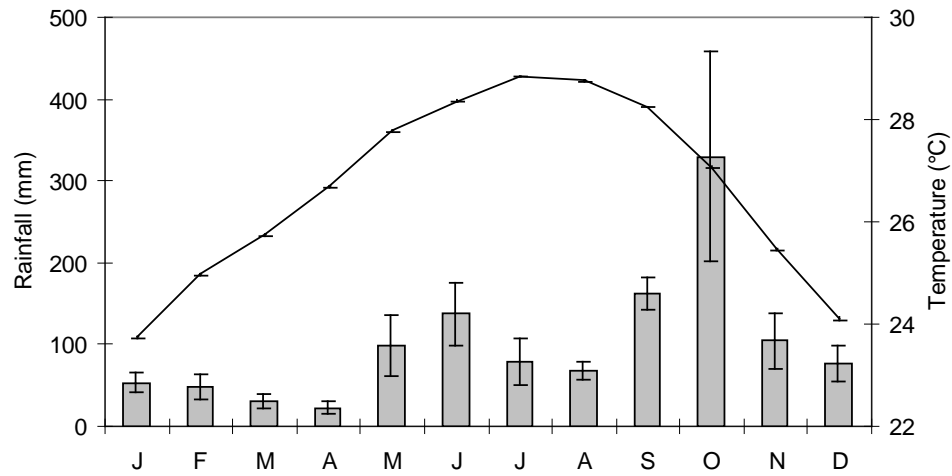


Figure 1.3. Mean precipitation (bars)  $\pm$  1SE and air temperature (solid line)  $\pm$  1SE in Sian Ka'an Biosphere Reserve, 2000-2007 (data provided by the National Meteorological Service; SMN 2007).

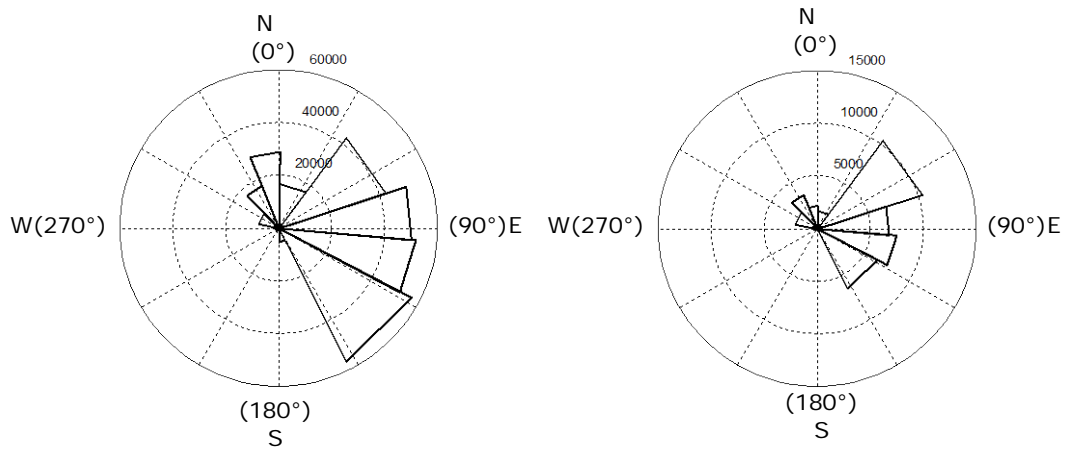


Figure 1.4. Prevalent winds in Ascension Bay for the period 2000-2007 (left) and during the year of the field campaigns 2007 (right). Labels on the concentric circles represent winds occurrence.

Table 1.2. Historic occurrence of hurricanes in the Sian Ka'an Reserve (source: <http://www.nhc.noaa.gov/pastall.shtml>). Before 1953 hurricanes were not given names. Categories for hurricanes are provided according to the Saffir-Simpson Hurricane Wind Scale (Marshall 2009). Tropical storm (TS) Dorothy was included because of the substantial damage reported.

Date	Storm	Category
Sep 1893	---	---
Sep 1905	---	---
Sep 1920	---	---
Sep 1928	---	3
Jun 1934	---	1
Aug 1947	---	2
Sep 1955	Hilda	4
Sep 1955	Janet	5
Oct 1969	Laurie	---
Aug 1970	Dorothy	TS
Sep 1974	Carmen	4
Oct 1995	Roxanne	3
Aug 1996	Dolly	1
Jul 2005	Emily	5
Aug 2007	Dean	5

Hurricane Dean was the strongest and most recent cyclone to impact Bahia de la Ascension and the Yucatan Peninsula. This typical tropical easterly wave (i.e., seasonal warm disturbances of the tropical North Atlantic Ocean) off the coast of Africa moved through the Caribbean and became a major hurricane, crossing the Yucatan Peninsula on 21 August 2007 as a category 5 storm on the Saffir-Simpson scale. Dean made landfall near Majahual, located 100 km south of Bahia de la Ascension, with a minimum barometric pressure of 905 hPa and maximum sustained winds of  $77 \text{ m s}^{-1}$  (Franklin 2008). Following Hurricane Dean's passage, organic material from the denuded adjacent mangrove wetland was observed, mainly in the southern part of the bay where some freshwater channels were obstructed and disappeared, while other waterways were formed through erosion and widening as a result of substantial rainfall and wind stress during the event. Such changes were evident during the rainy season sampling, which was carried out 54 d after the hurricane's impact. A quantitative assessment is still needed to understand the resilience of the system to such high-energy, meteorological phenomena.

## Materials and Methods

### *Water balance calculation*

The water balance of an aquatic ecosystem is undertaken by measuring the major water inflows and outflows during a given period of time (e.g., seasonally, yearly). The key terms of this relationship are precipitation (P), surface runoff (S), groundwater input (G), and evapotranspiration ( $E_T$ ), this latter represented with a negative sign as it constitutes a water loss from the system. Also, the advection of water through the inlet(s) must be included in this balance as it could represent either a gain or a loss (denoted by a  $\pm$  sign).

The karstic landscape of the Yucatan prevents fluvial discharges, therefore freshwater input to Bahia de la Ascension (BA) is through surface runoff and groundwater discharge, which for practical reasons are estimated together as ( $Q_{SG}$ ). Advection through the bay entrance would require thorough transverse sampling in cross sections of both inlets; such sampling was beyond the scope of the current study and, therefore, only the net water gain or loss in the system was calculated (Table 1.3).

The freshwater input ( $Q_{SG}$ ) was estimated using precipitation data for the Sian Ka'an Biosphere Reserve for the years 2000-2007 (SMN 2007), and using the following equation (Kjerfve 1990):

$$Q_{SG} = r * DBA * \Delta f / r$$

where  $r$  is rainfall, DBA is the drainage basin area (see quantification procedure below), and  $\Delta f/r$  is the dimensionless ratio of runoff plus groundwater to rainfall within the drainage basin. Both terms are represented on a seasonal scale. The runoff ratio was computed according to

$$\Delta f/r \approx e(-E_0/r)$$

where  $E_0$  is the potential evapotranspiration ( $m\ s^{-1}$ ) that is determined using the empirical equation (Holland 1978):



$$E_0 = 0.3805 e^{\left(\frac{-4.62 \cdot 10^3}{T}\right)}$$

where T (Kelvin) is the monthly average air temperature, while  $E_0$  represents the combined water that vaporizes from soil or flooded zones and the moisture that passes by active and passive processes through vascular plants to the atmosphere. This equation is based on the relationship between potential evapotranspiration and air temperature, assuming both a moisture-saturated soil and uniform vegetation (Medeiros and Kjerfve 1993).

The evaporation at the bay's surface was calculated using Thornthwaite's empirical formula for potential evaporation (1948):

$$E_t = 1.6 \left(10 T_i / I\right)^a$$

$$I = \sum_{i=1}^{12} \left(T_i / 5\right)^{1.514}$$

$$a = (492390 + 17920I - 77.1I^2 + 0.675I^3) * 10^{-6}$$

where  $E_{i}$  is possible evaporation for month  $i$  ( $\text{mm mo}^{-1}$ ),  $T_i$  is the mean monthly air temperature ( $^{\circ}\text{C}$ ), and  $I$  is a local heat index.

#### *Drainage basin area (DBA)*

Two SWIR (shortwave infrared) composite Landsat 7 ETM<sup>+</sup> images (bands 7, 4, 2) corresponding to 11 April 2002 and 4 October 2002 were downloaded from the USGS EROS archive (URL: <http://glovis.usgs.gov/BrowseBrowser.shtml>) to estimate the drainage basin area influencing Bahia de la Ascension. Because brightness values (i.e., reflectance) recorded in the SWIR spectrum are due primarily to moisture content, these three spectral channels improve the ability to discriminate between vegetated surface and bare soil (e.g., land-water boundaries and flood plains) on the Landsat 7 ETM<sup>+</sup> images (Jensen 2007).

The spectral patterns from both SWIR images were classified utilizing a Simple One-Pass Clustering Method (TNTmips, Microimages Inc. 2006) to place all cells into naturally

occurring spectral classes (i.e., non-supervised classification). Post-processing of this class raster included inspection of the spectral properties of each class and systematic comparison to available air photo information provided by a 1:50,000 topographic chart of the zone (e.g., partial “ground-truth”) (INEGI 2002). Finally, Didger-Digitizing software (Didger; Golden Software Inc., 2001) was utilized to digitalize and estimate the drainage basin area (DBA) of Bahia de la Ascension.

Table 1.3. Eight-year average flows for each month ( $\times 10^6 \text{ m}^3 \text{ mo}^{-1}$ ) (2000-2008) were used to compute the water balance in Bahia de la Ascension. Fresh water is the combined surface plus subsurface flows.

Month	Fresh water	Precipitation	Evapotranspiration
Jan	3	31	5
Feb	1	28	6
Mar	0	18	7
Apr	0	13	8
May	14	57	9
Jun	34	80	10
Jul	6	46	10
Aug	3	40	10
Sep	52	95	10
Oct	214	191	8
Nov	21	60	6
Dec	10	45	5

#### *Water residence time estimation*

Water residence time, defined as “the time it takes for any water parcel to leave the system through its outlet to the sea” (Dronkers and Zimmermann 1982), is the fundamental parameter utilized to address the relationship between hydrodynamic mechanisms and occurrence of distinct biogeochemical processes. The balance between water inflows and outflows in coastal ecosystems with limited exchange with sea largely controls their characteristic transport scales and thus, their retention capacity of waterborne constituents

(e.g., nutrients, biota, suspended material, pollutants). It is thought that even an overall quantification of the average time a water mass stays within BA before it is carried away from the system will assist in describing the variability of numerous ecologically important processes, including the outwelling of nutrients-enriched water and their proclivity to eutrophication.

The water residence time was calculated according to the LOICZ methodology (Gordon et al. 1996). An assumption underlying this formula is that the system's volume is constant in the long term ( $dV/dt = 0$ ), with deviations of this condition being accounted for by the residual flow ( $V_R$ ). The mixing flow ( $V_X$ ) was estimated utilizing salinity as a tracer, given its conservative nature. Hence, water exchange with sea is the most significant process concerning  $V_X$ . By dividing the total volume of the lagoon ( $V_{SYS}$ ) ( $m^3$ ) by the sum of  $V_X$  ( $m^3 d^{-1}$ ) and the absolute value of  $V_R$  ( $m^3 d^{-1}$ ), the average time (d) that any water parcel spends within the bay before it is flushed out through the inlets is the water residence time ( $\tau$ ):

$$\tau = \frac{V_{SYS}}{V_X + |V_R|}$$

#### *Hydrographic and dynamic variables*

Two field trips were carried out in Bahia de la Ascension to measure the spatial behavior of salinity as well as the temporal evolution of the water currents. The first sampling campaign was conducted late in the dry season (3-9 June 2007; right before the beginning of rainy season) and the second was late in the rainy season (14-20 October 2007).

#### *Spatial variability of salinity*

A flow-through sampling approach using a Dataflow® (Madden and Day 1992) was undertaken to continuously record salinity across the surface of the bay. The sampling tracks are shown in Figure 1.2. Prior to plotting the salinity data into contour maps, the spatial autocorrelation among sampling stations was quantified for both of the seasonal campaigns through a geostatistical approach utilizing GS+, Ver. 9 (Robertson 2008). An experimental semivariogram, which illustrates the variability associated with the distance among samples, was calculated to examine the degree of spatial dependence present in the salinity data (Isaaks and Srivastava 1989). A mathematical model (e.g., exponential, spherical, Gaussian) was fit to the cloud of points scattered over distance (x-axis) against

the semivariance (y-axis). The agreement between the model and the observations is measured by  $r^2$ , providing the criterion to select a specific model (i.e. the model with the highest  $r^2$  was chosen). The mathematical model was used to generate the salinity contour maps (Table 1.4).

Table 1.4.- Summary of the spatial autocorrelation analysis carried out for salinity during both seasons. The parameters shown are: the model fitted to data, range beyond which spatial autocorrelation among sampling units ceases, the proportion of the variance accounted by the fitted model (e.g., take values from 0 to 1), and the agreement between the experimental semivariogram vs. theoretical model accounted for by  $r^2$  (i.e., regression coefficient).

Season	Model	Range (m)	Proportion	$r^2$
Dry	Spherical	2,652	0.972	0.976
Rainy	Gaussian	16,000	0.778	0.693

#### *Cross-section CTD profiles*

CTD profiles (SBE-19plus, SeaBird Electronics, Inc.) were collected from the north and south inlets of Bahia de la Ascension to obtain the cross-section thermohaline distribution and assess the water mixing characteristics of the inlets.

#### *Temporal variability of the water currents*

The horizontal current velocity was recorded at the reef lagoon using an ADP (AWAC; Nortek AS) anchored outside the bay (Figure 1.2). The sampling frequency was 10 min during the 4 days spanning both seasonal campaigns.

#### *Variability of the water level in the reef lagoon (RL) and inner bay*

To assess water level variability both in the inner bay (Vigia Grande) and the adjacent marine environment (reef lagoon, RL), harmonic analysis was performed on the 89.5-h time series measurements made by CTDs (Diver; Van Essen Instruments) anchored at both localities during the two seasonal field trips in Bahia de la Ascension. By fitting individual harmonics to these data series the amplitude and phase were computed, both characterizing a particular tidal constituent (Pawlowicz et al. 2002). Tidal characteristics of

the western Caribbean have been identified as mixed semidiurnal, with a form number ( $F$ ) between 0.25 and 1.5 (Kjerfve, 1981).  $F$  is defined as the amplitude ratio:

$$F = \frac{(K_1 + O_1)}{(M_2 + S_2)}$$

Also, tidal excursion of the  $M_2$  component, or the horizontal distance a particle is able to move into the system with flood and ebb tide was estimated as:

$$L_{TE} = \int_0^{T/2} u dt = \frac{T}{\pi} u_0$$

where  $L_{TE}$  is the tidal excursion,  $T$  is the tidal period of the  $M_2$  constituent (= 12.42 h), and  $u_0$  is the maximum tidal velocity in the system inlet (this value was drawn from the current time series recorded in the reef lagoon during the June sampling campaign spring tides condition).

It is not intended that this tidal analysis will fully describe the behavior depicted by tides within the system; that would require a longer time series, including both spring and neap tides, to completely resolve the amplitudes and phases for the distinct constituents. Rather, this analysis is to assess the hydrodynamic traits of the dominant diurnal and semidiurnal frequencies across Bahia de la Ascension by comparing how these constituents are transformed as they travel across the bay (i.e., from the reef lagoon to the Vigia Grande moorings). Although the variability observed on such astronomical frequencies will be valid only for the timeframe of the sampling campaigns, it is my thought that the current information will provide insight to the range of differences of tidal frequencies between the outer and inner bay.

## Results and Discussion

### *Meteorology and hydrology*

Northeasterlies (i.e. trade winds) were both the most typical and strongest winds occurring in the Sian Ka'an Biosphere Reserve in 2007, when the current study was undertaken (Fig. 1.4). Peak northeasterly velocity during 2007 was  $14.14 \text{ m s}^{-1}$ , with an average of  $3.10 \text{ m s}^{-1}$ . This single year contrasted with the wind pattern exhibited over the 8-year (2000-2007) period, when southeast winds predominated (Fig. 1.4). The southeast winds were second in incidence during the year of the field campaigns, but with greater strong-winds persistence than trades, featuring a mean velocity of  $3.50 \text{ m s}^{-1}$  and maximum of  $8.91 \text{ m s}^{-1}$  (Fig. 1.4). Furthermore, north-northwest winds associated with the "Nortes" season showed a maximum velocity of  $6.17 \text{ m s}^{-1}$  and average of  $2.13 \text{ m s}^{-1}$ .

The  $1,200 \text{ km}^2$  drainage basin (DBA) of Bahia de la Ascension encompasses completely flooded zones (only in late rainfall season and including most of the drainage basin), partially flooded zones (during late dry season), and permanently flooded regions (e.g., slough; Fig. 1.2). The DBA estimated for Bahia de la Ascension in this study is roughly 40% of the catchment area reported by Aceves (1976), who calculated a drainage basin of  $2,949 \text{ km}^2$ . Aceves' estimation included a vast zone to the west (past the town of Felipe Carrillo Puerto 30 km west of Bahia de la Ascension), as well as a Late Tertiary geological formation (Miocene-Pliocene period) northwest of the bay, where well-developed forest vegetation exists over permanent non-flooded zones (Lopez-Ornat 1983).

The discrepancy between the Aceves' estimation and the current study's estimation of the drainage basin may be related to this study's use of spectral properties and aerial photography interpretation which would not account for any belowground features. The high porosity of the Yucatan karst leads to enhanced transmissivity (40% of the signal) of the Caribbean microtide ( $\approx 30 \text{ cm}$ ) through sinkholes located 5 km inland (Beddows 2003). These belowground features were not considered in the current drainage basin estimation, although their development reaches roughly 10 km inland (Beddows et al. 2007). However, the DBA boundary in this study nearly reaches 20 km inland, suggesting that a reasonable high percentage of this array of conduits discharging fresh water into the bay were included in the current DBA estimation.

The climatology of the SKBR is defined by seasonal varying precipitation rather than thermal oscillations (Fig. 1.3). September and October had the greatest precipitation (184 mm and 217 mm, respectively), followed by June (132 mm); 65% of the annual precipitation occurs during the rainy period between July-November (Fig. 1.3). Despite the seasonal rainfall regime, the Mexican Caribbean is characterized by a spatial heterogeneity due to tropical storms and meso-scale convective systems, (short-term cloud conglomerations associated with diurnal warming; Valdes et al. 2005). The geohydrological traits of the Yucatan karstic landscape may respond to a discontinuous spatial pattern of rainfall and send temporal fluctuating coastward freshwater supply after recharge of the aquifer.

The marked spatial variability of rainfall in the eastern coast of the Yucatan (Valdes et al. 2005) contrasts with the well-defined seasonal trend of alternating dry and rainy periods. Accordingly, high precipitation during late June, followed by another peak rainfall recorded around October was exhibited in the year when the field work was carried out. Furthermore, low pressure systems (e.g. hurricanes) occurring in the Yucatan during the late rainy season may bring high precipitation. These meteorological processes may account for up to 76% of the annual precipitation and explain 35% of the interannual variability in the SKBR, as recorded in 2005 when two category 5 hurricanes made landfall –one in the northern edge of the reserve (Emily), and the other (Wilma) 97 km to the north, off from the SKBR. The percentage of the interannual variability was estimated as the quotient of the Coefficient of Variation (CV) of monthly accumulated rainfall during the period 2000-2007 not including the precipitation from both hurricanes divided by the CV when the precipitation from these hurricanes was included ( $CV = [\text{standard deviation}/\text{mean}] * 100$ ).

Semi-enclosed, coastal ecosystems may experience dramatic hydrological effects due to seasonal rainfall variability, such as changes in the salinity spatial pattern and flushing time. Because of the strong temporal fluctuation in the precipitation regime of the Yucatan, coastal lagoons in the Peninsula are particularly sensitive to this seasonal trait, as observed in the Nichupte Lagoon, a choked ecosystem (i.e., lagoons with small ratio of entrance channel cross-sectional area to system's surface, leading to reduction of short-

term marine variability and long residence time; Kjerfve 1986) located 130 km to the north of Bahia de la Ascension and like this ecosystem, influenced by submerged groundwater discharge (Carruthers et al. 2005). A 19% reduction in the yearly precipitation led to a 56% increase in the flushing time of Nichupte (Merino et al. 1990). Based on a black-box model of water balance (i.e., budget model based on the mass balance of salt -LOICZ biogeochemical modeling guidelines; Gordon et al. 1996), the seasonal water residence time estimated for Bahia de la Ascension indicated that water is retained substantially longer during dry season (256 d) than in the rainy season (65 d), suggesting that interannual variation of direct rainfall onto the bay would alter the renewal time of the system and its salinity conditions.

This simple estimation provides insight into the importance that regional annual variability of rainfall plays in Bahia de la Ascension. Not only are precipitation trends directly affected, but this meteoric recharge of the regional aquifer promotes groundwater discharge towards the coastal zone due to high levels of the water head, thus favoring freshwater input to the landscape: wetlands-aquatic systems-adjacent marine zone. Also, occurrence of meteorological processes on an interannual scale, such as ENSO, may drive seasonal spatial salinity patterns across Bahia de la Ascension (Restrepo and Kjerfve 2000; Blanco et al 2006), as well as alter the vertical structure in the cross-section of the inlets zone, potentially affecting gravitational circulation and materials exchange with the ocean.

This response of the Yucatan's water storage was observed subsequent to Hurricane Gilbert in September 1988, which yielded an exceptional discharge, recharging the aquifer at 1.01 m above the recorded water table during the dry season of that same year (Marin 1990). Despite the hydraulic conductivity in the aquifer of the eastern Yucatan coast (ranges from  $10^1$  to  $10^3$  m d<sup>-1</sup>, Beddows 2004), it seems reasonable to expect that such high rainfall volume requires some time to percolate through the porous matrix and then be carried away to the transitional wetlands, and further on to the coastal zone via submerged groundwater discharge.

This phase shift in the freshwater outflow may generate a pulse-like discharge to the coastal bay during most of the year, rather than a constant input. Due to the karstic nature of the Yucatan, the groundwater discharge operates through physiographic features locally



named *cenotes*. This transient accumulation of fresh water within the nearby wetlands allows a variety of processes to occur while the water mass moves on sluggishly (i.e., laminar flow). The operation of such mechanisms may induce changes on the physical-chemical water properties, including nutrient-status and the removal of biotic and/or abiotic material from wetlands. When this water mass is flushed into the bay, it has the potential to alter the hydrographic spatial pattern of the receiving body of water on a variable basis, as a function of the amount of time the water resided within the adjacent ecotone, as well as the autochthonous biogeochemical traits and hydrodynamic features characterizing the system itself.

By comparing the precipitation recorded in the SKBR during the period 2000-2006 with that for the current sampling campaigns undertaken in 2007, it may be observed that rainfalls during the wet season of 2007 ( $0.15 \text{ m mo}^{-1}$ ) were below the average precipitation of  $0.21 \text{ m mo}^{-1}$  estimated in the wet season of the 7-year period. In contrast, precipitation during the 2007 dry season ( $0.09 \text{ m mo}^{-1}$ ) was higher than the mean rainfall of  $0.05 \text{ m mo}^{-1}$  recorded during dry seasons throughout the 7-year period. This seemingly atypical behavior of the precipitation might be linked to the moderate La Niña event occurring in June 2007 (UNAM 2007), which led to wetter than normal dry season conditions in the Yucatan Peninsula (Orellana et al. 2007) and, as will be presented later in this discussion, may have contributed to similar spatial distribution of salinity in both seasonal samplings.

It was estimated within an 8-year period (2000-2007) that 16% of the rainfall was converted into the joint surface runoff plus groundwater in Bahía de la Ascension during the dry season (i.e., freshwater input), whilst in the rainy season it was 68%. The monthly ratio of evaporation to precipitation is highly variable throughout the year, with a minimum of 4% in October during rainfalls and a high ratio, up to 60%, in April during the dry season. On the other hand, the amount of monthly variation exhibited by the freshwater input is larger than that of the direct rainfall onto the bay, which varied from about  $13 \text{ m}^3$  per month to about  $191 \text{ m}^3$  per month, a range of intra-annual variation of  $178 \text{ m}^3$  per month (with a range of 292% of mean value), while the range of intra-annual variation of joint runoff and groundwater into the bay was  $214 \text{ m}^3$  per month, or 719% of mean value. By inspecting the absolute magnitudes and amount of intra-annual variation of both the precipitation and fresh water it seems plausible that the salinity gradient of Bahía de la

Ascension is more strongly influenced by fluctuations on this latter term rather than rainfall variability.

Moreover, the seasonal water balance (precipitation plus freshwater discharge minus evaporation) consistently showed average positive net freshwater inputs to the bay of  $26 \times 10^6 \text{ m}^3$  per month in the dry season and  $142 \times 10^6 \text{ m}^3$  per month in the rainy season, while a volume of  $802 \times 10^6 \text{ m}^3$  per month was estimated for the annual budget. Assuming a constant water volume in the system (either seasonally or annually), the water balance indicates a water outflow from Bahia de la Ascension to the adjacent shelf. Considering these calculations, the time it takes the total volume of the system to be renewed is much larger (on the order of 6 times higher) than that estimated utilizing the LOICZ methodology (Gordon et al. 1996), although the ratio between the water residence times computed for dry and rainy seasons are nearly the same. It is likely that the effect of the mixing flow (accounted in by  $V_x$  according to the LOICZ method) derived from the strong salinity gradients observed in Bahia de la Ascension might reduce substantially the renewal time in the system compared to the water budget approach based solely on direct precipitation, freshwater flux, and evaporation.

#### *Variability of the water level in the reef lagoon (RL) and inner bay*

Because the water level data series obtained during October 2007 corresponded to neap tides, and arguably this record might be altered by meteorological processes co-occurring during the October campaign with a characteristic frequency (e.g., diurnal breezes, sun irradiance-influenced air pressure), the analysis of tidal constituents was focused on the sea-level response across the bay only during the June field trip (Figs. 1.5 and 1.6). Tides observed in the reef lagoon are clearly semidiurnal, with the main semidiurnal  $M_2$  constituent accounting for 56% of the water level (number of observations = 538; percentage of variance predicted/variance original = 63.5%). Impingement on this constituent as the tidal progressive wave crosses the bay was less pronounced than the main diurnal constituent ( $K_1$ ), which lagged water height in the inner bay by  $70^\circ$  relative to the reef lagoon. The observational evidence further suggests that diurnal tides are relatively more attenuated within the bay than semidiurnal tides, as the  $K_1$  constituent in Vigia Grande embayment was reduced during the June sampling to only 36% of the level

recorded in the reef lagoon, while the  $M_2$  principal-lunar tide was slightly attenuated to 88% of its recorded amplitude in the adjacent shelf.

The dampening of the  $K_1$  diurnal frequency and in less extent of the  $M_2$  semidiurnal frequency in the bay's interior during June may be a consequence of dissipation of the energy as the tidal wave enters the shallow water column of the Vigia Grande embayment. The narrow channel flanked by a sandbar endpoint at the north and an E-W lying sediment bank at the south, connecting the central basin (mean depth = 2.3 m) with the Vigia Grande embayment (mean depth = 0.5 m) might contribute to the attenuation of the tidal energy within the Vigia Grande subsystem.

This claim was further confirmed using a barotropic hydrodynamic model forced both with spring tides in the seaward boundary and uniformly distributed southeasterlies along the model domain (Chapter II). The previous scenario resembled prevailing conditions during the dry season campaign (Figs. 1.5 and 1.7). According to the model results, the water level was reduced to 58% in the Vigia Grande embayment and lagged nearly 4 h relative to the water level in the reef lagoon. Although the attenuation on the simulated water level record seems to be in congruence and intermediate between the reduction exhibited on both diurnal and semidiurnal frequencies in the June data series, larger time series are needed to fully resolve diurnal and semidiurnal frequencies and investigate the tidal characteristics on the water level fluctuations in Bahia de la Ascension.

It is thought that the remnant sea level variability on the measured data series of dry season sampling might be a result of a variety of forcing mechanisms operating over a broad range of time scales, from high frequency to seasonal meteorological processes (i.e., wind stress, barometric pressure systems and freshwater supply). Thus, the evident water level setup recorded in Vigia Grande within a 5-day period during the June campaign (0.18 m) might be explained by wind-driven water movement across the surface of this embayment. The effect of the southeasterly wind dominating during this sampling campaign would be enhanced in a semi-enclosed body of water as the Vigia Grande subsystem, than along open spaces such as in the reef lagoon (Kitheka 1996). Indeed, an average increase in the water level of the bay's interior was further observed utilizing a 2D hydrodynamic model (Chapter II) forced with spring tides and southeasterlies, but this

setup was substantially lower (0.05 m) than the observed during dry season sampling. It is thought that low-frequency meteorologically-induced water level fluctuations in Bahia de la Ascension, along with the imbalances due to widespread submerged aquatic vegetation stands and low-relief mangrove wetlands outlining the shallow bay's interior may lead to strong asymmetries of the tidal currents and in turn to water level slopes (Kjerfve et al. 1991).

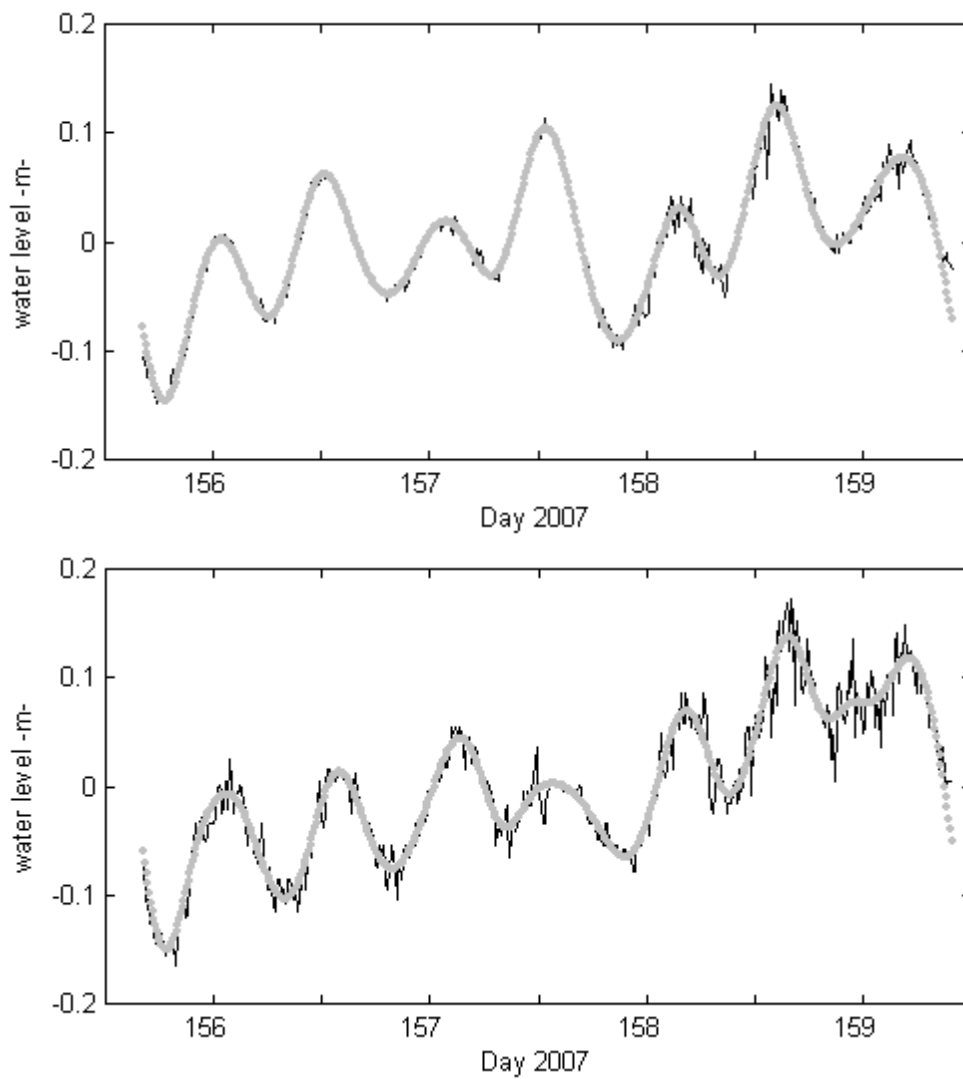


Figure 1.5. Measured (—) and 6-hr low-pass (.....) water level in Reef Lagoon (*upper*) and Vigia Grande (*lower*) during dry season (June 2007).

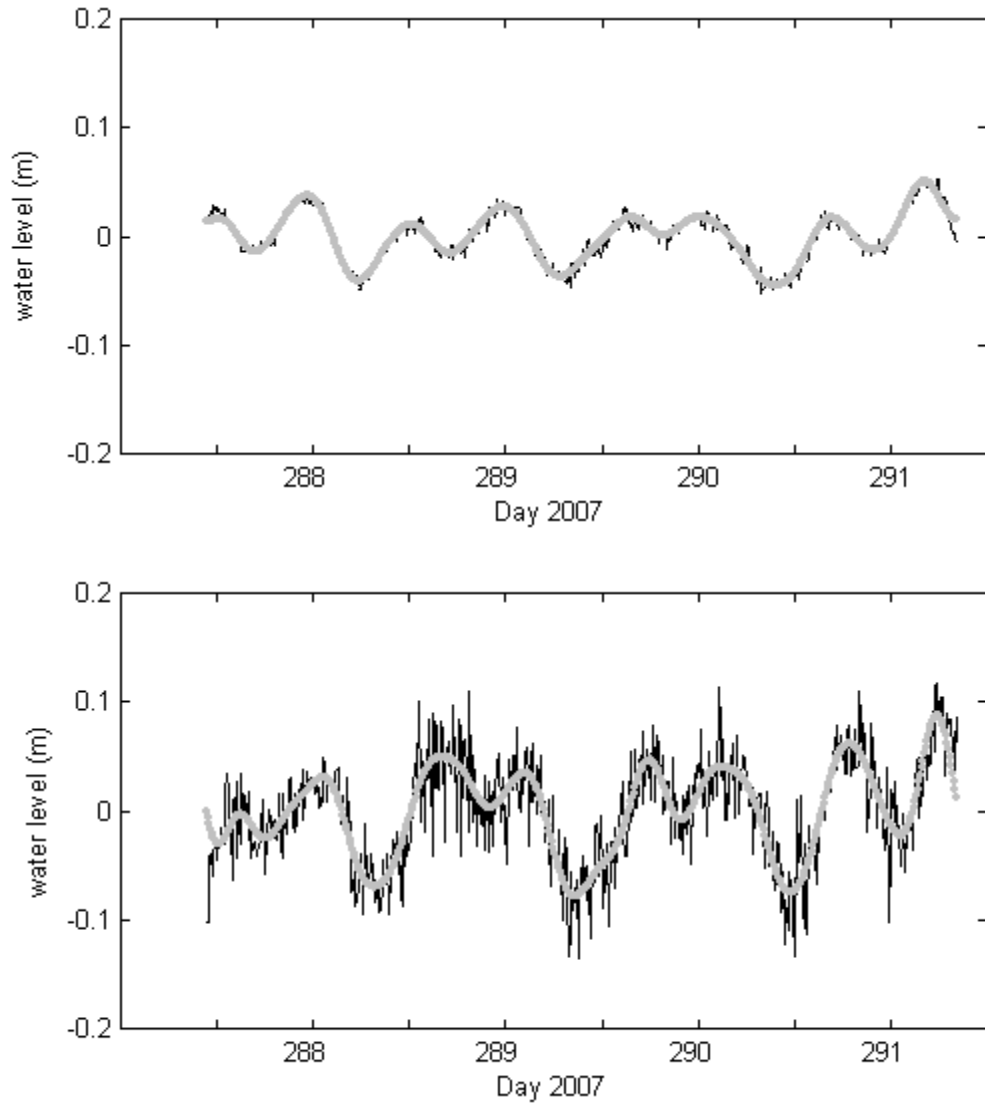


Figure 1.6. Measured (—) and 6-hr low-pass (.....) water level in Reef Lagoon (*upper*) and Vigia Grande (*lower*) during rainy season (October 2007).

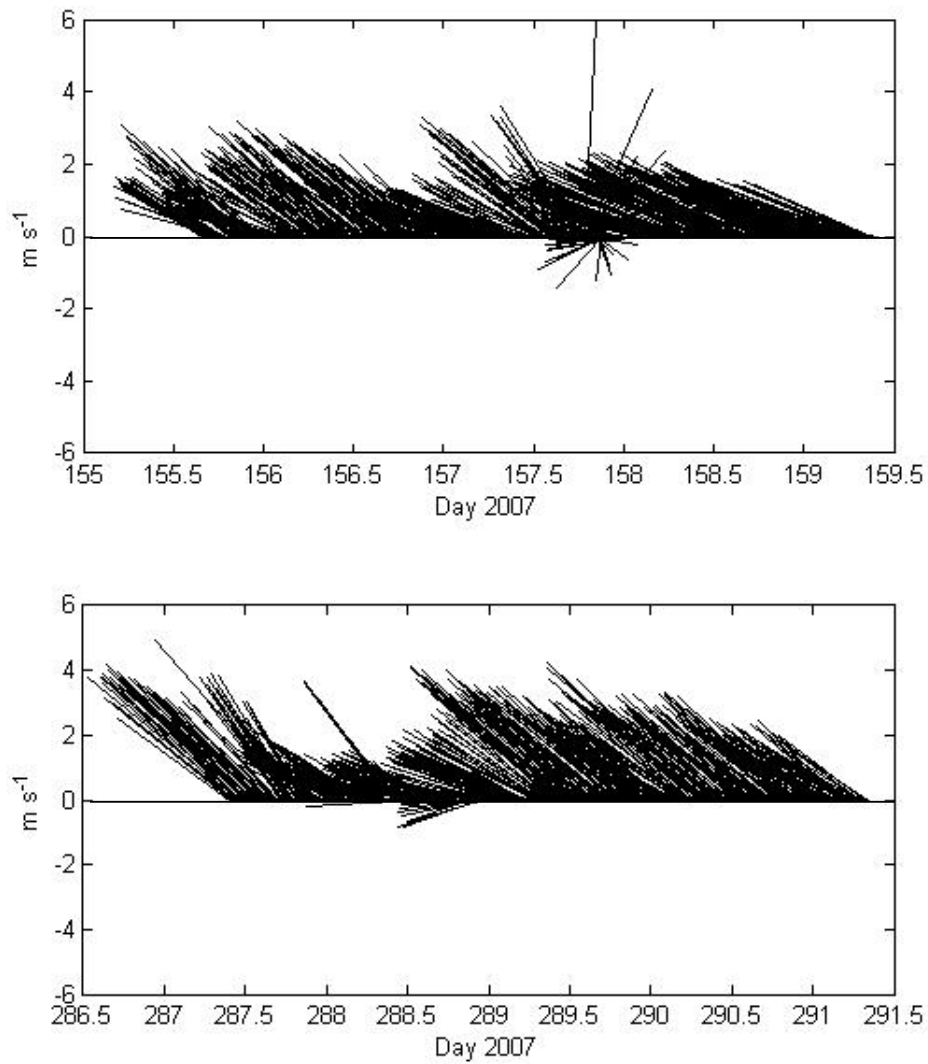


Figure 1.7. Winds in Ascension Bay during field trips: June 2007 (*upper panel*); October 2007 (*lower panel*).

### *Salinity spatial patterns*

Salinity across Bahia de la Ascension during the dry season varied from <1 to 35.7, with a mean of  $29.6 \pm 8.2$  (Table 1.5). The spatial distribution of salinity during this period exhibited lower values along the southwest portion of the system (i.e., Vigia Grande embayment) and higher salinities towards the marine front of the bay, with a remarkably strong horizontal salinity gradient at the inner bay—increasing from 16 to 30 within just 4 km to the east from Vigia Grande (Fig. 1.8). This estuarine salinity gradient in Bahia de la Ascension is associated with freshwater sources existing at the shallow southwestern side of the bay, where a number of marsh channels drain into the ecosystem (Fig. 1.2). The salinity variation during the rainy season ranged from 1 to 33.9, yielding an average salinity of  $22.4 \pm 8.9$ . Similar to the dry season, the spatial pattern during the rainfall sampling displayed a nearly normal gradient at the mouth of the bay (perpendicular to the ocean front; Fig. 1.8).

The ambient mesohaline prevailing during both seasonal samplings and the attenuated tidal influence suggested by the harmonic analysis indicates that such low-salinity conditions in Vigia Grande embayment are a perennial condition in the system throughout the year. Moreover, as previously explained the occurrence of interannual events as La Niña during 2007 has the potential to alter the water balance in this region and lead to atypical wetter dry seasons than usual, which may result in the similar spatial patterns of salinity recorded in both seasons (Fig. 1.8).

These findings indicate that the southwestern embayment Vigia Grande may represent a critical environment affecting the spatial pattern of salinity across the central basin. Thus, considering the limited tidal mixing across the channel connecting both subsystems, the occurrence of typical SE winds may modulate the extent to which freshwater discharged into this inner lagoon is either retained or propagated further into the bay.

Table 1.5.- Table showing the mean  $\pm$  SD, minimum, and maximum values of temperature and salinity during both samplings in two sites of Bahia de la Ascension (RL: reef lagoon and VG: Vigia Grande embayment).

Parameter	Dry season		Rainy season	
	RL	VG	RL	VG
Temperature (°C)	28.9 $\pm$ 0.24	29.1 $\pm$ 0.66	28.8 $\pm$ 0.29	28.7 $\pm$ 0.52
	28.5	27.9	27.9	27.2
	30.2	30.4	29.4	29.8
Salinity	--	16 $\pm$ 2.55	39.9 $\pm$ 0.45	12.3 $\pm$ 4
	--	10.5	37.9	3.9
	--	22.7	40.8	18

#### *CTD profile transects in the bay's ocean front cross-section*

Isotherms and isohalines were consistently vertical during the dry season, suggesting a completely mixed water column in the two inlets (north and south entrances) (Fig. 1.9). Yet, some differences were observed between the two openings, as mean temperature was higher at the north entrance ( $29.18 \pm 0.21$  °C) than in the shallower southern inlet ( $28.57 \pm 0.22$ °C). In contrast, a vertical structure was evident in the deepest channel corresponding to the northern entrance during rainy season (e.g., October sampling), featuring colder and fresher water overlying a slightly saltier and warmer water mass (Fig. 1.9). As expected, this condition was more sharply defined in the northern inlet, not only because it has a higher water column than the southern inlet, but also because it is placed proximate to the northern branch of the bay “La Ria” where a number of SGD vent into the system (personal observation). Water exchanges enhanced by ebb tides between this section and the northern portion of Bahia de la Ascension could control further flushing out of brackish water across the northern inlet. This condition is illustrated in the water residence times ( $\tau$ ) estimated for both seasons, with a substantially lower  $\tau$  during rainy season (65 d) than in dry period (256 d). Such a vertical pattern highlights the importance of baroclinic circulation processes in Bahia de la Ascension, given the microtidal regime and marked seasonal freshwater input experienced by this system (Tables 1.3 and 1.4).



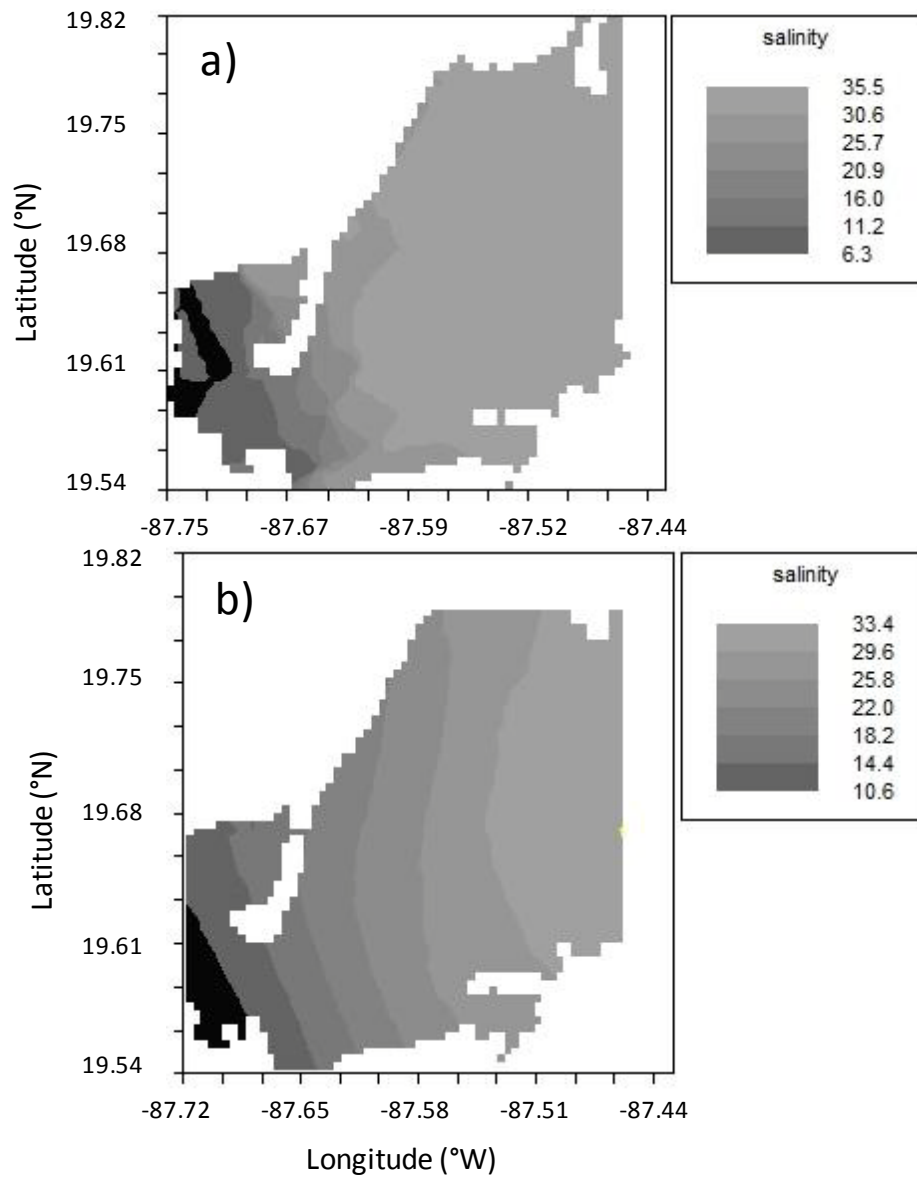


Figure 1.8. Spatial distribution of salinity during (*upper*) dry season sampling (June 2007) and (*lower*) rainy season sampling (October 2007).

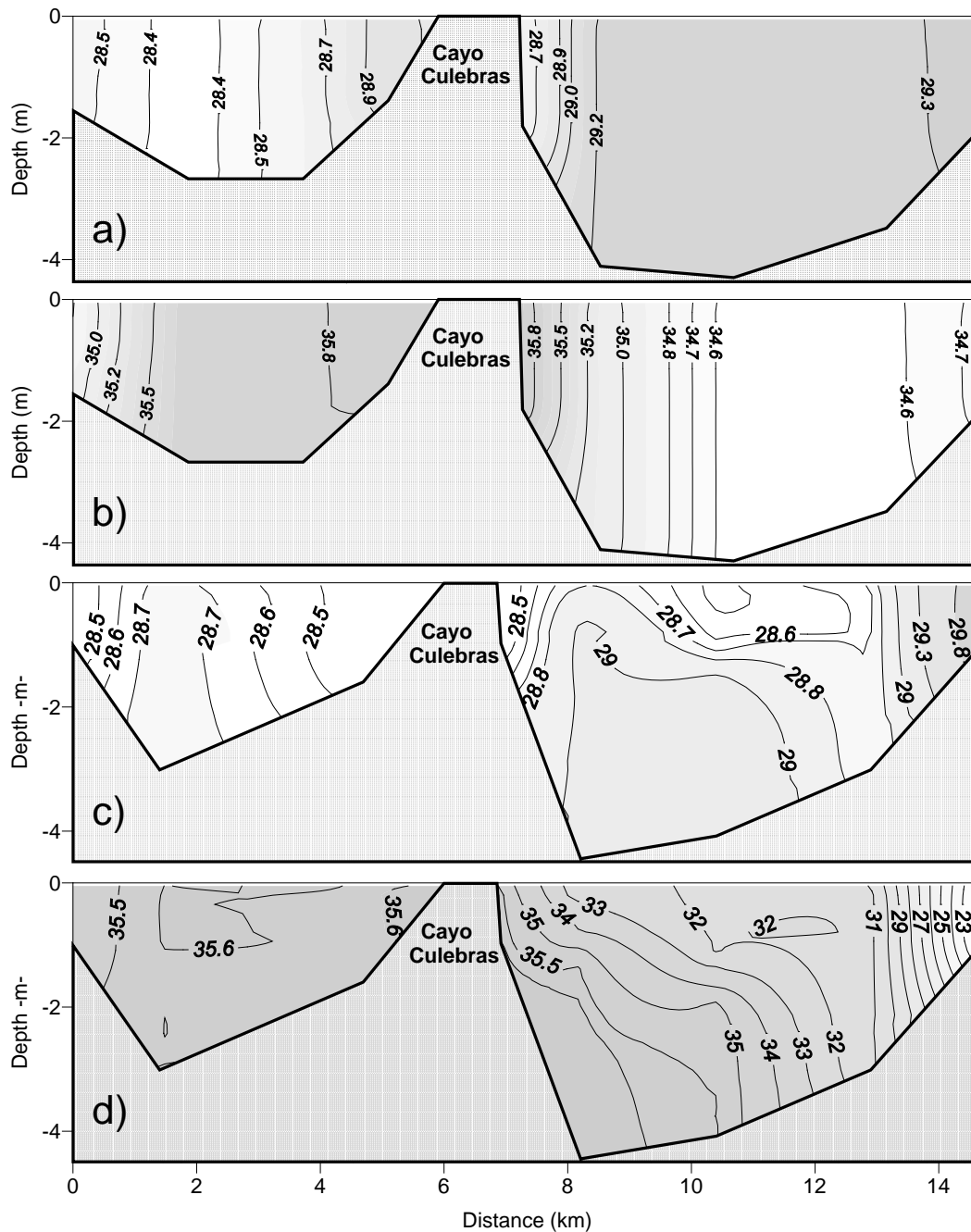


Figure 1.9. Temperature ( $^{\circ}\text{C}$ ) and salinity CTD profiles in the bay's inlets cross-sections during dry season (a, temperature; b, salinity) and rainy season (c, temperature; d, salinity).

### *Current time series*

Current oscillations in the reef lagoon depicted distinct variability patterns between both sampling campaigns. A more organized current pattern was observed in June, showing both stronger currents than in October and a marked change of current direction, roughly every 12 h (Fig. 1.10). This time-dependent behavior during the dry season may be a result of tide modulation throughout the period of the sampling campaign, as water elevation was greater during this field trip (range = 0.27m) than in October (range = 0.10m). The tidal influence during dry season not only defined more abrupt water level fluctuations and marked changes in current directions with a periodicity nearly that of the semidiurnal tide (Fig. 1.10), but it also partially explains the lack of vertical structure in the water column during this period (Fig. 1.9).

The distinct water current conditions characterizing both seasons might be a result of a stronger influence of tides in the dry season campaign carried out under spring tide versus a more prominent role of southeasterly winds during rainy season campaign undertaken during neap tides. Such differences are illustrated by the average current velocities corresponding to both samplings, which were substantially smaller ( $0.09 \text{ m s}^{-1}$ ) in the October than those of June ( $0.11 \text{ m s}^{-1}$ ). Also, strong peak ebb and northward currents established a  $\approx 0.40 \text{ m s}^{-1}$  NE instantaneous current in June, while in October during flood tide, a southward flow yielded a  $0.31 \text{ m s}^{-1}$  SW-trending instantaneous current. Despite the relatively slow currents measured in the rainy season, the significant freshwater input established a net outflow from the bay, which accounted for the shortest water residence time in this period (65 d).

These results strengthen the idea that Bahia de la Ascension is a heterogeneous ecosystem in both space and time. The influence on instantaneous flow by tides is limited to the inlets zone, with a dominant performance of wind stress and freshwater supply within the bay, particularly during neap tides. Furthermore, it is evident that the southwestern and southernmost sections of BA embody a transition zone between the marine influenced central basin and the wetland freshwater draining into the ecosystem, constituting a fundamental subsystem in the functioning of Bahia de la Ascension as the primary receiver of freshwater from neighboring mangrove wetlands. It is defined as an

environment of intensive mixing and intricate hydrodynamics which restricted circulation controls the propagation of brackish water mass farther into the main bay.

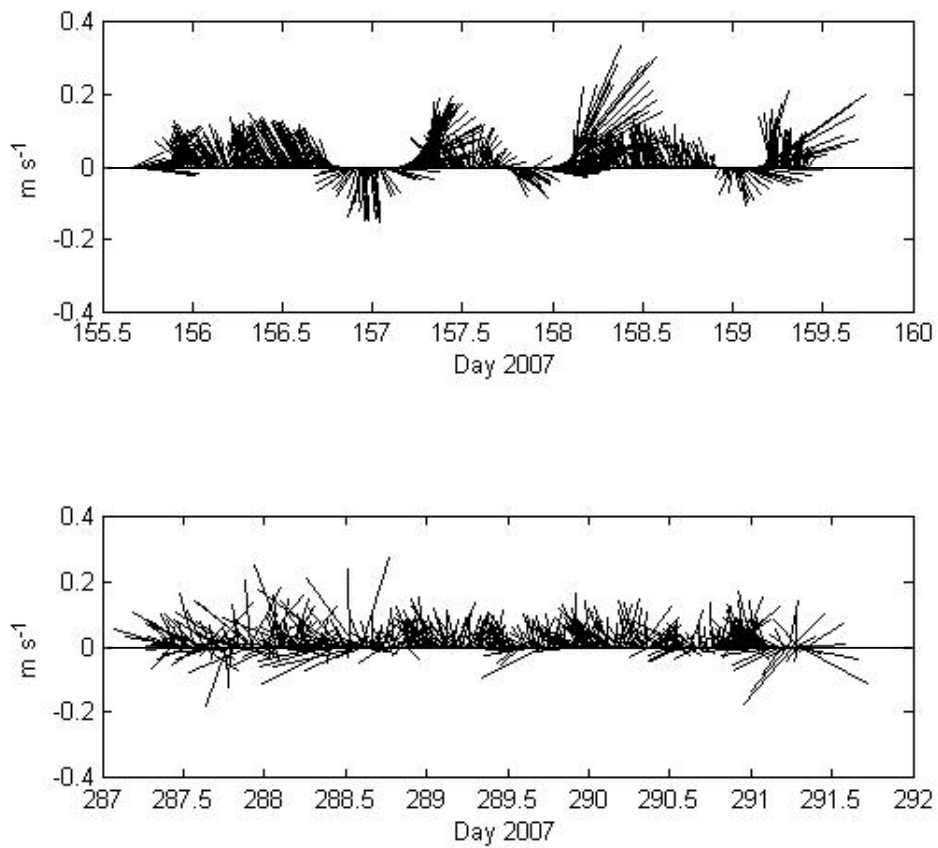


Figure 1.10.- Current velocities in the Reef Lagoon during dry season (*upper panel*) and rainy season (*lower panel*).

## Conclusions

Bahia de la Ascension is a shallow coastal lagoon characterized by strong SW-NE salinity gradients defined by freshwater supply from combined runoff and submerged groundwater discharges in the inner bay and strong tidal influence in the bay's central basin favored by the open seaward front.

The tidal energy is selectively attenuated in the interior of Bahia de la Ascension as diurnal frequencies are more readily filtered out than semidiurnal frequencies. Thus, water level setup observed in the bay's interior during the June sampling may be associated with other subtidal and wind-driven forcing functions.

The combined runoff and groundwater freshwater discharge into Bahia de la Ascension have larger fluctuations than direct rainfall into the system and thus have a greater potential to alter the seasonal salinity variations within the bay. However, the occurrence of strong intra-annual (e.g., hurricanes) or interannual events (e.g., ENSO, La Niña) influencing direct rainfall in the region may lead to substantial changes in the salinity spatial gradients within the bay. Moreover, a vertical density structure in the water column of the inlet zone was only evident in the rainy season, when rainfall peaks during the year (October).

## CHAPTER II

### MODELING OF HYDRODYNAMIC VARIABILITY IN A COASTAL BAY, YUCATAN, MEXICO

#### Introduction

The dynamic interplay among physical processes is of primary importance on the ecological integrity and overall health condition of aquatic ecosystems in the coastal environment (Nixon 1988; Wolanski 1994; Valiela 1995; Umgiesser and Neves 2005). The hydrodynamic setting defines the fluctuating nature of coastal systems as it modulates the rate and magnitude of key processes, such as salt and nutrient fluxes, relevant in the variability of water quality and productivity dynamics (Lee et al. 1992; Leichter et al. 2003; Hench et al. 2008).

The energy supplied by tides to a large extent controls the mixing and transport of materials in coastal ecosystems. This energy input represents a salient influence, even for restricted lagoons that are subjected to low tidal range, where it may account for up to 70% of the water level variability, driving a substantial advective water transport to the adjacent shelf (David and Kjerfve 1998). Nevertheless, tidally-driven effects might be confined to the inlet zone of these ecosystems, and be strongly dependent upon bathymetry, local geography (e.g., width of the offshore shelf; Redfield 1955), number of inlets, dimensions of the entrances, and channel width. Indeed, the open-boundaries condition of the coastal lagoons not only regulates the extent of exchange with sea, but it also exerts a main control over the coastal lagoon's functioning (Kjerfve 1986).

When the tidal range is small, long-term (in the order of months; e.g., seasonal) and short-term (in the order of hours; e.g., winds plus heat balances) meteorological forcing may have a greater influence on the coastal environment than tides (Smith 1977; Wong and Wilson 1984; Wong and DiLorenzo 1988). This non-tidal forcing can induce sea level oscillations with a period greater than a few days in the interior of coastal lagoons, altering the net transport trends. Additionally, the balance between freshwater influx and saltwater

incoming from the adjacent shelf may force gravitational circulation in estuaries and coastal lagoons. This circulation is responsible for the exchange of dissolved and particulate materials, as well as dispersion of biota, across the seaward boundary (Sheng et al. 1996; Brown et al. 2004; Cowen et al. 2006).

Because oceanographic phenomena constitute a major component of hydrological fluctuations in coastal ecosystems, and have profound implications on their dynamics and function, a proper grasp of the hydrodynamic mechanisms is essential to understanding the linkage between the physical process and the ecology of Bahia de la Ascension (BA), a shallow coastal bay in the Mexican Caribbean. Thus, the overall objective of this study is to assess the dynamic responses of water level, water discharge across inlets, and circulation patterns of BA due to the tides and winds. It is hypothesized that, given the microtidal regime of this region, winds should exert a more dominant effect on circulation than tides alone.

### **Study Site**

Bahia de la Ascension (BA) is located within the Sian Ka'an Biosphere reserve (19° 40' 32.76" N; 87° 32' 30.87" W) on the east coast of the Yucatan Peninsula, in the Mexican Caribbean. It is a shallow ecosystem, with an average depth of 2.3 m and a maximum depth of 6.8 m at the north inlet (Fig 2.1). The surface area of the bay is 580 km<sup>2</sup> and its total mean water volume is 1,330 x 10<sup>6</sup> m<sup>3</sup>. The tidal characteristics of this region are defined as a mixed, semi-diurnal, microtidal regime, dominated by the principal lunar M<sub>2</sub> component of 0.074 m (Kjerfve 1981). The tidal range is <0.20 m within the bay, which experiences a tidal prism of 105 x 10<sup>6</sup> m<sup>3</sup> per semidiurnal cycle. BA receives significant freshwater input (357 x 10<sup>6</sup> m<sup>3</sup> yr<sup>-1</sup>) through both diffuse and point sources draining from a 1,200 km<sup>2</sup> hydrological basin (computed according to the Schreiber model; Medeiros and Kjerfve 1993). The estimated water residence time in this system during dry and rainy seasons, respectively, is 256 days and 65 days (computed according to the LOICZ methodology; Gordon et al. 1996). The ratio of groundwater input to tidal prism in BA is nearly 1% in the rainy seasons and only 0.07% in dry seasons (Chapter I).

For a more extended explanation of methods and discussion of results regarding the water balance in Bahia de la Ascension see Chapter I.

## **Materials and Methods**

The spatial variability of water level and currents in Bahia de la Ascension, the estimation of net water discharges across boundaries, and an assessment of the time-averaged flow under tidal forcing and different wind conditions scenarios were addressed using a barotropic (2D) hydrodynamic model.

### *Model setup*

A depth-averaged, free-surface hydrodynamic model was implemented using the Delft 3D system (WL-Delft hydraulics) in 2D mode. The model simulates non-steady flow resulting from tidal and meteorological forcing. The space in the model domain was partitioned using a Cartesian, curvilinear, adaptive grid-cell arrangement with 23,200 nodes and  $\Delta x$  varying from 100 m inside the bay (the site of interest), to a coarser horizontal resolution  $\approx 1,000$  m on the shelf (Fig 2.2). To avoid potential boundary effects, a weakly-reflective open boundary was positioned 15 km seaward from the reef barrier (distance was defined according to the availability of bathymetric data in this region).

### *Sensitivity tests*

Before the hydrodynamic model could be used to study the circulation of Bahia de la Ascension, sensitivity tests were conducted to assess the stability of the model under constant conditions and varying model parameters. The tests included: (i) sensitivity to time step and (ii) conservation of water volume, along with defining a suitable grid resolution to solve relevant oscillations (Courant number). These tests provide objective means by which the model's performance can be judged. Moreover, accurate calibration of the model was needed to verify its capacity to reproduce observations. The model was found to be robust. Information concerning the forcing functions, simulation time, and other relevant aspects of distinct model runs (e.g., period of time removed from start up until steady state) is presented in Table 2.1.



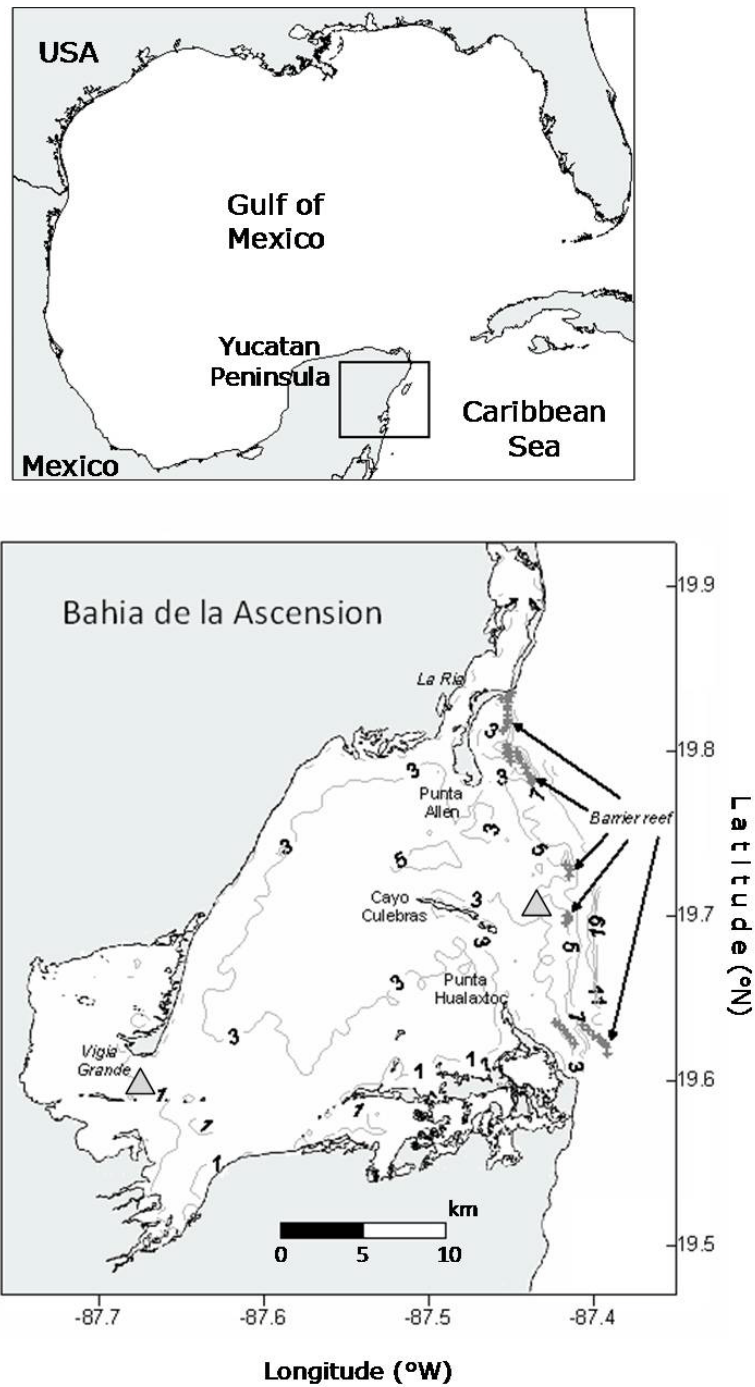


Figure 2.1. Map of the Gulf of Mexico and Bahía de la Ascension in the Western Caribbean. Isobaths are given in meters. Grey triangles represent moored instruments during 2007 field campaigns (current profiler and CTD in the reef lagoon and CTD at the inner bay).

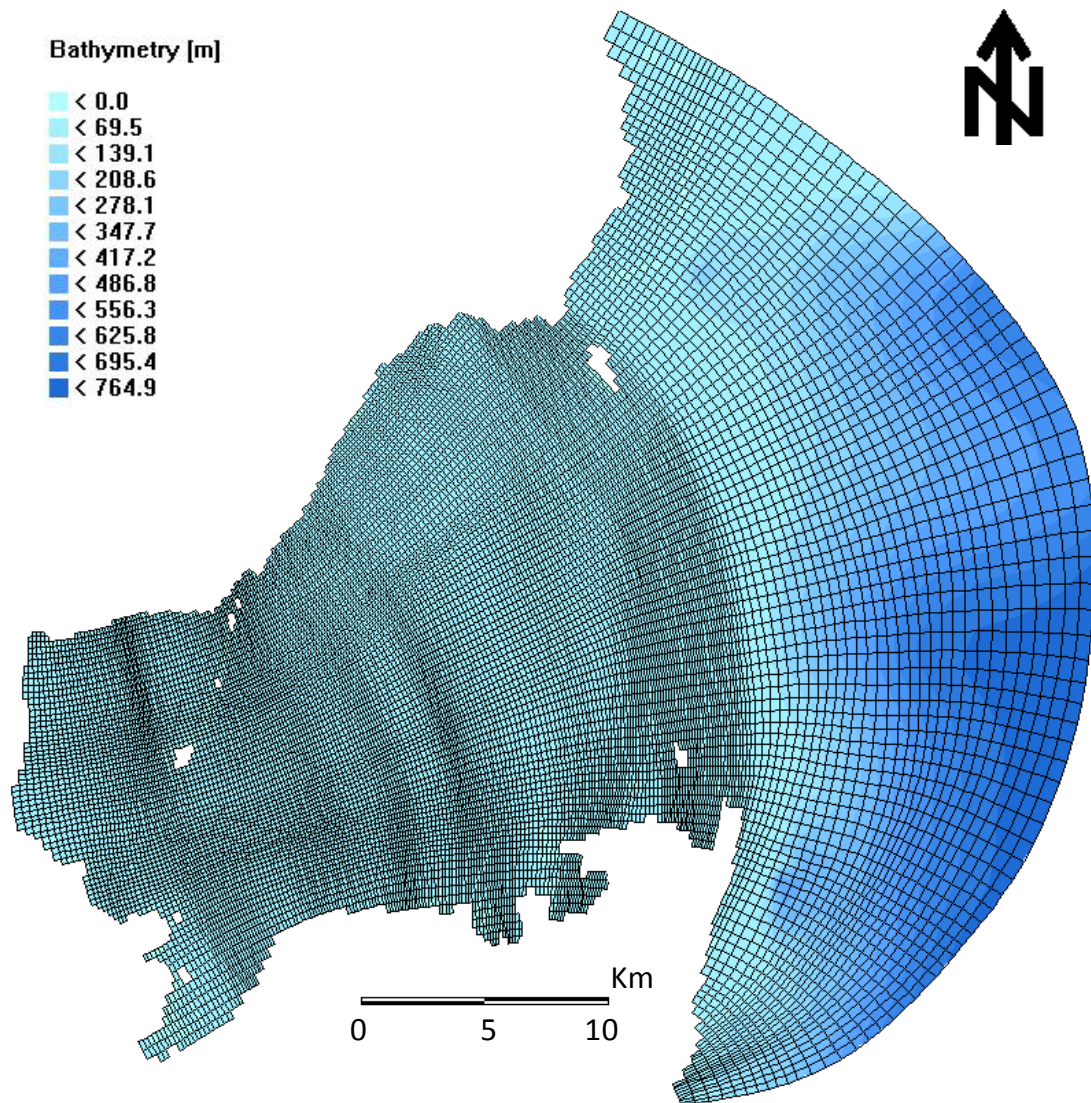


Figure 2.2. Adaptive grid of the model domain.

Table 2.1. The simulations run on the hydrodynamic model including forcing functions and simulation times utilized on the distinct cases. Eight-day long simulations were used for the wind forcing simulations because “Nortes” are characteristically short-lived episodes in the Yucatan Peninsula.

	Cases	Forcing function	Simulation time (days)	Observations
Stability tests	Kinetic energy	$M_2$ tide	10	Three $\Delta t$ 's tested: 1, 3, and 9 min
	Volume conservation	$M_2$ tide	30	Experiment carried out with $\Delta t= 3$ min
Reliability tests	Calibration and Validation	Observations of surface elevation	4	Time series collected in the reef lagoon for calibration; validation using data series recorded in the bay's interior
Hydrodynamic simulations	Tides and winds	Spring tide ( <b>ST</b> )	8	Spring tides plus real winds. Data uniformly distributed across the domain
		ST + northeasterlies		
		ST + southeast wind		
		ST + “Nortes” (N-NW)		

(i) *Sensitivity to time step*

The existence of unrealistic velocity oscillations due to numerical instabilities in the model was assessed by tracking the evolution over time of the system's kinetic energy ( $E_k$ ) (Enríquez et al. 2010). The total kinetic energy of the bay was calculated as

$$E_k = \iint \frac{1}{2} \rho (u^2 + v^2) dx dy$$

where  $\rho$  is density, and  $u$  and  $v$  are east-west (x-axis) and north-south (y-axis) velocities, respectively. Given constant forcing conditions (i.e.,  $M_2$  tidal component),  $E_k$  should increase to a certain level and stabilize; otherwise, uncontrolled velocity fluctuations building up over time will lead the model to break down. Such anomalous behavior in the simulations will be detected by  $E_k$ .

The sensitivity to time step test finds the most efficient  $\Delta t$  among three distinct values (1 minute, 3 minutes, and 9 minutes).  $E_k$  achieved stability after two semi-diurnal cycles (24 h from startup) for the three time-steps evaluated, with an average  $E_k$  of  $6.25 \times 10^5$  joules accumulated throughout the system (Fig. 2.3). Thus, the model is stable under conditions used in this study. Although  $\Delta t = 9$  minutes exhibited larger  $E_k$  during the whole simulation than  $\Delta t = 1$  min and  $\Delta t = 3$  min, the three distinct time-steps demonstrated minimum differences among each other (Fig. 2.3). However, due to comparatively higher computational requirements when using a  $\Delta t = 1$  and failure on the Courant number criteria (i.e.  $>10$ ) for  $\Delta t = 9$ , the  $\Delta t = 3$  minutes was chosen for the simulations. This latter time-step represented the option meeting both accuracy in reproducing important spatial length scales and stability for the current barotropic model (WL-Delft hydraulics).

(ii) *Water volume conservation test*

The water volume conservation test was implemented to ensure that the model neither accumulated water nor lost water in the system such that it would eventually dry out after successive simulations (i.e., volume needed to be conserved). For this purpose, the total time integral of fluxes through the bay-shelf boundary at both inlets was evaluated. This integral needed to be close to zero after a long simulation. Considering the results of the *sensitivity to time step* assessment, fluxes across the boundary were computed beginning with the 3<sup>rd</sup> tidal cycle to avoid potential start up instabilities. Since fluxes across the bay-

shelf boundary approached a zero value over the 30-day simulation, and the water exported to the nearshore constituted only 0.002% of the 1% tidal prism estimated for Bahia de la Ascension, it was concluded that the model is volume-conservative (Figure 2.4).

#### *Model calibration and validation*

The model was calibrated by adjusting the bottom friction coefficient until reaching a water level close to that observed in the inner bay during dry season sampling (June). For this stage, the model was forced in the open boundary with the 89.5-hour-long water level time-series collected using a CTD (Diver; Van Essen Instruments) in the reef lagoon during the same dry season campaign. This data series was first high-pass filtered using a Discrete Fourier Transform filter to keep only those frequencies above 0.5 cpd (e.g., diurnal, semidiurnal). Further calibration was limited to tuning the bottom roughness formulation: two different Manning roughness coefficients of  $n = 0.04$  and  $0.07$  (independent of units), and a Chezy coefficient (default in Delft) of  $C = 40 \text{ m}^{1/2} \text{ s}^{-1}$  were applied in distinct model runs (Figure 2.5). These roughness values are within those reported for macrophyte-dominated habitats (e.g., 0.03-0.30; Dawson and Robinson 1984) and utilized in studies to parameterize the bottom friction in shallow ecosystems colonized by aquatic vegetation (e.g., 0.02-0.20; Morin et al. 2000).

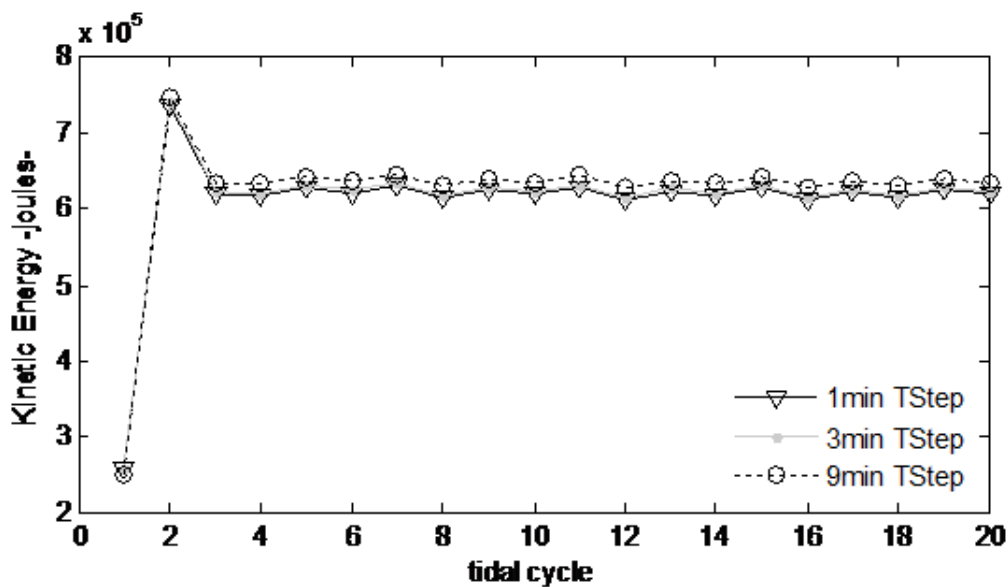


Figure 2.3. Kinetic energy ( $E_K$ ) calculated every  $\Delta t$  at individual nodes and presented as the integral (accumulated) for the whole system at every semidiurnal cycle. Three time-steps:  $\Delta t=9$  minutes,  $\Delta t=3$  minutes, and  $\Delta t=1$  minutes, were tested for a 10-day simulation.

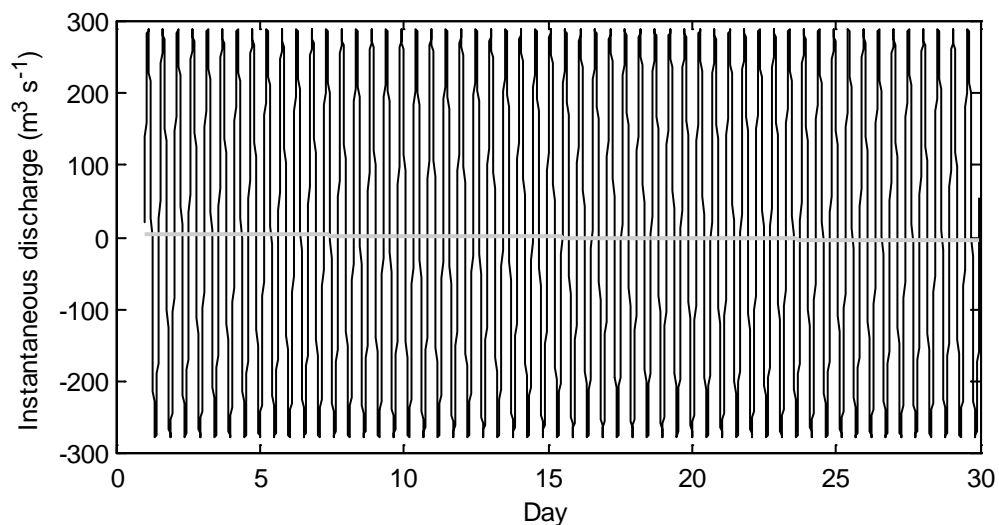


Figure 2.4. Modeled water discharge (black line) across the bay-shelf boundary in the water volume conservation test. The signal was low-pass filtered using a running-average with window size equal to the semidiurnal tidal cycle. A regression line (grey line) was fitted to the filtered discharges by the least-squares method to quantify the potential trend of the oscillations.

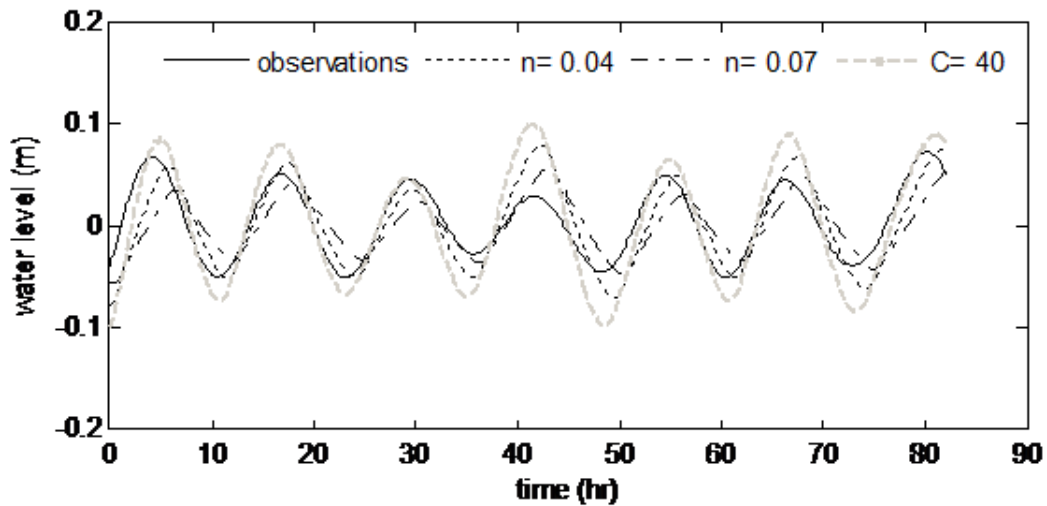


Figure 2.5. Water level series at the Vigia Grande (VG) mooring. Observations compared with simulated data obtained through different bottom roughness coefficients.

The model's capability to reproduce the surface elevation behavior in Bahia de la Ascension was determined by comparing the observed and the modeled water level (Fig. 2.5). A 4-day water level time-series recorded (CTD Diver) at the inner zone of the bay (Vigia Grande embayment) during June 2007 was used (Fig. 2.6). The agreement between modeled and measured water level was quantified utilizing the root-mean square (RMS) and the relative mean absolute error (RMAE), both statistics widely used to evaluate accuracy of numerical models (Fernandes et al. 2001; Walstra et al. 2001; Sousa and Dias 2007). The smallest difference between the water level observed and that predicted by the model at the inner bay corresponded to a Manning coefficient equal to 0.04, yielding a Relative Mean Absolute Error  $\approx 0.15$  (Table 2.2). According to the error categorization provided by Sutherland et al. (2004), RMAE values lower than 0.2 are qualified as an excellent match between predictions and observations.

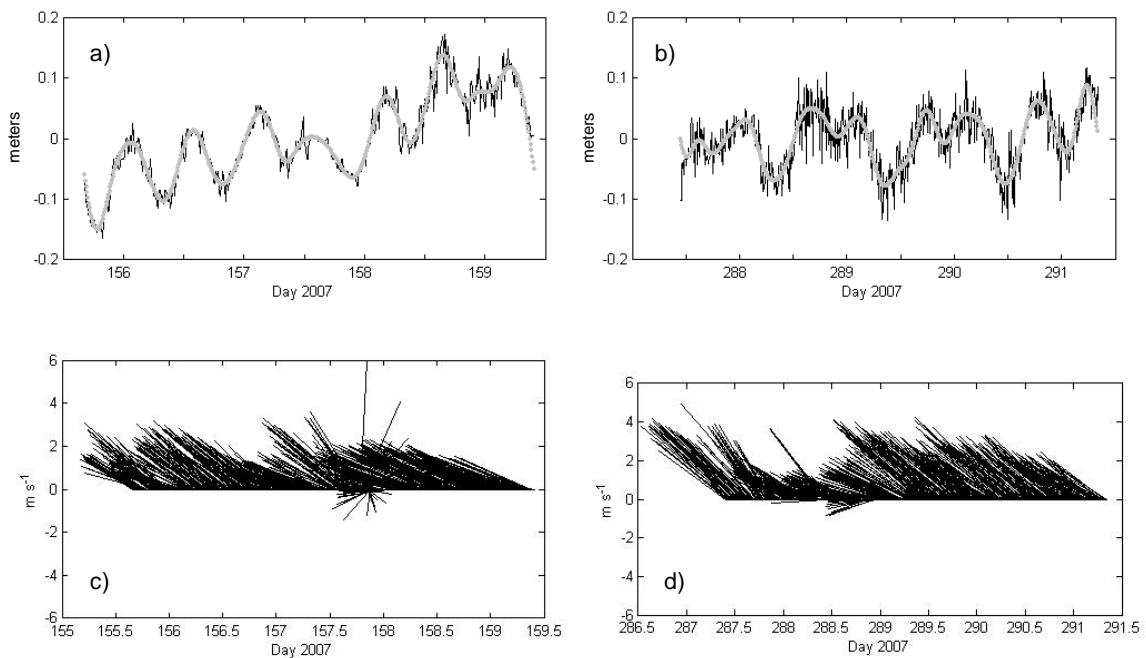


Figure 2.6. Water level (measured — and 6-hr low-pass ••••) and wind velocity time series in Vigia Grande during dry season sampling (a and c) and rainy season sampling (b and d). High frequency oscillations were eliminated from the raw water-level data by using a discrete Fourier transform filter.

Table 2.2. The summary of statistics of the model performance. RMS = Root Mean Square; RMAE = Relative Mean Absolute Error (a value  $<0.2$  corresponds to an excellent agreement; Sutherland et al. 2004).

Bottom friction formulae	RMS	RMAE
Chezy, $C= 40 \text{ m}^{1/2} \text{ s}^{-1}$	0.0416	0.6164
Manning, $n= 0.04$	0.0387	0.1486
Manning, $n= 0.07$	0.0401	0.2440



### *Hydrodynamic simulations*

The model was forced at the seaward boundary with a water level time series reconstructed from local tidal constituents reported for Cozumel Island, located 60 km north of BA (Kjerfve 1981). Besides the tidally forced case, a series of simulations comprising tides plus distinct typical wind conditions in the region were carried out:

1. Northeasterlies (Trade winds)
2. Southeasterly winds
3. Northwest-North winds (*Nortes*)

The three wind events were simulated using real, time-varying data (Fig. 2.7) (collected with a 10-minute frequency by a Vaisala automatic weather station 35 km from the study site) rather than prescribing artificial, steady winds. This was done to elucidate the ecosystem's hydrodynamic response to the most prevalent local wind scenarios under real conditions as much as possible. It has been recognized that using unidirectional/constant velocity wind data sets may over value the wind stress influence on water circulation, whilst time-varying responses of semi-enclosed ecosystems hydrodynamics to short-term processes (e.g., seiches) might be over looked (Staneva and Stanev 1998; Enríquez et al. 2010).

Wind events were selected by ensuring that the distinct data series included both a minimum direction persistence over an 8-day period and relatively high velocities according to the mean values reported for this zone (Chapter I). This duration defined for the simulations is tied to the characteristic duration of *Nortes* (i.e., winds from the N and NW associated with polar high-pressure fronts featuring low air temperature), which is limited to a few days in the Yucatan Peninsula. It is thought that by keeping a standard simulation time, the comparison of model results obtained along distinct cases would be more duly accomplished. Finally, the spring and neap tidal cycles were centered at the midpoint of each of the 8-day simulations run. As previously mentioned, tides were obtained from local tidal constituents according to Kjerfve (1981). The scenarios modeled are summarized in Table 2.1.

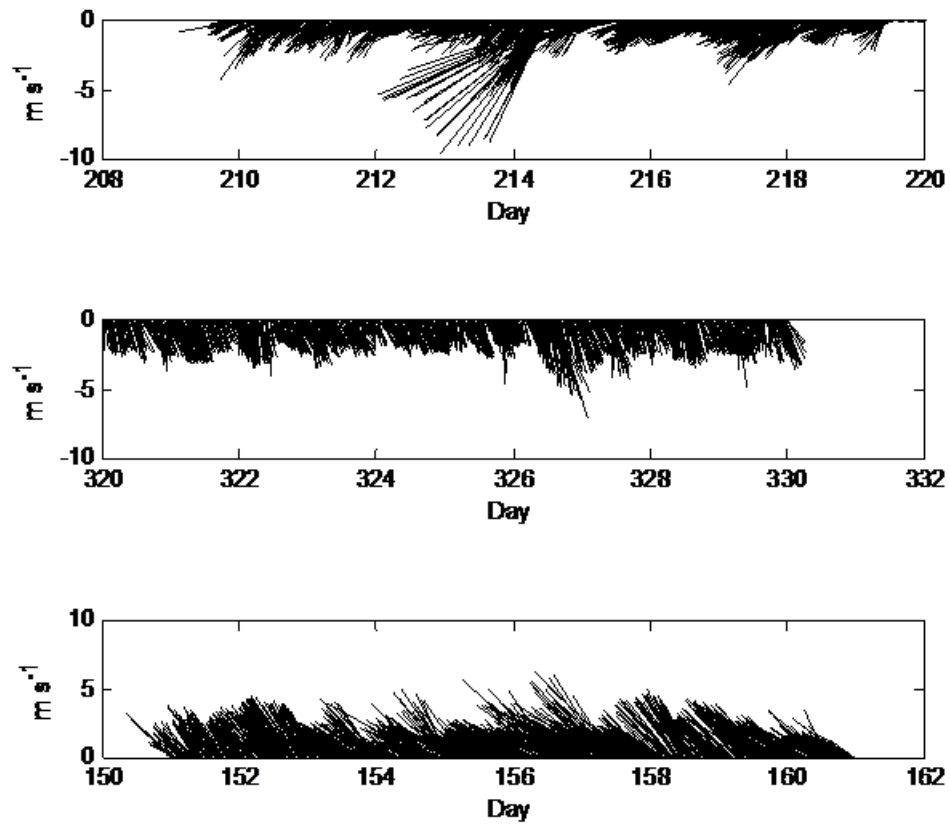


Figure 2.7.- Three wind events occurring in 2007 and utilized in combination with tides to force the hydrodynamic model: Trades (top); north winds (middle); and southeast winds (bottom).

## Results and Discussion

### *Net water volume discharge*

When the model was forced with tides only, the results indicated the net water discharge (defined here as water exported from the bay is positive discharge, whilst negative discharge is water inflow to the bay), estimated over 14 semidiurnal cycles (i.e., first day removed from the 8-day simulation run for stability reasons), was negligible both for spring ( $25,180 \text{ m}^3$ ) and neap tides ( $725 \text{ m}^3$ ) compared with the tidal prism ( $105 \times 10^6 \text{ m}^3$ ). The average water displacement during spring tides yielded a net inflow to the bay, while a residual outflow to the sea was estimated during neap tides. The force of winds only added to this pattern, with a maximum bay-directed net discharge observed among the wind scenarios, where southeasterly winds drove the peak net inflow of  $-29,909 \text{ m}^3$ , followed by the Trades with a discharge of  $-27,098 \text{ m}^3$ .

Following a  $9.8 \text{ m s}^{-1}$  wind gust (Fig. 2.7, upper panel), an exceptionally high water discharge was seen within a single tidal cycle during the Trades scenario (Fig. 2.8). The behavior of this event in time scale (i.e., period similar to tidal) suggests the water elevation difference and subsequent peak discharge may be a wind-induced seiche (which is abruptly damped) occurring in the bay (Mortimer 1953). Although the contribution of such an event was lessened in the average flow (i.e., net water discharge), the implications for nutrients and oxygen exchange between the bay and adjacent sea might be relevant to the metabolism of the whole system (Reynolds-Fleming and Luettich 2004). Thus, it is necessary to determine whether this salient process is a real seiche within Bahia de la Ascension, and to assess both the extent of its vertical amplitude and the associated lateral transport. Moreover, north wind forcing (i.e., “*Nortes*”) had only a marginal influence on the net discharge, as the water volume imported into the bay was nearly the same amount displaced by the tide only scenario (Fig. 2.8).

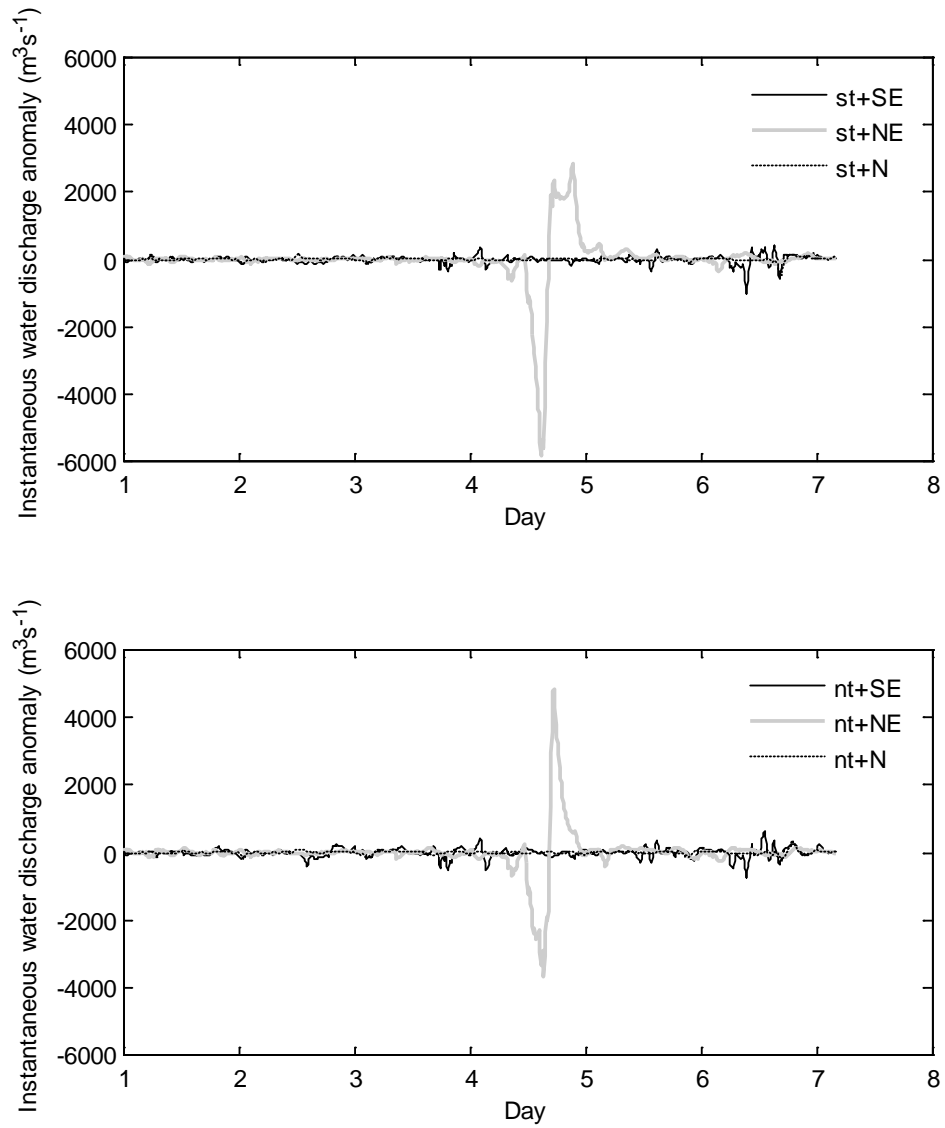


Figure 2.8. Instantaneous water discharge anomaly (tides plus wind forcing minus the tides base case) across the bay-shelf boundary. Upper panel corresponds to spring tides (st) and lower panel is neap tides (nt) plus wind events: southeasterlies (SE); Trades (NE); and north winds (N).

### *Instantaneous currents*

The instantaneous currents observed when water motion within BA is forced only by the tidal input showed that the ebb-tide does not generate a seaward water motion as expected. This was due to a phase shift between the water level time series utilized to force the model in the opened seaward boundary (15 km from the reef lagoon) and the water level response into the bay. Yet, bay-directed currents across the north entrance were still evident during ebb-tide, as well as in the inner-most bay, where large water level differences between the central basin and the bay's interior ( $\approx 8$  cm) favored water moving into the Vigia Grande embayment during this tidal phase (Figure 2.9a). During flood tide, the main currents in the inlets zone also indicated a water inflow to the bay, particularly across the southern entrance. However, current velocities rapidly decelerated once they reached the central basin (Figure 2.9c).

When southeasterly winds were added to the model, a similar current pattern (e.g., magnitude and direction) as that for tides alone was found (Fig. 2.9a). The phase shift in the Vigia Grande embayment (average depth of 0.5 m) of the bay's interior may be a consequence of tidal attenuation due to friction when the progressive tidal wave enters shallow water (Fig. 2.10). The circulation under Trade winds plus spring tides case showed that wind-driven water moving against the bay boundary caused an increase in the water level (i.e., setup) within the VG embayment ( $\approx 10$  cm) during flood tide (Fig. 2.11d). This water level slope induced by Trades is still lower than that recorded in the inner bay (18 cm) during 5 days of persistent southeasterly winds (e.g., please see *Variability of the water level in the reef lagoon (RL) and inner bay* in the Results and Discussion section of Chapter I). The barotropic field associated with this scenario might reduce water transport from the main bay into VG during episodes of persistent easterlies, unless a return flow mechanism through the bottom layer is established to maintain the water exchange with the central basin (Kjerfve 1994).

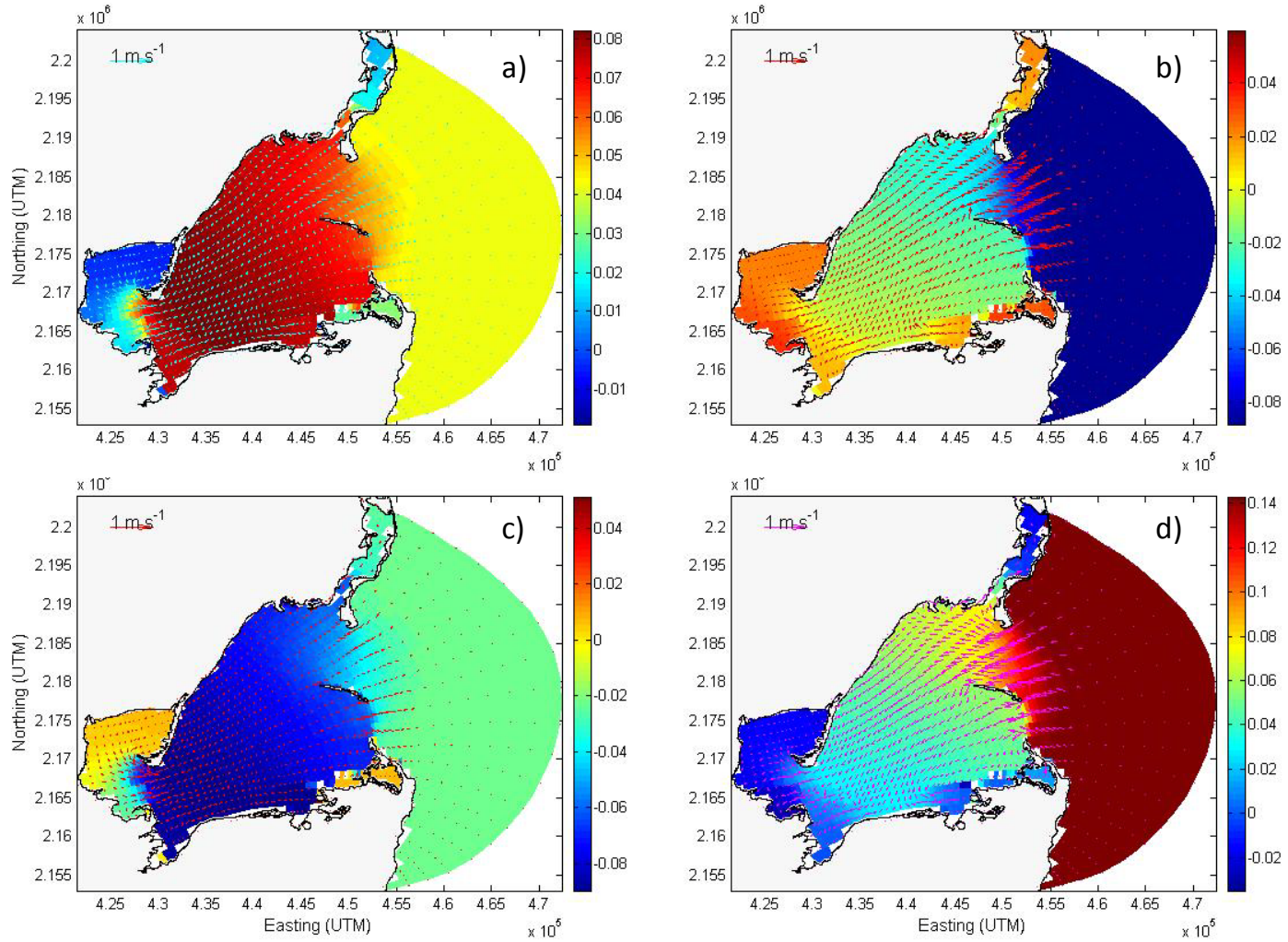


Figure 2.9. Instantaneous water-level (m) and currents ( $\text{m s}^{-1}$ ) when the model is forced with only tides during four instantaneous tidal phases: a) ebb; b) low; c) flood; and d) high.

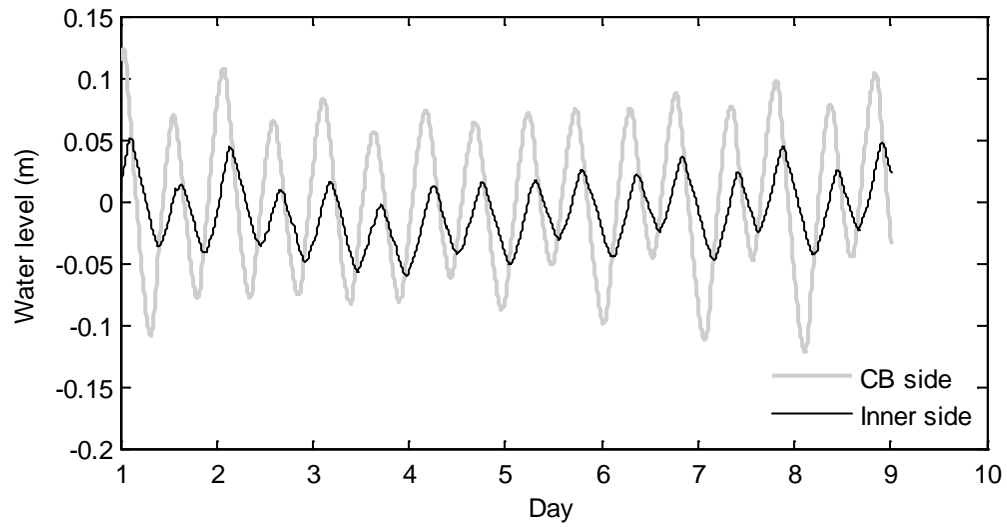


Figure 2.10. Modeled water level obtained in both the inner (Inner) and outer (CB) portions of the channel connecting Vigia Grande embayment with the bay's central basin under the spring tides plus southeast winds scenario (comparable to the condition observed during the June sampling).

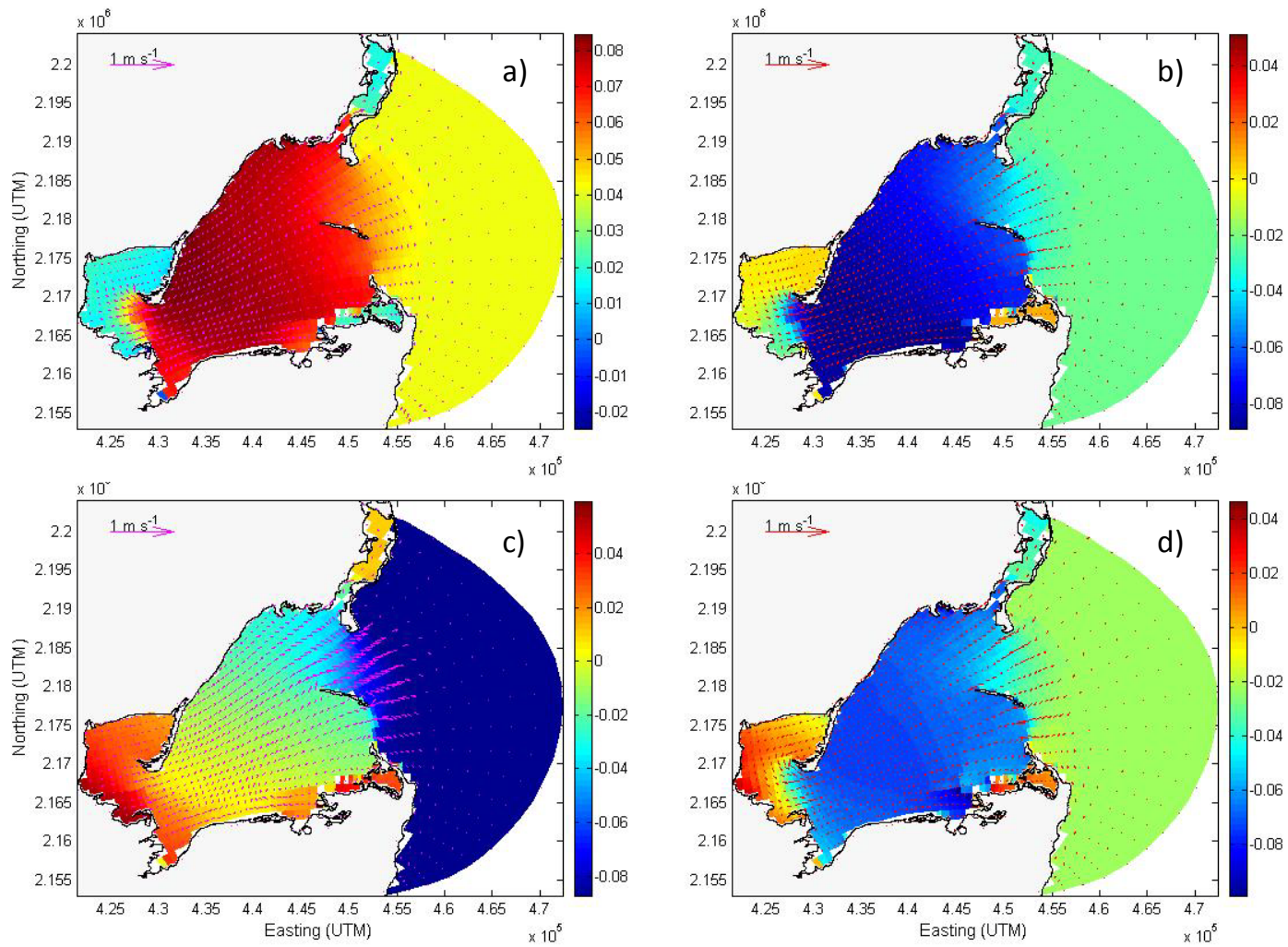


Figure 2.11. Instantaneous water level (m) and currents ( $\text{m s}^{-1}$ ) when the model is forced with tides plus a) SE winds in ebb tide; b) "Nortes" in flood tide; c) Trades in low tide; and d) Trades in flood tide.



### *Residual currents*

The tide-averaged currents over 14 semidiurnal cycles (i.e., first day removed from the 8-day simulation run for stability reasons) simulated under the effect of astronomical tides showed a clockwise cell flowing around Cayo Culebras mangrove cay (CC) in the inlets zone, having water inflow through the south inlet and outflow at the north inlet. Net tidal flow in the VG embayment is minor and limited to the channel between this inner subsystem and the central basin (Fig. 2.12a). This condition is a consequence of tidal energy dampening just past the channel into the VG embayment (Fig. 2.10) (e.g., please see *Variability of the water level in the reef lagoon (RL) and inner bay* in the Results and Discussion section of Chapter I).

The circulation pattern corresponding to the southeasterly wind plus tide simulation exhibited a prevalent northward residual flow parallel to the reef barrier (mean velocity of  $0.05 \pm 0.02$  SD  $\text{m s}^{-1}$  and  $0.10 \text{ m s}^{-1}$  maxima), which caused a bay-directed transport through the south inlet. At the southwestern edge of the bay, two oppositely-directed, net flows ( $0.04 \pm 0.01$  SD  $\text{m s}^{-1}$ ) occurred along the Vigia Grande channel (Fig. 2.12b). Circulation from the SW towards the central bay is evident through the northern section of this waterway, whereas an inflow to VG is established at the southern half. This lateral current variability points out the relevance of wind-driven transport on the turnover times for the inner-most bay.

The circulation-constrained VG embayment (e.g., inner bay) is the receiving water body of substantial freshwater input and abundant nutrients drained from neighboring ecosystems (see Chapters I and III of this dissertation). Because of the attenuation of the tidal energy within VG, it is likely that this subsystem would experience a variable extent of isolation from the main bay in the absence of a wind-controlled mechanism of water motion. This wind-driven propagation of water properties farther into the central basin along the salinity gradient has the potential to alter a number of physical-environmental traits in Bahia de la Ascension such as thermohaline characteristics in the water column and heat fluxes across the system, as well as ecologically significant processes such as the trophic status and health of the abundant submerged aquatic vegetation (Chapter III).

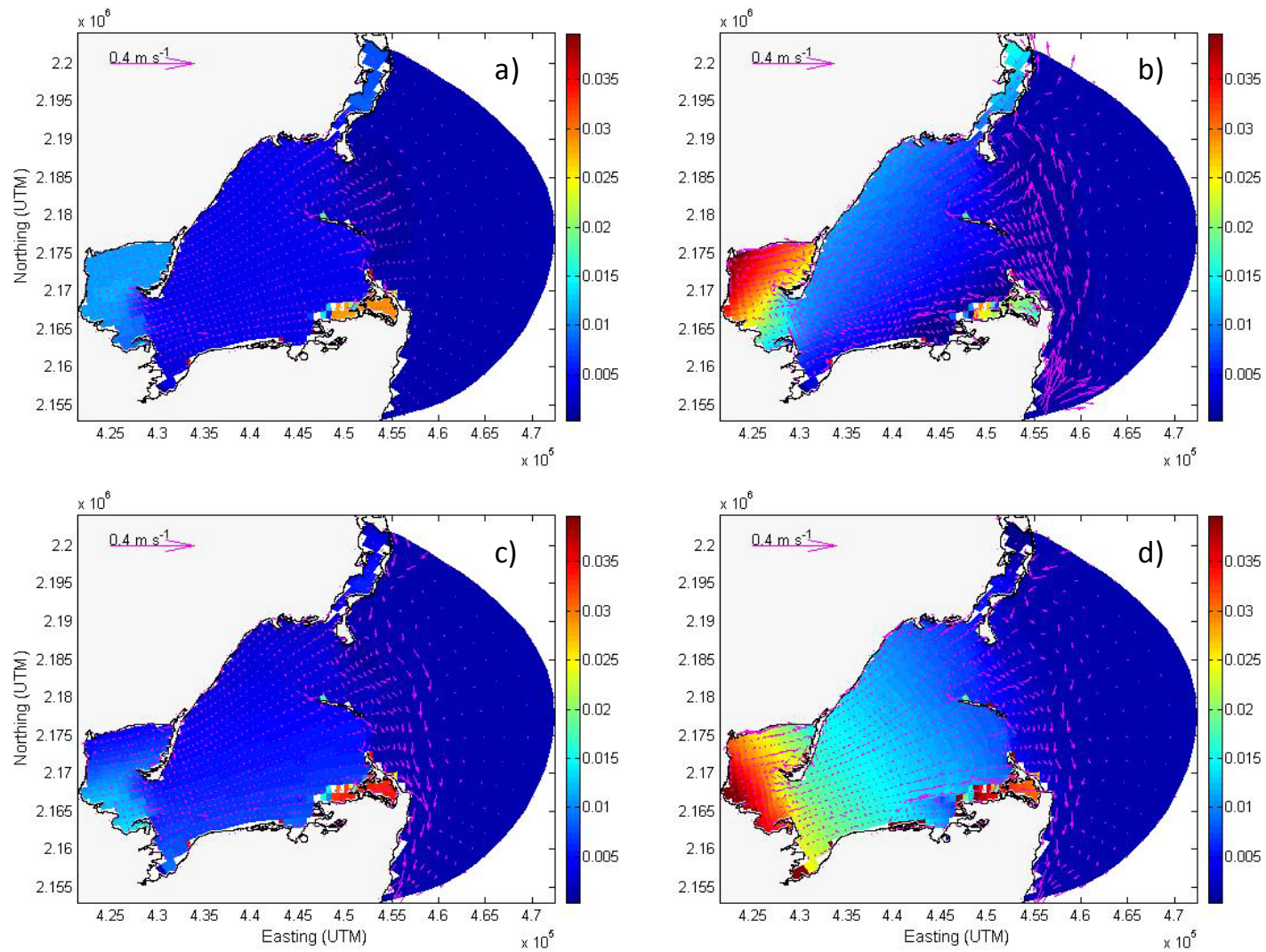


Figure 2.12. Seven-day-average water level (m) and residual currents ( $\text{m s}^{-1}$ ). Four scenarios are shown: a) tides alone; b) tides plus southeast wind; c) tides plus "Nortes" event; and d) tides plus Trades.

The simulation results with the NW-N wind (i.e., “Nortes”) and tides combined forcing showed an active alongshore, southward water transport with peak current velocity of  $0.04 \text{ m s}^{-1}$ . The water enters the system through the north entrance while it flows out through the south inlet. A slight response in the water level was seen at the southern section of the VG embayment, characterized by an elevation of about 10 mm relative to the rest of the bay (Fig. 2.12c). In the light of these results, it is considered that the *Nortes* wind is not as relevant for the circulation pattern of BA as it is in the coastal ecosystems of the Yucatan’s north coast. Indeed, northern polar cold-fronts constitute dominant hydrometeorological processes in the northern Yucatan, inducing an evident marine influence on its coastal lagoons, along with longer water residence times during the season comprising such events (Medina-Gomez and Herrera-Silveira 2009). The geographic location of Bahia de la Ascension (e.g., “Nortes” show a trajectory from the continent in BA instead of from the ocean as in the Yucatan’s north coast) contributes to relieve the potential effects of such events along the system’s surface.

During the Trade wind event, a prevalent southward coastal circulation with peak current velocity of nearly  $0.07 \text{ m s}^{-1}$  was observed. The residual current field showed a lateral circulation along the northern entrance, featuring a net water inflow in the northern half of this inlet, while water is exported along the section adjacent to the CC cay (Fig. 2.12d). There is also a residual flow into the bay through the southern entrance. As in the southeasterlies plus tides simulation case, the Trades and tidal joint forcing exhibited a water level increase in the inner-most section of the bay, although in the latter case the level gradient showed a smoother distribution along the NE-SW plane of the bay than with the southeasterly winds forcing (Fig. 2.12d). It is considered that such a pattern occurs because northeasterly Trades act over the system’s surface in the same direction as the system’s main axis, optimizing its forcing effect on the water level field. This increase in water level in VG relative to the central basin might reduce the barotropic pressure gradient between both points and depress water transport from the main bay into the system’s interior. Also, it is thought that such a mechanism would serve to spread the hydrographic properties characterizing the southwestern-most subsystem (i.e., Vigia Grande embayment) farther into the bay during episodes of persistent Trade winds.

The mean currents modeled under a tidal-southeasterly winds joint forcing were lower than

those recorded with an ADP (AWAC; Nortek AS) during dry season sampling. This field campaign was carried out during spring tides and featured four days of steady SE wind in the zone of the bay, with average current velocity of  $0.11 \pm 0.06$  SD  $\text{m s}^{-1}$  and peak flow of  $0.39 \text{ m s}^{-1}$  ( $n= 550$ ) in the reef lagoon (see Results and Discussion section of Chapter I under the *Current time series* subtitle). Such discrepancies might be a consequence of the bottom roughness formulation utilized as a boundary condition for the hydrodynamic model, not only for the SE wind forcing, but for all cases run (Table 2.2). While setting a uniformly distributed Manning friction coefficient ( $n = 0.04$ ) throughout the domain allowed parameterization of a well-developed submerged aquatic vegetation dominating the bay's floor in BA (Morin et al. 2000), the seasonally-varying growth and density traits featuring the aquatic benthic vegetation communities are obviously not accounted for by the homogenous boundary definition of the model domain (Chambers et al. 1991; Kjerfve et al. 1991). The species diversity characterizing BA and associated attributes as variable morpho-functional traits, along with their spatial distribution patterns, add architectural complexity to the bottom, leading to a distinct degree of friction acting on the water currents and potentially influencing the heterogeneity of the circulation patterns (Cotton et al. 2006). Finally, the floor of the reef lagoon in BA is virtually lacking seagrasses and is dominated by coarse sand instead, which likely represents a smoother surface for the water motion and as a consequence, favors stronger flowing currents than inside the bay.

## Summary and Conclusion

The simulation of the circulation patterns in Bahia de la Ascension under the dynamic forcing of tides and three typical wind conditions occurring in the Mexican Caribbean, showed that, despite this system's microtidal regime, tides influence significantly the water transport through both inlets, although stronger currents corresponded to the northern entrance, featuring a peak velocity of  $0.25 \text{ m s}^{-1}$  along the seaward endpoint of Cayo Culebras during spring tides. This effect, however, is limited to the inlets and seaward portion of the main bay, as tidal currents substantially decelerate in the upper reaches of the central basin.

Wind stress, on the other hand, strongly alters the water movement due to tidal influences;

currents in BA characteristically exhibited parallel motions to that of the winds acting in the zone. The wind effect is more vividly illustrated along the southern boundary of the bay and in the inner-most bay. Trade winds generated maximum currents of  $0.11 \text{ m s}^{-1}$  in the VG embayment with an average velocity of  $0.04 \pm 0.01 \text{ SD m s}^{-1}$ . Trades played a prominent role in the water transport from the bay's interior to the main bay and, although the circulation pattern under SE winds is similar to that resulting from the spring tides and Trades joint forcing, maximum southeasterly wind-induced currents were only one half of that observed in the Trade winds case.

Overall, the SE wind case featured two oppositely directed currents: water advected into the central basin through the northern half of the channel between the inner system and the central basin and net water inflow to the inner bay through the southern half of the same channel (Fig. 2.12b). This exchange is enhanced by the wind-driven setup in the northwest portion of the VG embayment and associated pressure gradient. Additionally, sustained SE wind stress maintains a net water inflow across the inlet which is roughly 18% greater than the water imported to the bay during the spring tides case.

Given the constrained tidal circulation in the interior of VG, it is considered that, whilst relatively strong instantaneous tidal currents ( $0.06 \text{ m s}^{-1}$ ) may contribute to maintaining the channel between the inner bay and the central basin by eroding the depth and cross-section area, the subtidal energy input by sustained easterlies (i.e., residual flow) on the water motion play a salient role in moderating the depositional rate of this embayment and prevent its infilling with sediment from the adjacent mangrove wetland. Thus, it is asserted that Vigia Grande embayment constitutes a critical subsystem for the evolution of water properties farther along in the main bay.

The first hydrodynamic model of Bahia de la Ascension proved to be an appropriate tool to evaluate the circulation patterns of this system under the influence of tides and winds. Tide is an important forcing function controlling the hydrodynamics of BA, as tidal phase alters both instantaneous and time-average flow in the inlets zone and the bay's central basin, while winds enhance water circulation from the system's interior to the main bay, particularly when acting along the main northeast-southwest axis of the bay (i.e., Trades and southeasterly winds). The influence of winds on the transport phenomena is evident

within the Vigia Grande embayment, where tidal frequencies seemed to decline on the west side of the channel connecting the main bay with the system's interior. Thus, the energy input due to winds constitutes a major driving force on the circulation in this subsystem. Net discharges are relatively larger across the north inlet than in the south inlet, although instantaneous current velocities are higher in the latter.

## CHAPTER III

### SEASONAL RESPONSES OF *THALASSIA TESTUDINUM* TO THE PHYSICAL-ENVIRONMENTAL SETTING IN A SHALLOW COASTAL BAY OF THE WESTERN CARIBBEAN

#### Introduction

Submerged aquatic vegetation (SAV) communities constitute a major biological feature of coastal zones around the globe, proliferating across sandy sediments of shallow seas (Spalding et al. 2003). Within SAV communities, the marine angiosperms (generically seagrasses) provide a variety of ecological functions, such as stabilization and trapping of sediment, regulation of nutrient recycling, and dissipation of wave energy (Constanza et al. 1997). Because seagrasses are important habitat for numerous aquatic organisms (Lipcius et al. 1998; Bloomfield and Gillanders 2005), seagrass die-off episodes have been associated with decreases in the abundance of seagrass-related fish and benthic invertebrate dwellers (Fourqurean and Robblee 1999). The functional connectivity between seagrasses and neighboring mangrove wetlands ecosystems is through both tidally-driven and nekton-facilitated organic material exchange, which is significantly mediated by bacterial remineralization processes (Yañez-Arancibia et al. 1993; Hemminga et al. 1994; Holmer and Bachmann-Olsen 2002).

In the western Caribbean (WC), these benthic habitats are found both as monotypic or mixed beds colonizing nearshore waters. The specific composition of the SAV in the WC typically comprises the seagrasses *Thalassia testudinum*, *Halodule wrightii*, and *Syringodium filiforme*, as well as *Ruppia maritima* in oligohaline systems, accompanied by rhizophytic algae and epiphytes (Littler and Littler 2000). *Thalassia testudinum* is ubiquitous along shallow bays and coastal lagoons of the WC, where it develops extensive stands usually adjacent to mangrove forests and coral reefs. The ecological resilience of this long-lived clonal species was documented after hurricanes Gilbert (category-5) in September 1988 and Wilma (category-4) in October 2005, two strong hurricanes that made landfall near Puerto Morelos reef lagoon, in the Mexican Caribbean (van

Tussenbroek 1994; van Tussenbroek et al. 2008). The enhancement of vertical growth in surviving short-shoots counteracted burial of the leaf-producing meristems, leading to recovery of the abundance level exhibited by *Thalassia* in this coastal lagoon prior to occurrence of those hurricanes.

Seagrasses in the waters of the Yucatan Peninsula face threats to their well-being from sources other than natural disturbances. Unconfined aquifers are susceptible to contamination from human activities and the submerged groundwater discharges (SGD) draining the extensive groundwater network of the Yucatan may provide the pathway for contaminant delivery into the coastal zone. Cultural eutrophication increases epiphytism on seagrass blades and increases macroalgal abundance across the substrate, leading to a drastic reduction in seagrass production and coverage (Tomasko and Lapointe 1991; Wear et al. 1999). The rate of tidal exchange in circulation-restricted coastal ecosystems regulates the persistence of this deleterious process (Madden and Kemp 1996). If continued, highly diverse canopies may become monotypic beds through the removal of less adapted seagrass species (Zimmerman et al. 1996), leading the coastal systems to undergo an overall ecological phase shift. Because massive tourism is driving economic development in the Mexican Caribbean, an exacerbation of cultural eutrophication and resulting processes along the coastal zone might be expected (Orth et al. 2006). The vulnerability of the Mexican Caribbean makes evident the need for baseline information about the relationship between the physical environment and the biological communities, which have high connectivity across this karst, coastal landscape.

*T. testudinum* is distributed across the shallow coastal bay Bahia de la Ascension (Fig. 3.1), having developed under the distinct spatial salinity gradients and environmental conditions of this system. The objectives of the current study are to explain the seasonal and spatial variations in biomass and shoot density of the seagrass *Thalassia testudinum* by evaluating the physical forcing factors that contribute to the observed patterns. Vigia Grande (the inner embayment of BA, site 2 in Fig. 3.2) receives fresh water by surface and groundwater discharges, and it is hypothesized that the presence of *T. testudinum* there is connected to the high inorganic nutrient delivery to this subsystem from the adjacent mangrove wetland. However, the mesohaline regime of Vigia Grande may pose a physiological constraint (osmotic stress) to the *T. testudinum* population, which would



inhibit the aerial component development (i.e., lower above/belowground biomass ratio) compared to the marine-influenced sections within the bay (site 1 in Fig. 3.2).

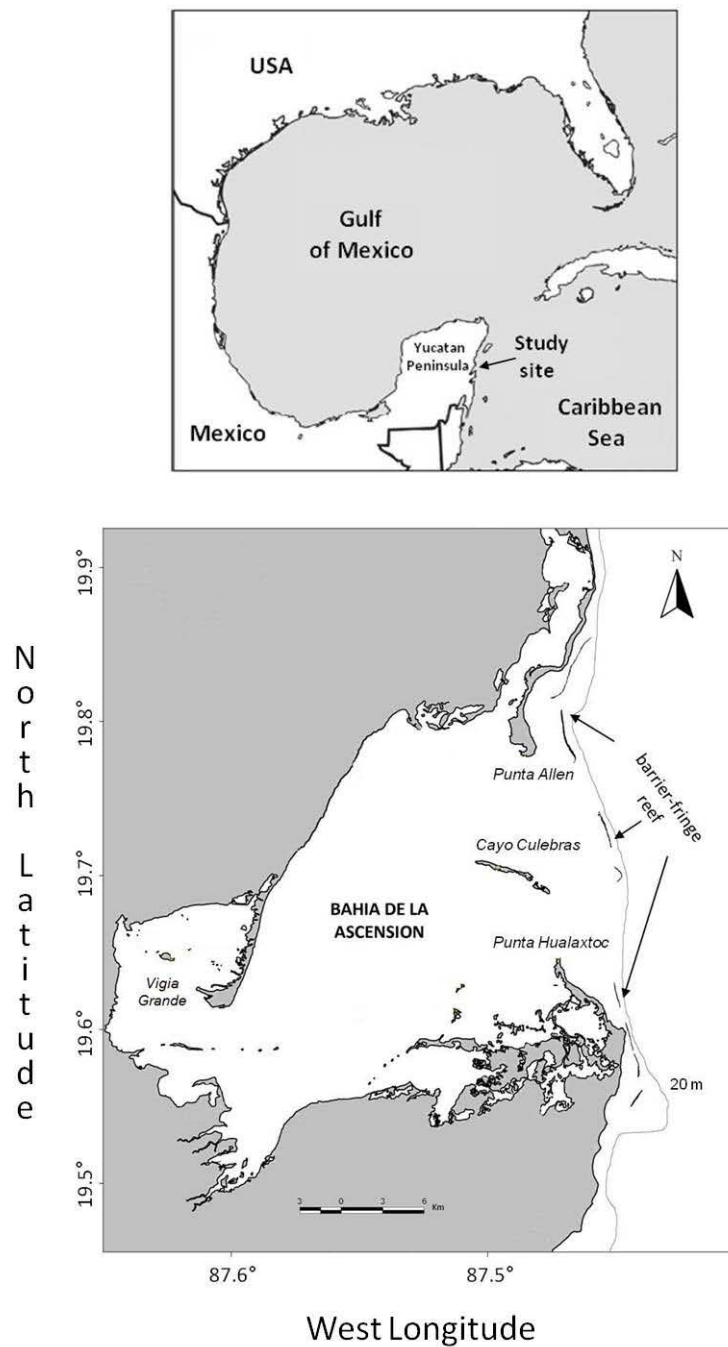


Figure 3.1. Map of Bahia de la Ascension in the Western Caribbean. Coordinates are given in decimal degrees.

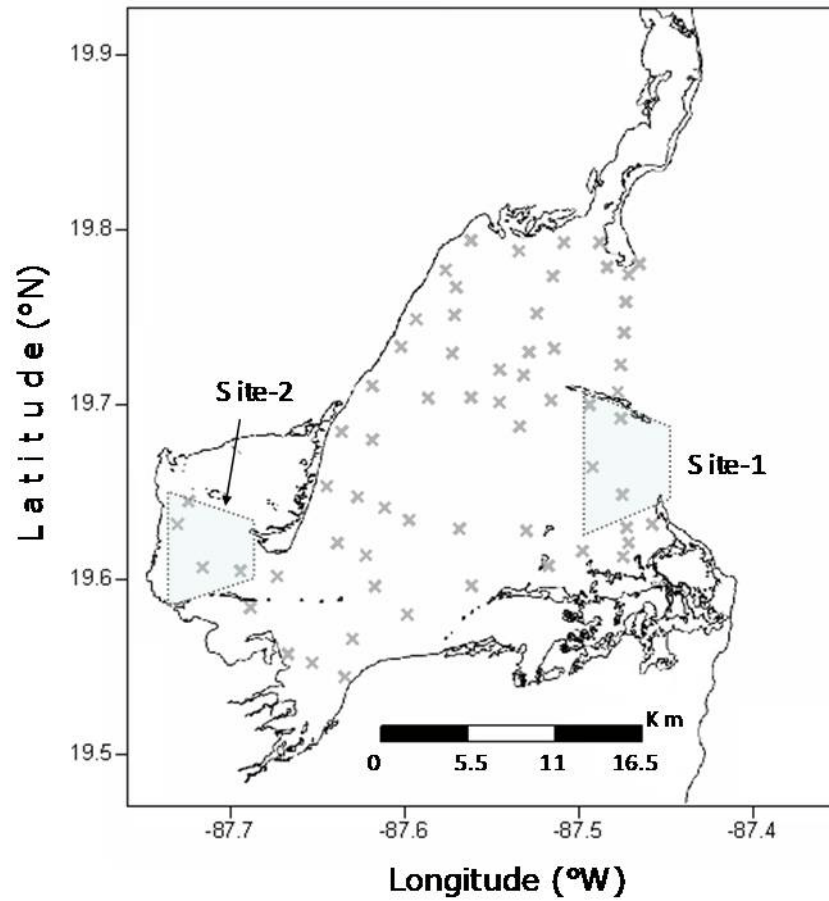


Figure 3.2. Study site with 62 sampling stations (crosses). Also, two *T. testudinum* beds referenced in the hypotheses are shown (site-1: Cayo Culebras stand, and site-2: Vigia Grande stand).

## Study Site

Bahia de la Ascension, part of the the Sian Ka'an Biological Reserve, is a shallow coastal bay on the eastern Yucatan Peninsula. It is confined by two headlands, Punta Hualaxtoc on the south and Punta Allen on the north. The latter is the location of a small fishing village ( $\approx 600$  population; INEGI 2008), which is the only populated site along the bay's coastline. The valuable resources that Bahia de la Ascension provides to the local inhabitants, such as the traditional commercial spiny lobster fishery, recreational fisheries operation, and recent burgeoning commercial activities associated with tourism, are tied directly and indirectly to the environmental well-being of this ecosystem.

The bay's main axis is oriented SW-NE. It has a surface area of  $580 \text{ km}^2$  and a drainage basin of  $1,200 \text{ km}^2$ . The mean depth of the bay is 2.2 m, with a maximum of 6.8 m in the main, E-W oriented tidal channel located between Punta Allen and Cayo Culebras (CC), a mangrove cay in the middle of the main bay-reef lagoon boundary (Fig. 3.1). The semi-continuous coral reef defining the seaward boundary of Bahia de la Ascension is a segment of the Mesoamerican barrier reef system (MBRS), a coral barrier reef extending along four countries of the Western Caribbean: Mexico, Belize, Guatemala, and Honduras.

Climate in the Sian Ka'an Reserve is warm, sub-humid, with a mean annual temperature  $> 22^\circ\text{C}$  overall and  $> 18^\circ\text{C}$  during the coldest month (January). This region is influenced by a marked dry-rainy seasonality, with winter rainfall accounting for about 10% of the annual mean and the precipitation ranging from 1,200 mm to 1,500 mm. Although Bahia de la Ascension lacks surface fluvial discharges, it receives a significant amount of freshwater through submerged springs (SGD) and surface streams connected to waterways within the nearby mangrove forest and draining into the southwestern-most portion of the bay (Fig. 3.1).

The freshwater flux in Bahia de la Ascension is characteristic of an estuarine ambient, that is, a partially enclosed shallow coastal body of water affected by marine influence and containing sea water measurably diluted by freshwater inflow (Pritchard 1967). However, the sea water dilution in Bahia de la Ascension is by groundwater discharge rather than a river as in true estuaries. Geomorphologically, the bay is separated from the sea by a large

barrier reef (discontinuous on its southern portion) and connected to the marine ambient through a main tidal channel (on its north section), typical of coastal lagoons (Kjerfve 1994). Such traits deeply influence the bay's functioning and thus, the definition of a coastal lagoon will be adopted for Bahia de la Ascension. Tides in the zone are defined as mixed and semi-diurnal, featuring a micro-tidal regime with the principal lunar  $M_2$  as the dominant component (Kjerfve 1981).

The system features the entire biological corridor including mangrove forest, shallow water bodies, seagrass meadows, and coral reef barrier. The widely distributed submerged aquatic vegetation in Bahia de la Ascension is dominated by the seagrass species *Thalassia testudinum*, which extends from the marine-influenced reef lagoon to the mesohaline environment at the inner-most portion of the bay (Vigia Grande). The ecological functions of Bahia de la Ascension are expected to be well-preserved because of the bay's location within the protected Sian Ka'an Reserve, making the bay a suitable site for this research. It is expected that the information from this study will shed light on the connectivity issue across the biological corridor in the Caribbean, and through cross-comparisons with other tropical ecosystems (Rivera-Monroy et al. 2004), it may assist in the achievement of relevant generalizations about their functioning. This information in addressing issues related to the intense agriculture and tourism development surrounding this region.

## **Materials and Methods**

Four sampling campaigns were undertaken in 2006 and 2007; two during the dry season (June) and two during the rainy (October) season. Sixty-two stations (Fig. 3.2) were sampled for hydrographic parameters and *Thalassia testudinum* variables.

### *Hydrographic variables*

Water samples were collected at mid-depth (CTD profiles exhibited lack of vertical stratification at all the 62 sampling stations during the field campaigns; data not shown) along the bay for nutrients and chlorophyll-*a* determinations under a discrete sampling scheme.

Additionally, a continuous flow-through sampling with high spatial resolution (<30 m horizontal distance amongst stations) of temperature (Signet 8860 Sensor; range: -25°C to 120°C; accuracy:  $\pm 0.5^\circ\text{C}$ ), salinity (Signet Conductivity Sensor; 10.0 cell constant for range of 100-200,000  $\mu\text{S}$ ), and colored dissolved organic matter (CDOM; WETStar fluorometer; sensitivity: 0.100 ppb quinine sulfate dihydrate) were taken across Bahia de la Ascension using a Dataflow® (Madden and Day 1992) only during the rainy season (October) 2007 campaign, due to malfunctioning of this device.

The treatment of samples, laboratory processing, and methods of determination of nitrite, nitrate, ammonium, silicate and phosphate, and chlorophyll-a were completed according to Medina-Gómez and Herrera-Silveira (2003).

#### *Biological variables*

Submerged aquatic vegetation was surveyed using the Braun-Blanquet technique for a rapid visual assessment of SAV cover (Fourqurean and Rutten 2003). This technique consists in having GPS-positioned transects of  $\approx 50$  m length, each separated by 100 m. Yet, transects should represent the entire seagrass area and thus, their total length might be rather variable. The samples were taken at regular intervals across transects (10 m), so that biomass and density gradients in seagrass beds could be defined. Four replicate quadrants (0.02 m<sup>2</sup>) were sampled at each of the 62 resulting stations using SCUBA equipment. All seagrass species were listed, and a score based on the estimated cover of each species in that quadrant was assigned (Table 3.1). Density and abundance were computed from observations in those quadrants for a given site (Fourqurean and Rutten 2003). The collection of samples and treatment of biomass was undertaken according to the CARICOMP methods manual for seagrass communities (CARICOMP 2001).

Table 3.1. Interpretation of the Braun-Blanquet scores utilized for rapid assessment over the seagrass meadows.

Score	Description
0	Species absent from a quadrat
0.1	Species represented by a solitary short shoot, <5% cover
0.5	Species represented by a few (<5) short shoots, <5% cover
1	Species represented by many (>5) short shoots, <5% cover
2	Species represented by many (>5) short shoots, 5%-25% cover
3	Species represented by many (>5) short shoots, 25%-50% cover
4	Species represented by many (>5) short shoots, 50%-75% cover
5	Species represented by many (>5) short shoots, 75%-100% cover

The analysis of the vegetation response to seasonal environmental gradients was carried out in the current study by comparing the variability of *Thalassia testudinum* along three distinct sites (i.e., Vigia Grande -Class 3, the central bay -Class 4, and Cayo Culebras -Class 8) out of eight classes previously identified through a supervised classification of *Thalassia testudinum* distribution in Bahia de la Ascension (Arellano 2010; Fig. 3.3). In such classification effort, training zones with known cover (documented by field observations in the bay; e.g., sparse shoots, bare sand) were used as “seeds” to identify spectrally similar pixels on a Landsat ETM<sup>+</sup> image (taken on 21 April 2000). Using the maximum likelihood (Gaussian) classification algorithm, a systematic extrapolation of such spectral signatures from the zones with known cover to unknown pixels across the image was accomplished (Kappa index = 0.809) (Arellano 2010).

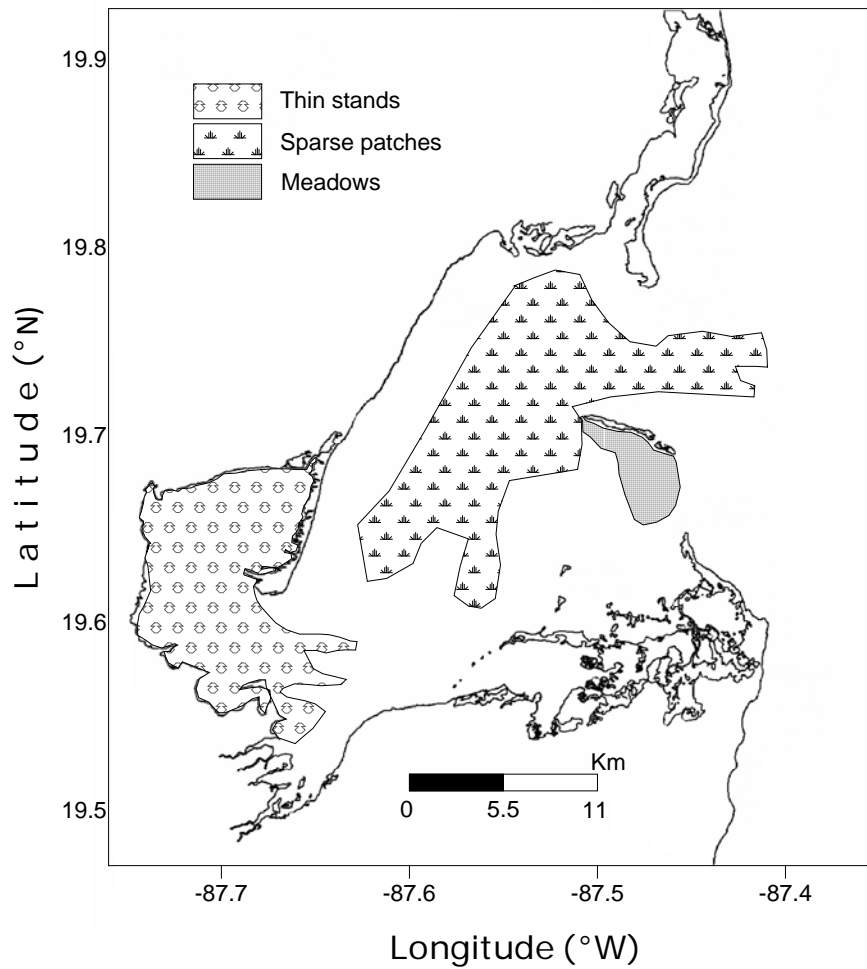


Figure 3.3. Three distinct *Thalassia testudinum* beds classified according to morphometric, structural, and density attributes from a Landsat ETM<sup>+</sup> image (Arellano 2010). Thin stands (class 3): patch sizes of only a few centimeters long and shoot densities  $<200 \text{ m}^{-2}$ ; Sparse patches (class 4): patches covering tens of centimeters, with mean density  $\approx 350 \text{ m}^{-2}$  and average aboveground biomass  $>300 \text{ g DW m}^{-2}$ ; Meadows (class 8): bed sizes  $>10 \text{ m}$ , average density of  $955 \text{ m}^{-2}$  and aboveground biomass of  $1,978 \text{ g DW m}^{-2}$ .

### *Statistical analysis*

A Principal Component Analysis (PCA) was applied to the physical-chemical parameters (temperature, salinity, dissolved oxygen, pH, and CDOM) and dissolved inorganic nutrients ( $\text{NO}_2^-$ ,  $\text{NO}_3^-$ ,  $\text{NH}_4^+$ , SRP, SRSi) to identify the key variables controlling the water quality in Bahia de la Ascension. All sites and years (2006-2007 sampling campaigns) were combined to carry out two seasonal PCA's (e.g., dry and rainy seasons).

ANOVA's for the hydrographic and water quality parameters allowed decomposing the variance of each parameter into two components: a between-group component and a within-group component. The between-group estimate to the within-group estimate ratio was accounted by the F-ratio. Finally, p-values for the F-test were calculated and inspected for statistically significant differences (p-value < 0.05) among the means of a given parameter corresponding to the distinct levels of a "treatment" at the 95.0% confidence level. On the other hand, Kruskal-Wallis Test was utilized to test the null hypothesis that the medians of the distinct seagrass parameters are the same. Since biological parameters were not normally distributed, medians instead of means were reported. P-values were assessed for statistically significant difference amongst the medians at the 95.0% confidence level.

Coefficients of variation (CV) were estimated for both environmental and biologic parameters as it constitutes a normalized measure of dispersion of their probability distribution. The CV is calculated as the ratio of the standard deviation to the mean times 100. Since the CV is expressed as a percentage and is a dimensionless number, it is suitable for comparison among data sets. All the statistical analyses were performed utilizing STATGRAPHICS Plus for Windows 4.1.



## Results

### *Water quality*

Mean values of physical-chemical parameters will be reported throughout this section and are summarized in Table 3.2. Also, the terms “zones” and “classes” will be used equivalently along the results and discussion, unless something different is indicated.

The water temperature was generally less variable in Vigia Grande than in the central basin (CB), or Cayo Culebras (CC), with statistically minimum values during rainy season 2007 across the bay. During the 2006 dry season, the lowest mean temperature of the study was observed in the central bay (Class 4), while peak values and wider variability corresponded to CC (Class 8) during this same campaign. This latter location had a trend of decreasing temperature across sampling campaigns (Fig. 3.4a).

Salinity was fairly homogenous across the central basin, highly variable and exhibiting marked low mean values in Vigia Grande, while both a fluctuating behavior and minimum salinities were observed in Cayo Culebras during rainy season 2007. In general, salinities recorded during the 2007 campaign were lower than those observed in 2006, with the minimum values in each class occurring during the 2007 rainy season. An anomalous pattern in Vigia Grande was recorded during 2006: rainy season salinities were higher than in the dry season (Fig. 3.4b). During the 2006 campaign, the average percent of dissolved oxygen in Vigia Grande was statistically significant lower than in the central basin and Cayo Culebras; also, the mean values measured in the 2007 dry season were significantly higher at all sites than those measured in the 2007 rainy season (Fig. 3.4c).

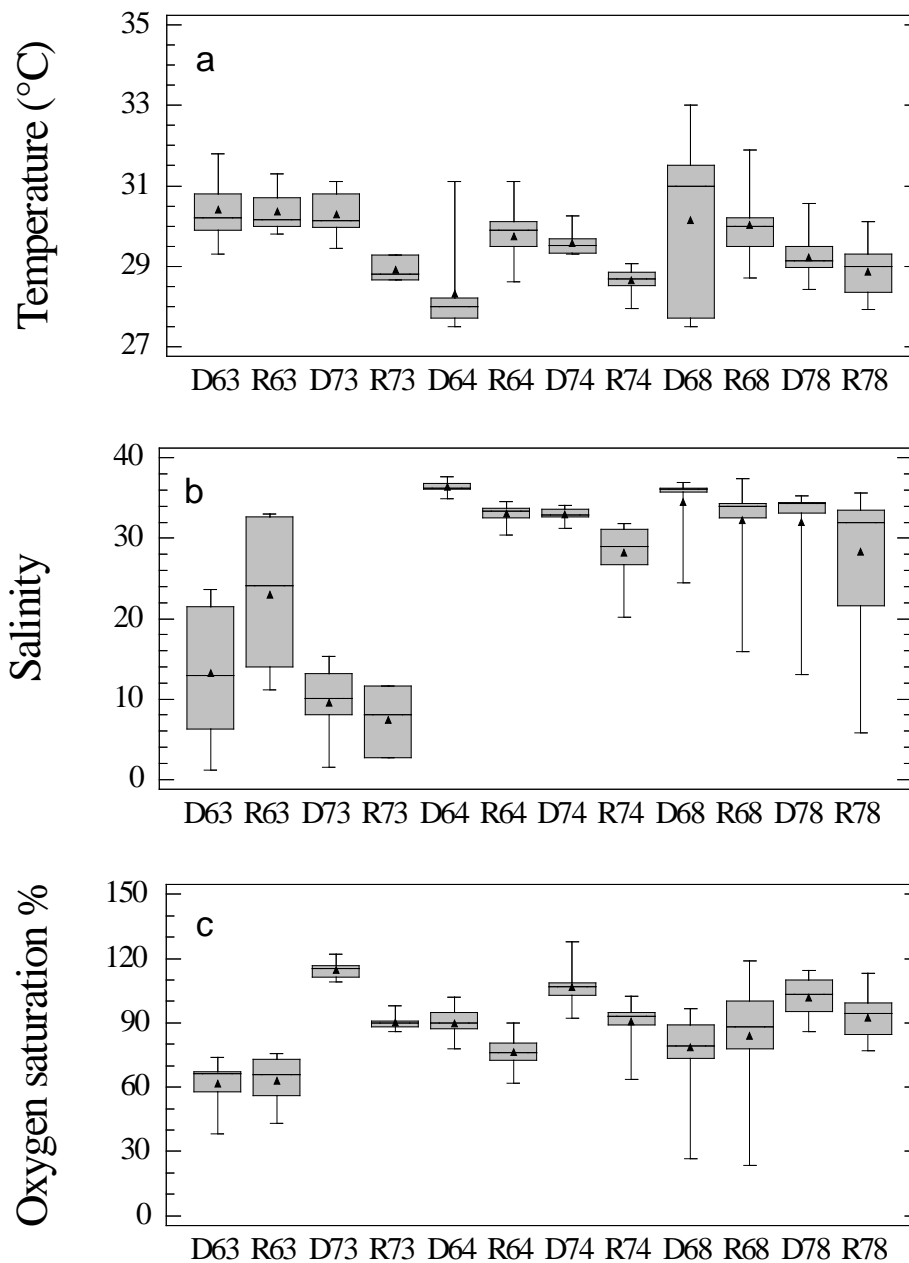


Figure 3.4. Seasonal variability of hydrographic properties in Bahia de la Ascension during the 2006 and 2007 sampling campaigns. Mean is represented by a triangle and median is the horizontal line into the box, 25th and 75th percentiles are the top and bottom of the box, while the 5th and 95th are located on the tips of the whiskers. The labels on x-axis: 1<sup>st</sup> letter represents the climatic season (D= dry; R= rainy); 1<sup>st</sup> number designs the year of sampling campaign (2006 or 2007); the 2<sup>nd</sup> number denotes the corresponding class according to the supervised classification of *T. testudinum* depicted in Figure 3.3.

Table 3.2. Seasonal water quality parameters (mean values  $\pm$  1 standard deviation) at 3 sites (e.g., supervised classification) across Bahia de la Ascension during 2006-2007: Vigia Grande at the inner bay (VG), bay's central basin (CB), and Cayo Culebras at the seaward boundary (CC). Temperature is given in °C and inorganic nutrients concentration in  $\mu\text{M}$ .

Param.	Dry season						Rainy season					
	VG class 3 (N=15)		CB class 4 (N=32)		CC class 8 (N=37)		VG class 3 (N=16)		CB class 4 (N=37)		CC class 8 (N=33)	
Temp	30.4	0.7	28.8	1.1	29.8	1.6	30.0	0.8	29.4	0.7	29.6	0.9
Sal	12.1	7.7	35.2	1.8	33.5	4.9	19.4	11.4	31.4	3.2	30.9	6.6
$\text{NO}_3^-$	1.2	2.2	0.3	0.3	0.6	0.7	1.2	0.9	0.8	0.9	0.7	0.4
$\text{NH}_4^+$	6.0	4.4	4.1	4.8	2.6	2.2	6.8	4.3	5.2	2.6	4.6	3.2
$\text{PO}_4^{-3}$	1.8	0.8	1.5	1.2	0.6	0.5	1.1	0.4	1.3	0.6	1.4	0.8
$\text{SiO}_4$	142.4	75.6	14.5	11.0	25.6	19.5	101.0	42.1	33.8	33.4	26.2	23.2

### *Inorganic nutrients*

#### Nitrogen

Both maximum concentrations and greater variability of  $\text{NO}_3^-$  was found during the 2007 dry season in Vigia Grande compared to the other sites during this same campaign, as well as in the 2006 sampling campaign. The overall seasonal pattern of increasing nitrate concentrations during the 2006 rainy season was inverted in the 2007 campaign, when all the classes showed a pattern of decreasing concentrations during the rainy season, although only Vigia Grande actually exhibited significant differences ( $p$ -value of the F-Test  $\ll 0.05$ ) (Fig. 3.5a).

Higher mean  $\text{NH}_4^+$  concentrations and greater variability was observed in Vigia Grande compared to the central basin and Cayo Culebras for both seasons at 2006 and 2007 (Fig. 3.5b). Yet, the inner bay lack of the seasonal difference among ammonium values recorded elsewhere in the system. Such seasonal behavior was, on the other hand, evident both in the central bay and Cayo Culebras during the 2007 sampling campaign, when maximum  $\text{NH}_4^+$  concentrations were observed in rainy season.

### Phosphate

Mean phosphate concentrations in the 2006 dry season were statistically lower than values determined in rainy season at the three classes (Fig. 3.5c). This seasonal relationship changed for Vigia Grande and the central basin during the 2007 campaign, when peak  $\text{PO}_4^{3-}$  and more variable concentrations were recorded during the dry season. Such differences, however, were not statistically significant (p-value of the F-Test > 0.05).

### Silicate

Three different patterns of SRSi variability were observed in the zones studied. Silicate concentrations in Vigia Grande were substantially higher than those of the central basin or Cayo Culebras, with highest value recorded during the dry season and decreasing values over the 2006-2007 campaigns (Fig. 3.5d). Farther into the bay's central basin, mean SRSi concentrations exhibited higher values during the 2006 rainy season than in the preceding dry season. Although seasonal mean SRSi concentrations in CB were not significantly different during the 2007 sampling (p-value of the F-Test >0.05), the values in the rainy season had a more scattered distribution (CV = 94.4%). Cayo Culebras showed a seasonally homogeneous distribution in the distinct campaigns, although atypically high SRSi concentrations occurred in all samplings.

### *Principal Component Analysis (PCA)*

The first three principal components (PC) taken from the combined hydrographic and inorganic nutrients data accounted for 65% and 62% of the total variance during dry and rainy season campaigns, respectively (Table 3.3). During the dry season, PC-1 explained the opposite fluctuations of salinity versus silicate and CDOM, which defined the terrestrial *runoff plus groundwater discharge* gradient. The PC-2 extracted from the data for the dry season indicated that ammonium and urea varied in opposite direction along the ordination axis. These chemical species are significantly influenced by the external input (both natural and anthropogenic) and thus, PC-2 was named the *mineralization* gradient. The PC-3 described the behavior of nitrite and phosphate and the inverse variability of the oxygen saturation percent. The variability of this set of hydrographic parameters may be reflecting the occurrence of local, bacteria-mediated breakdown of organic matter through respiration into the sediments. This relationship was synthesized as the *nutrients recycling* component in Bahia de la Ascension.

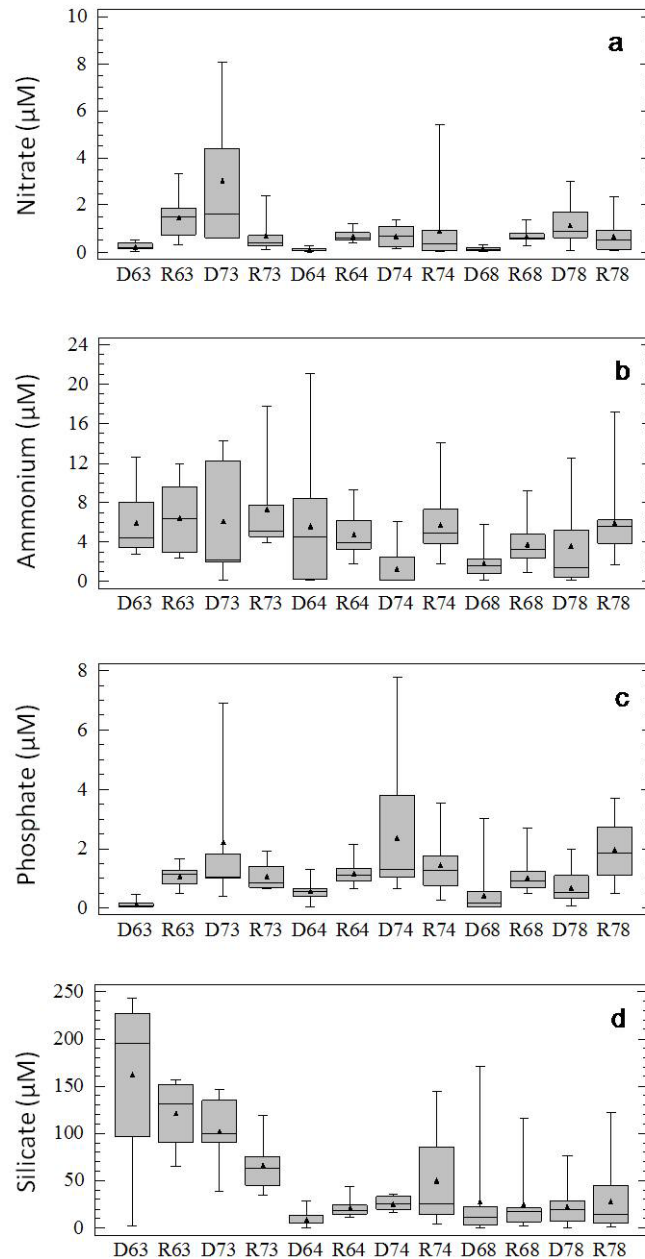


Figure 3.5. Seasonal variability of inorganic nutrients in Bahia de la Ascension during the 2006 and 2007 sampling campaigns. Mean is represented by a triangle and median is the horizontal line into the box, 25th and 75th percentiles are the top and bottom of the box, while the 5th and 95th are located on the tips of the whiskers. The labels on x-axis: 1<sup>st</sup> letter represents the climatic season (D= dry; R= rainy); 1<sup>st</sup> number designs the year of sampling campaign (2006 or 2007); the 2<sup>nd</sup> number denotes the corresponding class according to the supervised classification of *T. testudinum* depicted in Figure 3.3.

During the rainy season analysis, the PC-1 was defined by the silicate and salinity gradient, thus accounted for by the *groundwater input* component. The evident co-variation of nitrite and nitrate in PC-2 during rainfall suggests it might be depicting the gradient of nitrogen loss through  $\text{NO}_3^-$  reduction, thus constituting the PC-2 as the *denitrification* component. The concurrent dynamics of PC-3 exhibited by the oxygen saturation percent and ammonium concentrations (i.e., reduced nitrogen species) may indicate that this component captured the biogeochemical decomposition of organic material into the oxic stratum of sediments (i.e. not involving  $\text{NO}_3^-$  as a secondary electron acceptor). Such sediment layer may be widened owing to the oxygen production by the seagrass beds and further pumped into the roots/rhizome complex. Thus, this was called as the *seagrass oxygen production-benthic mineralization* component.

Table 3.3. Seasonal Principal Component Analysis (PCA) in Bahia de la Ascension during 2006-2007.

Season	Eigenvalue.	Key variables	Component name	% variance	Cum. %
Dry	I: 3.66	Sal, SRSi, CDOM	<i>Runoff - GD</i>	36.6	36.6
	II: 1.76	$\text{NH}_4^+$ , urea	<i>Mineralization</i>	17.6	54.2
	III: 1.12	$\text{O}_2$ %, $\text{PO}_4^{-3}$ , $\text{NO}_2^-$	<i>Nutrients recycling</i>	11.2	65.3
Rainy	I: 3.23	SRP, $\text{NH}_4^+$ , urea	<i>Groundwater input</i>	32.3	32.3
	II: 2.22	Sal, temperature	<i>Denitrification</i>	22.2	54.5
	III: 1.39	$\text{NO}_3^-$ , $\text{O}_2$ %	<i>Benthic production</i>	13.9	68.4

### *Biologic variables*

The nomenclature derived from the supervised classification of *Thalassia testudinum* over Bahia de la Ascension will be utilized throughout the description of the seagrass parameters (Table 3.4). Medians instead of means will be reported along this section due to that seagrass variables did not show a normal distribution. Besides, structural parameters data (biomass, blades length and width) are only available for the 2006 sampling campaign; data on shoot density and abundance are available for 2006 and 2007 campaigns.

### Biomass

Significantly lower aboveground biomass levels were recorded in the rainy season vs. dry season for all the three zones (Kruskal-Wallis test;  $p$ -value  $\ll 0.05$ ), with the most salient seasonal difference observed at the inner bay (Vigia Grande embayment, class 3). Cayo Culebras (class 8) showed both the highest median aerial biomass ( $980 \text{ g DW m}^{-2}$ ) and the greatest variability among the classes, with a range of  $1,542.9 \text{ g DW m}^{-2}$  during the dry season, while class 4 had the lowest biomass levels for both seasons. No significant differences were detected, however, between the amount of aboveground biomass observed in class 8 and class 3 during the dry season, even though biomass in the latter were more narrowly centered on the median of  $853.7 \text{ g DW m}^{-2}$  (range of  $544.5 \text{ g DW m}^{-2}$ ; Fig. 3.6a).

Belowground biomass exhibited a similar pattern, characterized by overall lower values in rainy season than in the dry season, and a strong seasonal varying behavior in the inner bay (class 3). However, no significant seasonal belowground biomass differences were recorded in Cayo Culebras stand (class 8), which exhibited the highest median biomass of  $667.56 \text{ g DW m}^{-2}$  in dry seasons (Fig. 3.6b).

### Aboveground/Belowground (AB/BG) biomass ratio

The AG/BG ratio showed an overall seasonal pattern of decreasing values in the rainy season, featuring ratios  $>1$  only during the dry season. Although seasonal AG/BG differences were statistically significant at the 95% confidence level for each class (Kruskal-Wallis test;  $p$ -value  $\ll 0.05$ ), this trend was more prominent in class 3 than in the central bay, suggesting that relatively more extreme environmental conditions may occur

in the inner bay along the year cycle than in the rest of the system. Also, variability increased from the bay's interior (class 3) towards the bay-nearshore boundary, in the inlets zone (class 8). The highest average above/belowground biomass ratios of 1.50 and 1.16 were observed during the dry season in classes 3 and 8, respectively (Fig. 3.6c).

Table 3.4. Seasonal structural and demographic parameters (median values and coefficient of variation percent) of *Thalassia testudinum* at three sites (supervised classification) across Bahia de la Ascension: Vigia Grande at the inner bay (VG), bay's central basin (CB), and Cayo Culebras at the seaward boundary (CC). ab: aboveground and bb: belowground biomasses are given in g DW m<sup>-2</sup>, A/B is aboveground/belowground ratio, and short shoot (SS) density as individuals m<sup>-2</sup>.

Parameter	Dry season						Rainy season					
	VG class 3 (N=10)		CB class 4 (N=21)		CC class 8 (N=21)		VG class 3 (N=10)		CB class 4 (N=21)		CC class 8 (N=21)	
ab <sup>a</sup>	854	21%	488	92%	980	72%	87	14%	38	45%	306	87%
bb <sup>a</sup>	590	10%	406	65%	668	49%	292	23%	249	19%	608	44%
A/B <sup>a</sup>	1.4	28%	1.1	54%	1.3	57%	0.3	35%	0.2	36%	0.5	73%
SS dens <sup>b</sup>	75	83%	75	94%	164	98%	329	68%	186	85%	214	98%

<sup>a</sup> Data corresponding to the 2006 sampling campaign.

<sup>b</sup> Data corresponding to the 2006-2007 sampling campaigns.



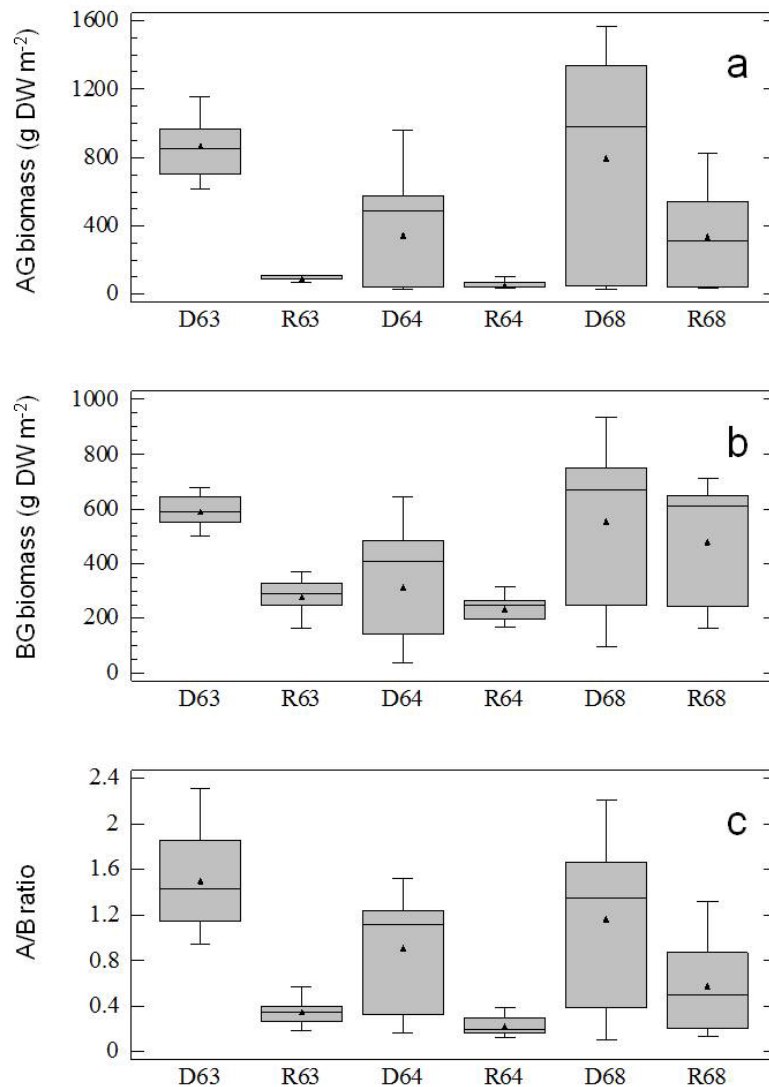


Figure 3.6. Intra-annual variability of seagrass aboveground biomass (a), belowground biomass (b), and aboveground/belowground ratio (c) across *T. testudinum* vegetation classes (i.e. supervised classification) in Bahia de la Ascension during 2006. Mean is represented by a triangle and median is the horizontal line into the box, 25th and 75th percentiles are the top and bottom of the box, while the 5th and 95th are located on the tips of the whiskers. The labels on x-axis: 1<sup>st</sup> letter represents the climatic season (D= dry; R= rainy); 1<sup>st</sup> number designs the year of sampling campaign (only 2006 field work available for these parameters); the 2<sup>nd</sup> number denotes the corresponding class according to the supervised classification of *T. testudinum* depicted in Figure 3.3.

### Leaf length and width

The length of *Thalassia* leaves showed a clear seasonal variability, characterized by statistically significant shorter blades in the rainy season across the bay. This intra-annual pattern was more apparent in the inlet zone (i.e., Cayo Culebras, class 8). Class 8 *Thalassia* exhibited the longest blades, with median length of 26.3 cm and 13.1 cm for dry and rainy seasons, respectively. *Thalassia* leaves developing in Cayo Culebras were characterized by an ample variability in both seasons, yielding coefficients of variation of 54.65% and 45.14% in dry and rainy seasons, respectively. This variable growth was clearly more marked during dry season, which varied within the interval of 3.9-35.3 cm (Fig. 3.7a).

A similar overall pattern to that portrayed by blades length was observed with the leaf width, featuring consistently more variable (CV= 57.70 % and 47.22 % in dry and rainy seasons, respectively) and wider leaves in *Thalassia* individuals growing in Cayo Culebras than in other classes during both seasonal campaigns (Fig. 3.7b). The seasonal difference in blade width was however not as great as was seen in blade lengths, particularly in Cayo Culebras, where no significant differences were detected between medians for both seasons.

### Abundance and shoot density

Overall, the median abundance of *T. testudinum* depicted a spatial pattern of lower abundance in the inner-most zone of the bay and increased abundance near the boundary of the adjacent reef lagoon (Fig. 3.8a). Temporal fluctuations were characterized by peak abundances during the dry season and lower abundance in the rainy season. This seasonality was more consistent in classes 4 and 8, although *Thalassia* abundances in the central basin (class 4) dropped more abruptly during rainy season.

The shoot density showed a trend of increasing numbers both seasonally and interannually during the two years of this study: densities were higher during the rainy season compared to dry season. The comparison amongst medians utilizing the Kruskal-Wallis Test indicates that differences (e.g., intra-annual and interannual) in the bay's interior and central basin are statistically significant at the 95% confidence level. This pattern, however, was more evident in the Vigia Grande zone (class 3), which exhibited a

low median density of shoots in the 2006 dry season ( $64 \text{ m}^{-2}$ ), intermediate densities in the 2006 rainy season and 2007 dry season (261 and  $323 \text{ shoots m}^{-2}$ , respectively; no significant differences between each other), and significant peak shoot densities ( $748 \text{ shoots m}^{-2}$ ) during the 2007 rainy season (Fig. 3.8b). This latter value is the highest median density of shoots recorded among the three zones of Bahia de la Ascension in this study.

The same pattern of increasing shoot densities during rainy season campaigns and during 2007 with respect to the preceding year was evident both in the central basin (class 4) and towards the sea boundary of the bay (class 8), although greater variability was recorded at this location compared to the other zones. Furthermore, no significant differences were observed among samplings in CC, as the medians estimated during both seasons in 2007 were nearly the same (Fig. 3.8b).

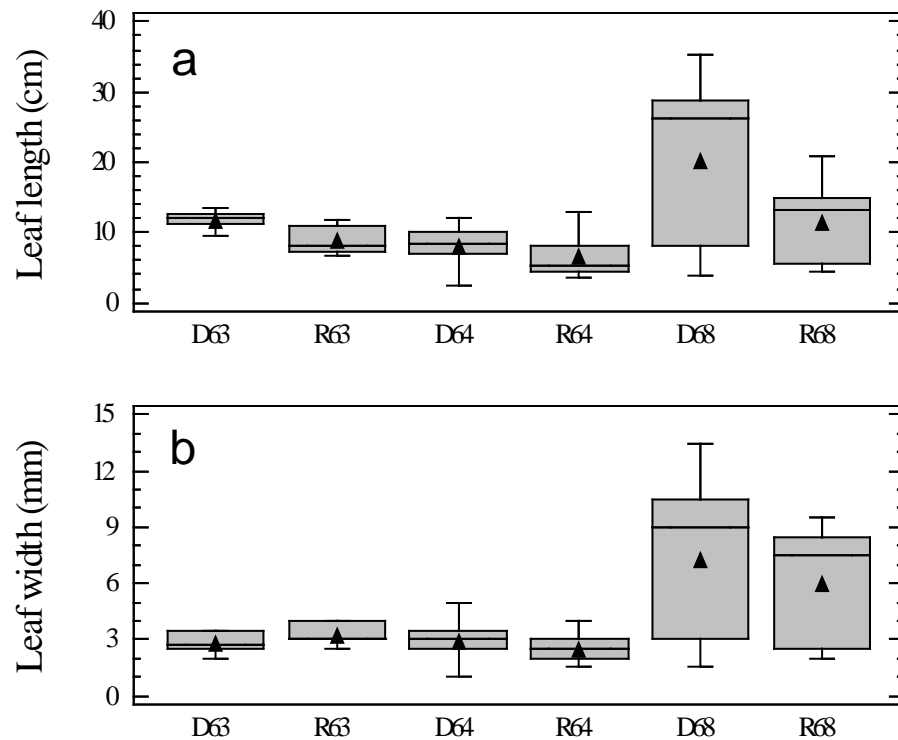


Figure 3.7. Intra-annual variability of *Thalassia* leaf morphometry across vegetation classes (i.e. supervised classification) in Bahia de la Ascension during 2006. Mean is represented by a triangle and median is the horizontal line into the box, 25th and 75th percentiles are the top and bottom of the box, while the 5th and 95th are located on the tips of the whiskers. The labels on x-axis are as follows: 1<sup>st</sup> letter represents the climatic season (D= dry; R= rainy); 1<sup>st</sup> number designs the year of sampling campaign (only 2006 field work available for these parameters); the 2<sup>nd</sup> number denotes the corresponding class according to the supervised classification of *T. testudinum* depicted on figure 3.3.

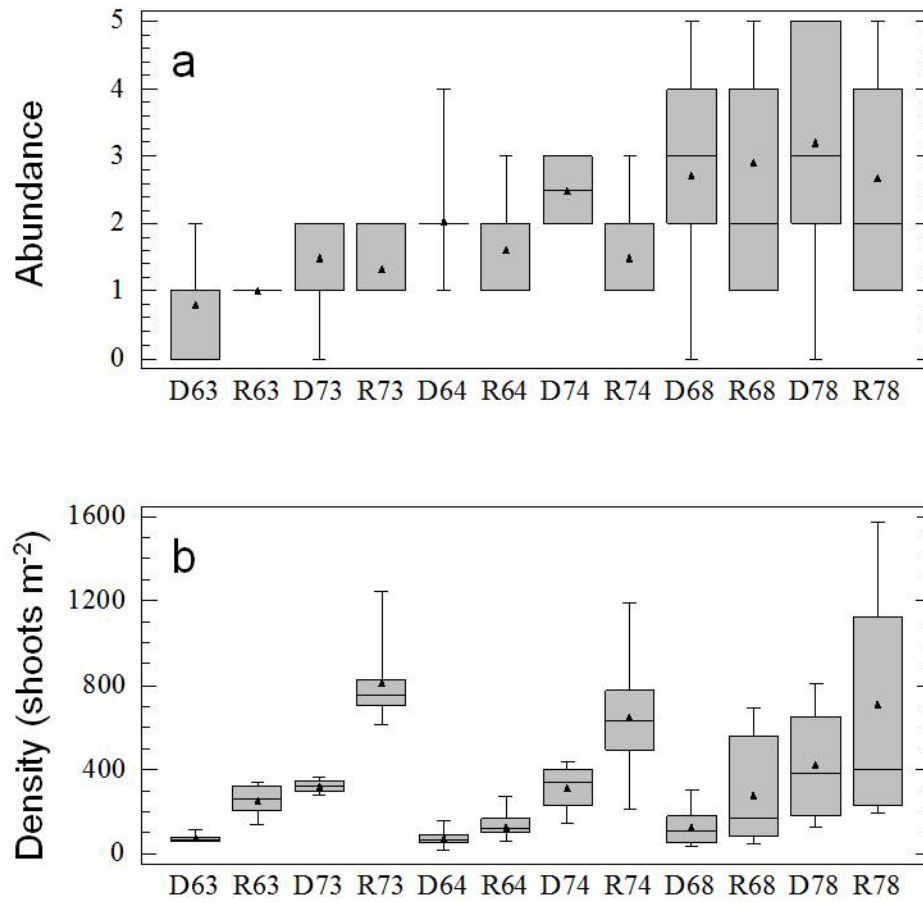


Figure 3.8. Seasonal variability of *Thalassia* abundance (given in Braun-Blanquet scores) and shoot density across vegetation classes (i.e. supervised classification) in Bahia de la Ascension during 2006-2007. Mean is represented by a triangle and median is the horizontal line into the box, 25th and 75th percentiles are the top and bottom of the box, while the 5th and 95th are located on the tips of the whiskers. The labels on x-axis: 1<sup>st</sup> letter represents the climatic season (D= dry; R= rainy); 1<sup>st</sup> number designs the year of sampling campaign (2006 or 2007); the 2<sup>nd</sup> number denotes the corresponding class according to the supervised classification of *T. testudinum* depicted in Figure 3.3.

## Discussion

The seagrass *Thalassia testudinum* is widely distributed across Bahia de la Ascension (BA) occupying  $\approx 90\%$  of the system's floor. Despite the spatial-temporal varying nature of the hydrodynamic forcing and freshwater input, implying a highly fluctuating distribution of relevant resources for the vegetation stands within the system and thus, featuring a heterogeneous physical environment, this stenohaline species (Zieman 1975) colonized from the marine-influenced zone in the seaward boundary and central basin to the bay's interior, where copious freshwater discharge contributes to establish a recurrent nutrient-enriched, mesohaline climate.

The average *T. testudinum* aboveground biomass of  $399.3 \text{ g DW m}^{-2}$  recorded in Bahia de la Ascension is higher than the mean value of  $214 \text{ g DW m}^{-2}$  estimated for this species on a global context, whilst the average belowground biomass of  $402.8 \text{ g DW m}^{-2}$  is consistent with the mean biomass ( $400 \text{ g DW m}^{-2}$ ) reported for the world's *Thalassia* meadows (Duarte and Chiscano 1999). Total median biomass of  $1,004 \pm 686 \text{ g DW m}^{-2}$  in BA is also within the range of biomasses estimated for other *Thalassia* stands in the Caribbean ( $1,045.1 \text{ g DW m}^{-2}$  in Discovery Bay, Jamaica; Gayle and Woodley 1998). However, average biomass of  $4,116 \text{ g DW m}^{-2}$  (Koltes et al. 1998 for Carrie Bow Cay, Belize, a mangrove cay with low freshwater drainage about 300 km south of this site) is well above the mean biomass measured in BA (Table 3.5). These *T. testudinum* biomass differences across the Caribbean emphasize the high site-specific variability of the species.

Moreover, *Thalassia* showed significant differences in biomass, leaf size, as well as shoot density and abundance levels among zones (classes) within Bahia de la Ascension. The variation in patterns of structural, morphometric, and individual growth exhibited by the clonal population across the bay were related to differential resource availability and fluctuations in the magnitude of distinct stressors within the system (Bell and Tomlinson 1980). The *Thalassia* biomass in the Vigia Grande embayment supports the preceding assumption. Even though this subsystem receives abundant nutrients through surface discharges and submerged springs to this subsystem, the associated low salinity prevented the seagrass from attaining a more developed biomass, compared to the *Thalassia* beds in the coastal lagoon of Twin Cays about 320 km to the south of in Bahia

de la Ascension, in the western Caribbean. Koltes et al. (1998) reported *Thalassia* biomass of  $4,116 \pm 681$  g DW  $m^{-2}$  in summer in Twin Cays, one of the highest for this species. This seagrass meadow lies near mangrove communities and such a high biomass level might be a result of outwelling from the adjacent mangrove. It is important to note that the site in Belize is lacking significant freshwater input, in contrast to the bed developing in Vigia Grande, where freshwater supply was coupled with intense inorganic nutrients and CDOM input (Tables 3.2-3.4).

Table 3.5. Average biomasses (g DW  $m^{-2}$ ) and short shoot densities ( $m^{-2}$ ) in shallow ecosystems of the Gulf of Mexico and the Caribbean Sea. Information drawn from CARICOMP - Caribbean Coral Reef, Seagrass and Mangrove Sites (Kjerfve 1998), except for Hall et al. 1999.

Site	Total biomass (g DW $m^{-2}$ )	Shoot density ( $m^{-2}$ )	Authors
Bahia de la Ascension, Mexico	1000.2	579.5	Current study
Carrie Bow Cay, Belize	4321.9	1010	Koltes et al. 1998
Cayo Coco, Cuba	1522.7	660	Alcolado et al. 1998
Discovery bay, Jamaica	1045.1	--	Gayle and Woodley 1998
Puerto Morelos, Mexico	1409.7	510	Ruiz-Renteria et al. 1998
Florida Bay, U.S.A.	46	539.3	Hall et al. 1999

In contrast to other studies carried out in the northeastern Gulf of Mexico reporting virtually no influence of groundwater over the seagrass meadows (Rutkowski et al. 1999), the relevance of groundwater discharges on the seagrass development has been consistently observed on the coast of the Yucatan Peninsula (Carruthers et al. 2005; Medina-Gomez and Herrera-Silveira 2006; Mutchler et al. 2007). Groundwater discharge has a great potential to alter the nutrient status within the coastal systems of the Yucatan, which is particularly important to long-life cycle seagrass species such as *Thalassia testudinum*. In the coastal ecosystems of the Mexican Caribbean the precipitation regime strongly controls the chemical composition of *Thalassia* leaves, as peak phosphorus concentrations on leaf tissue are related to heavy rainfall events (Carruthers et al. 2005). That inland nutrients are actually moving into the coastal systems through biological communities along the Mexican Caribbean (e.g., SAV) emphasizes the need to clarify more accurately the implications of such alterations on the nutrient status of its habitats.

Although the main external nutrients delivery in Bahia de la Ascension is arguably explained by groundwater, unlike other coastal lagoons of the Yucatan Peninsula (Herrera-Silveira and Comin 1995; Medina-Gomez and Herrera-Silveira 2003; Young et al. 2008), a joint freshwater supply from both submerged discharges (SGD) and surface channels sourced inland through fractures in the regional aquifer (Beddows 2004) operates in this ecosystem. The variable residence time of this groundwater remains within the wetlands may induce substantial changes on its hydrographic properties (e.g. CDOM enrichment, pH lowering, heat gain through sun radiation) before the water is advected into Bahia de la Ascension. This functional coupling between the mangrove forest and seagrass meadows is a common feature in coastal landscapes where such ecosystems coexist along a biological corridor as in Bahia de la Ascension (Hemminga et al. 1994).

Moreover, peak phosphate concentration of  $\approx 7 \mu\text{M}$  determined in the water column of the freshwater-influenced bay's interior in dry season 2007 is exceptionally high for karst environments as the Yucatan Peninsula (Herrera-Silveira and Comin 1995; Medina-Gomez and Herrera-Silveira 2003; Valdes and Real 2004), where P is readily removed from the water column by precipitation in the presence of calcium (Cable et al. 2002). Even the  $\text{PO}_4^{-3}$  concentrations observed during the rainy season 2007 of up to  $\approx 2 \mu\text{M}$  seem higher compared to those reported in other karst tropical coastal lagoons when the mesohaline condition of the inner bay is considered, as higher phosphate adsorption by calcite occurs under low salinity conditions in karstified environments (Millero et al. 2001).

It is thought that such phosphate levels are associated with benthic decomposition of the organic matter channelized through surface streams into VG, as P fluxes from sediments to interstitial water (and further to the water column by wind-driven resuspension or bioturbation) are significantly correlated with the organic matter content in the substrate (Valdes and Real 1994). Besides, phosphate availability has been widely recognized as limiting the seagrass development in biogenic carbonate substrates (Fourqurean et al. 1992) and positive relationships have been reported between *Thalassia* biomass and productivity, and phosphate additions to the ambient (Herbert and Fourqurean 2009). Thus, *Thalassia* beds growing within VG embayment may benefit, at least seasonally, from the organic material discharge into the system. Both low salinity and seagrass roots



uptake may explain lower water column SRP concentrations during rainy season 2007, when rainfall associated with the hurricane Dean was recorded (Chapter I). Deviation from this seasonal pattern in Cayo Culebras may be due to that this zone is rather sea-influenced than VG and CB (Fig. 3.5).

The rainy season aboveground biomass in the partially enclosed and wetland-influenced Vigia Grande embayment is at the upper level of standing crop reported for *Thalassia* (50-80 g DW m<sup>-2</sup>) adjacent to a mangrove waterway located 132 km to the north of Bahia de la Ascension along the Mexican Caribbean (Ruiz-Renteria et al. 1998). Also, the average total biomass recorded in Vigia Grande during the 2006 dry season (1461.23 DW m<sup>-2</sup>) is well above the biomass level (295.9 DW m<sup>-2</sup>) reported for a freshwater-influenced *Thalassia* bed in Manatee Bay, Florida (Irlandi et al. 2002). On the other hand, the mean biomass of 366.4 DW m<sup>-2</sup> for this inner section of the bay during the rainy sampling campaign is comparable to the values observed in Florida (Irlandi et al. 2002).

The significant development exhibited by *Thalassia testudinum* at the inner bay might be explained not only because of the nutrients supply from neighboring ecosystems, but also due to its circulation characteristics. Indeed, the reduced tidal energy input and wind-driven circulation featuring this embayment (Chapter II) may effectively enhance availability of the allochthonous supply (e.g., inorganic nutrients, CDOM) for further vegetation uptake into Vigia Grande. It is argued that both increased residence times within VG subsystem, along with wind stirring leading to a thickness reduction of the diffusion boundary layer onto leaves (e.g., breakdown of assimilation gradients), would favor carbon availability and nutrients influx to plants and consequently, a high overall net growth of the vegetation in this site (Koch 1994; Cornelisen and Thomas 2004).

Also, despite silicate concentrations in Vigia Grande subsystem were consistently above those recorded in the CB and CC along the 2006-2007 campaigns, the relatively lower silicate values observed in this embayment during rainy season compared to that in dry season seems to disagree the most typical condition found in the Yucatan, as groundwater discharges (SGD) have been reported as the primary SRSi inputs in the coastal lagoons (Herrera-Silveira and Comin 1995). Alternatively, prominent concentrations during dry season in the circulation-constrained VG embayment might be a result of peak

evaporation rate during droughts, which along with these ions affinity to remain in solution for long, would lead to an apparent silicate increase during the droughts period (Jacobs et al. 2008). Yet in the inner-most bay, the previous mechanism would represent another link between the hydrodynamics and the nutrients status in Bahia de la Ascension that awaits further observations and validation.

Seagrass populations growing in such circulation-limited systems are, however, more susceptible to deterioration of its water quality, either due to excessive nutrient delivery (e.g., eutrophication) or high organic matter loading and accumulation, which may lead to a high sulfide concentration in the sediments and thus, an overall decrease in the health of *Thalassia testudinum* stands (Tomasko et al. 1996; Eldridge et al. 2004). This subtle equilibrium between the health of the seagrass bed growing in Vigia Grande and its hydrodynamics emphasizes the importance of easterlies-induced residual circulation within this embayment, which has proven to be a primary factor controlling net water displacement (e.g., residual flow) between the inner bay and the main bay (Chapter II).

The average *Thalassia* shoot length (10-15 cm) in the Vigia Grande embayment, along with the extent of lignification of the roots/rhizome system (buried about 30 cm deep in the fine-sand sediment), suggests this is actually a mature population developing under mesohaline conditions. Yet, a poor transparency regime within the water column and pervasive osmotic stress of this shallow subsystem constrains shoot production, which showed sparse distribution with a scheme of small, radial-growing patches (50 cm average diameter), separated by ample bare soil spaces. This sparse distribution of the *Thalassia testudinum* stand in Vigia Grande is consistent with the lowest salinity-tolerance limit reported for this species (Moore 1963).

The median shoot density of  $\approx 580$  shoots  $m^{-2}$  in Bahia de la Ascension is well below the number of individuals reported for a dense *Thalassia* bed in Carrie Bow Cay (1,010 shoots  $m^{-2}$ ), but above the densities regionally observed across the Caribbean (Table 3.5). On the other hand, the unusually high density recorded in the bay's interior during the 2007 rainy season (a maximum of 1,250 shoots  $m^{-2}$ ) is comparable to that reported by Koltes et al. (1998) for *T. testudinum* occurring interspersed with *S. filiforme* and a calcareous algae

across a shallow shelf in the western Caribbean ( $960 \pm 250 \text{ m}^{-2}$ ); a bed characterized by deep sediment ( $\geq 1 \text{ m}$ ) and high-nutrient delivery from the adjacent mangrove community

Peak number of *T. testudinum* shoots in Vigia Grande lagoon during the 2007 rainy season might be attributed to the significant organic material input following the passage of Hurricane Dean. While low and less variable  $\text{NO}_3^-$  concentrations in the 2006 dry season might be explained through prevailing high denitrification rates enhanced by a temperature rise in the water column (e.g., ammonium, a reduced nitrogen species, exhibited higher mean concentrations and greater variability in Vigia Grande relative to the central basin and Cayo Culebras for both seasons at 2006 and 2007), diminished  $\text{NO}_3^-$  values during the 2007 rainy season are likely due to Hurricane Dean. As previously explained, in addition to submerged groundwater discharge directly to the bay, surface channels drain water into Vigia Grande as the result of fissures in the limestone located several kilometers from the discharge point. Since a relatively greater amount of the damage generated by hurricanes is carried out well inland by winds (Cablak et al. 1994; Smith et al. 1994) rather than the storm surge itself (e.g., highly focused along the coast), it is likely that an enhanced delivery of denuded organic matter into the system occurred during the hurricane passage due to the amount of vegetation debris produced.

Remineralization of the hurricane-associated organic matter load to Vigia Grande embayment was at the expenses of dissolved oxygen and nitrate, both parameters showing an evident decline in Vigia Grande during rainy season 2007 (Figs. 3.4c and 3.5a). Additionally, the evident seasonal behavior of ammonium both in the central bay and Cayo Culebras during the 2007 sampling campaign (e.g., no seasonal pattern in VG as substantial organic matter supply is likely a perennial trait), featuring maximum  $\text{NH}_4^+$  concentrations in rainy season may be also tied to the bacterial-mediated organic matter breakdown (e.g., denitrification) and further advection-diffusion towards the seaward boundary of Bahia de la Ascension.

In the opposite direction from VG (i.e., seaward), *Thalassia testudinum* co-occur with *Halodule wrightii* in a mixed vegetation community windward of Cayo Culebras (CC), a small, NW-SE lying sandy cay with well-developed mangrove cover (e.g. *Rhizophora mangle*, *Conocarpus erectus*, and *Laguncularia racemosa*) contiguous to the reef lagoon,

which divides the bay's ocean front into a northern and southern portion. The shallow (<0.6 m) and sheltered bay side of Cayo Culebras had the most developed *T. testudinum* stand in Bahia de la Ascension, suggesting that the benign conditions, calm waters and fine-grained, deep sediments ( $\geq 1$  m) found in this zone might enhance the recycling of organic matter and suitable rhizome development. A higher survival rate has been reported for short shoots inhabiting low exposure localities such as back-reef zones, rather than those developing on the reef lagoon and along the coastal edge in other *Thalassia* meadows of the Mexican Caribbean (van Tussenbroek 1994).

Although Vigia Grande and Cayo Culebras show similar average depth (0.5 m and 0.6 m, respectively) and arguably both locations receive daily saturating light levels, they harbor quite different *Thalassia* beds, not only in terms of shoot distribution and abundance, but also in terms of their leaf morphometric characteristics (Table 3.4). It is thought that the contrasting patterns exhibited by *Thalassia testudinum* at these sites are a function of the frequency and magnitude with which their particular environmental pressure schemes operate, combined with the inherent ability of *Thalassia* to recover from disturbances. This claim is supported by the relatively shorter and narrower blades observed on *Thalassia* individuals growing in Vigia Grande compared to those collected seaward of Cayo Culebras (Fig. 3.7). An inverse relationship between the width of *Thalassia* leaves and freshwater influence has been observed in Biscayne Bay, Florida as well (Irlandi et al. 2002), suggesting that the leaf morphologic traits recorded from shoots developing in Vigia Grande are tied to the freshwater input in the bay's interior.

Some salient characteristics in Bahia de la Ascension resemble that described for Florida bay. As in this estuarine lagoon system (Nuttle et al. 2000), circulation in BA is restricted in some inner sub-basins due to geomorphology traits and microtidal regime. Both ecosystems are influenced by a marked dry-wet seasonality and are downstream from large watersheds. They have mangrove wetlands along their landward boundary, and harbor dense seagrass stands and low phytoplankton development. In general, BA tends to be more nutrient enriched than the oligotrophic Florida Bay, due to the importance of groundwater discharge and because marsh filtration is absent in the Sian Ka'an Biological Reserve.

The shoot density increase observed in BA during the rainy season was coupled with an abrupt reduction in abundance (Figures 3.7a and 3.9b), indicating that these new recruited individuals were downsized (e.g., length and width) compared to those present in the dry season. However, all sampling stations had a drastic decrease in the aboveground/belowground ratio, indicating that the belowground biomass was less significantly affected by the seasonal change (Fig. 3.5b). One could argue that the significant inorganic nutrients and dissolved organic matter delivered to Vigia Grande early in the rainy season (i.e. when accumulated enriched material is removed from surrounding systems) may have stimulated shoot recruitment. Furthermore, these vegetatively produced individuals may grow throughout the rainy season by producing new blades and thus sustain an overall abundance increase together with shoot density (Fig. 3.7a). Further meteorological events during the rainy season – tropical storms or a strong hurricane in late summer – may lead to a decline in shoot density; whilst the development of surviving shoots through the translocation of non-structural carbon are enhanced (Burke et al. 1996). This might be a consequence of both the high freshwater flux and water-borne nutrients associated with hurricanes and a rapid colonization by young shoots in the available open spaces on the substrate.

When comparing the shoot density observed before and after Hurricane Dean in August 2007, an increase in the number of individuals in Vigia Grande (class 3) and central basin (class 4) was found. However, this seasonal pattern of shoot density is less evident towards the bay's seaward boundary (Fig. 3.7b). It may be due to the shelter provided by this meadow and because the influence of the freshwater flux is dampened as it gets closer to the ocean front. While a steep decline in abundance was observed at all sites (Fig. 3.7a), in the cay and Vigia Grande these decreases were not significantly different from those observed at these same sites in the preceding dry season. This relationship suggests that strong wind stress accompanying this cyclone trimmed out the canopy cover to the levels observed during the October 2007 campaign, apparently on a larger extent at the open spaces (e.g., central basin) than at the bay's interior (e.g., Vigia Grande) and sheltered locations (e.g., Cayo Culebras).

These results suggest that the *Thalassia* stand growing in Vigia Grande transforms the environmental pressure into a dual stress: osmotic and light stress (this latter deduced

from the shallowness and prevalent wind stress over the embayment), without the possibility of a useful steady ecophysiological adjustment. This prevalent condition would ultimately result in relatively more restricted limits to individuals inhabiting this embayment (e.g., statistical variability), in terms of their structure in a given climatic season compared to that observed in the *Thalassia* bed developing in Cayo Culebras (see coefficients of variation in Table 3.4 for each class). The optimum environmental status pertaining to Cayo Culebras allows the vegetation growing in this zone not only to display a larger variability, but also preserve its structural traits across successive seasons. As a consequence, a comparatively more stable seasonal growth pattern will be exhibited by this marine-influenced meadow than the *Thalassia* thriving in the bay's interior (i.e., marked seasonal differences in all the structural parameters; Figures 3.6-3.8).

It is thought that the current study gives a basic understanding about the most relevant processes molding the observed patterns of variability in *T. testudinum* structure. This knowledge will help natural resources managers gather new relevant information from landscape features present across Bahia de la Ascension, in order to design and implement an effective management program to quantify and maintain the environmental health of the seagrass habitat. One essential aim of such a framework should be to accomplish not only the preservation of the vegetation abundance and coverage, but also to maintain the biological diversity of the seagrasses to such a level that the structural integrity and optimal ecological value of this community for the biological assemblages inhabiting it are ensured.

## **Conclusions**

Investigating the responses of *Thalassia testudinum* biomass, shoot densities, and abundance to the environmental variability in the karst, shallow coastal bay of Bahia de la Ascension revealed the plasticity of this species, which was found inhabiting a wide range of salinity levels across the system, from marine to permanently mesohaline ambient (salinity <16), yielding in this latter environment a peak total biomass of 1,800 g DW m<sup>-2</sup> in the dry season. Also, seasonal shoot recruitment coincided with peak nutrients delivered during the rainy season, with maximum average density of shoots in the mesohaline

embayment Vigia Grande following a strong hurricane. Conversely, *Thalassia* stand developing in Vigia Grande exhibited narrower biomass variability compared to that of the seagrass beds inhabiting the central basin and the inlet zone.

The exogenous nutrients and organic material supply to Vigia Grande embayment, in the inner-most bay, is likely the main reason that *Thalassia testudinum* is able to develop under such low-salinity ambient and exhibit biomass levels, numbers of individuals, and aerial/belowground biomass ratios comparable to the seagrass growing in the more optimum environment of Cayo Culebras, in the inlet zone. Whilst the hydrographic setting of this embayment adds environmental pressure to the aquatic vegetation, including increased turbidity and low salinity, this monotypic bed displays a set of ecological mechanisms to withstand environmental fluctuations. Thus, the seagrass *Thalassia testudinum* developing in Vigia Grande turn this fluctuating environment into a more stable habitat that may be readily exploited by other macrophyte dwellers. Finally, the proximity of the seagrass bed growing in Vigia Grande to the terrestrial-hydroscape interface defines the higher sensitivity of this vegetation stand to changes in the watershed compared to the plants developing in the central basin and Cayo Culebras.

## CHAPTER IV

### CONCLUSIONS

Along the karstified Yucatan coastal zone the spatial-temporal trends in hydrographic properties are regulated by the fresh water input via underground conduits that are recharged through precipitation. Thus, poor land-use practices in the watershed of the coastal zone as well as human activity throughout the coastal systems along the Caribbean can result in environmental disturbance. In the case of the Yucatan Peninsula (YP) the disturbance is redoubled because the main factor driving economic development of the Mexican Caribbean (eastern YP) is the massive tourism industry, which has led the so-called "Mayan Riviera" to experience one of the fastest growth rates in Latin America (5-year compound avg. annual population growth rate = 6.4%; INEGI 2008).

This study highlights the linkage between the hydrological heterogeneity of the shallow coastal bay, Bahia de la Ascension (BA), and the oceanographic component, as well as an evaluation of the highly interdependent nature of the seagrass *Thalassia testudinum* within the karstic bay. BA is located within UNESCO's Sian Ka'an Biosphere Reserve (SKBR) along the Mexican Caribbean. The analysis of water quality and climatologic data showed that the combined runoff and submerged groundwater discharge (SGD) into BA were greater than direct rainfall input and thus, has a greater potential to alter the seasonal salinity variations within the system. This hydrometeorological control on the hydrographic patterns also includes hurricanes, which may influence the interannual precipitation variability up to 36%, suggesting that alterations in both the magnitude and frequency of these atmospheric processes may drive substantial changes on the salinity spatial gradients within BA.

The dominance of runoff plus SGD established a marked horizontal SW-NE estuarine salinity gradient in BA and also affected tidally-driven exchange, as tidal energy is attenuated in the inner bay. On the other hand, the barotropic model made evident that Trades and southeasterly winds enhanced the residual flow in the system's interior, emphasizing the relevance of short-term meteorological forcing on the flushing



characteristics of the brackish and nutrient-enriched southwest inner bay. Therefore, while the salinity regime in the reef lagoon and the bay's central basin is strongly affected by tides, the salinity at the inner bay is controlled by the freshwater variability, which is strongly modulated by short-term (wind stress) and intra-annual (e.g., hurricanes) processes. Events occurring over broader time-scales (e.g., ENSO, La Niña) may also have far-reaching indirect consequences on the spatial patterns of salinity due to their influence on regional rainfall.

*Thalassia testudinum*, which is widely recognized as a stenohaline seagrass species, was able to grow in the mangrove-fringed, mesohaline inner bay, although environmental stress was evidenced in morphometric traits, as leaf lengths and widths were positively correlated with the SW-NE salinity gradient. However, comparable biomass levels were seen in the southwest (mesohaline) and northeast (marine-influenced) extremes of BA. Aerial biomass showed marked differences between dry and rainy seasons along the bay; the seasonal pattern varied negatively with salinity, while the variability within sites exhibited an opposite trend along the SW-NE bay's axis.

A seemingly spatial-temporal pattern was depicted by the belowground component, yet only the inner bay showed statistically significant seasonal differences. Indeed, the aboveground variability (peak aerial/belowground ratio >2.3) is a remarkable trait of the *Thalassia* bed growing in the mesohaline, inner zone compared to the aquatic vegetation developing in the main bay. The relationship between nutrient distribution and above/belowground ratio suggested that *Thalassia* favors development of the aerial component as nutrients availability increases.

*Thalassia* average total biomass of  $1,004 \pm 686$  g DW m<sup>-2</sup> in BA is within values reported for other coastal zones in the Caribbean, but below that of beds growing in nearby southern mangrove cays having low freshwater input. Mean shoot density in BA is  $589 \pm 328$  m<sup>-2</sup>, with peak values during rainy season, a feature more pronounced in the inner bay's environment of low salinity-high nutrients regime, dampened tidal influence, and wind-driven residual circulation. Also, *Thalassia* abundance exhibited a consistent inverse correlation with density during both dry and rainy seasons, except for the southwestern-

most system. This contrasting pattern between density and abundance was more salient following passage of a strong hurricane affecting the SKBR.

These results show that the ecological integrity of the seagrass *T. testudinum* habitat is largely based upon a balance among physical processes. Indeed, despite this species ability to tolerate low salinities because of the high nutrient inputs occurring at the inner, wetland-influenced bay, the mesohaline ambient may inhibit the increase of areal coverage (i.e., abundance) as well as favor the development of other typical brackish species (e.g., *Ruppia maritima*). Thus, it is argued that man-induced modifications on this subtle balance will have undesirable consequences for the overall health condition of the seagrass habitat in Bahia de la Ascension.

BA is part of a natural protected area, SKBR; however, it may be impacted by tourism-related development occurring outside the Reserve. The high functional connectivity between coastal ecosystems on this karstified environment creates the possibility for water quality to be adversely modified through potential pollution of the water supply, which would impact this site and the Reserve. This in turn would negatively affect the fledgling tourism beginning within the region of Bahia de la Ascension.

## REFERENCES

- Aceves, M., 1976. Recurso Agua. In: Estudio Geográfico y Socioeconómico del Estado de Quintana Roo. Boletín de la Sociedad Mexicana de Geografía y Estadística. Tomo 1 Capítulo III. México, D.F., p. 121.
- Arellano, L., 2010. Caracterización especial de la distribución de *Thalassia testudinum* (Banks ex König) en una bahía tropical, México. Tesis de Doctorado. Centro de Investigación y de Estudios Avanzados del Instituto Politécnico Nacional, Unidad Mérida.
- Back, W., Hanshaw, B.B., 1970. Comparison of chemical hydrogeology of the carbonate Peninsulas of Florida and Yucatan. *Journal of Hydrology* 10, 330-368.
- Back, W., Hanshaw, B.B., Pyle, T.E., Plummer, L.N., Weidie, A.E., 1979. Geochemical significance of groundwater discharge and carbonate solution to the formation of Caleta Xel Ha, Quintana Roo, Mexico. *Water Resources Research* 15(6), 1521-1535.
- Beddows, P.A., 2003. Yucatan Phreas, Mexico. In: Gunn, J. (Ed.), *Encyclopedia of cave and karst science*, Routledge Taylor & Francis Group, New York, 786-788.
- Beddows, P.A., 2004. Groundwater hydrology of a coastal conduit carbonate aquifer: Caribbean Coast of the Yucatan Peninsula, México, Mexico. PhD dissertation. University of Bristol, UK. xix. 303 pp.
- Beddows, P.A., Smart, P.L., Whitaker, F.F., Smith, S.L., 2007. Decoupled fresh-saline groundwater circulation of a coastal carbonate aquifer: spatial patterns of temperature and specific electrical conductivity. *Journal of Hydrology* 346, 18-32.
- Bell, A.D., Tomlinson, P.B., 1980. Adaptive architecture in rhizomatous plants. *Botanical Journal of the Linnean Society* 80, 125-160.
- Blake, E.S., Rappaport, E.N., Landsea, C.W., 2007. The deadliest, costliest and most intense United States tropical cyclones from 1851 to 2006 (and other frequently requested hurricane facts). NOAA, Technical Memorandum NWS-TPC-4, 48 pp.
- Blanco, J.A., Vilorio, E.A., Narváez, J.C., 2006. ENSO and salinity changes in the Ciénaga Grande de Santa Marta coastal lagoon system, Colombian Caribbean. *Estuarine, Coastal and Shelf Science* 66, 157-167.
- Bloomfield A.L., Gillanders, B.M., 2005. Fish and invertebrate assemblages in seagrass, mangrove, saltmarsh, and nonvegetated habitats. *Estuaries* 28 (1), 63-77.
- Brown, C.A., Holt, S.A., Jackson, G.A., Brooks, D.A., Holt, G.H., 2004. Simulating larval supply to estuarine nursery areas: how important are physical processes to the supply of larvae to the Aransas Pass Inlet. *Fisheries Oceanography* 13, 181-196.
- Burke, M.K., Dennison, W.C., Moore, K.A., 1996. Non-structural carbohydrate reserves of eelgrass *Zostera marina*. *Marine Ecology Progress Series* 137, 195-201.
- Butterlin, J., 1958. Reconocimiento geológico preliminar del Territorio de Quintana Roo. *Boletín de la Asociación Mexicana de Geólogos Petroleros* 10, 531-570.

- Cable, J.E., Reide-Corbett, D., Walsh, M.M., 2002. Phosphate uptake in coastal limestone aquifers: a fresh look at wastewater management. *Limnology and Oceanography Bulletin* 11, 29-32.
- Cablk, M.E., Kjerfve, B., Michener, W.K., Jensen, J.R., 1994. Impacts of hurricane Hugo on a coastal forest: assessment using Landsat TM data. *Geocarto International* 2, 15-24.
- Caribbean Coastal Marine Productivity (CARICOMP). Methods manual, levels 1 and 2: manual of methods for mapping and monitoring of physical and biological parameters in the coastal zone of the Caribbean. Centre for Marine Sciences, University of the West Indies, Mona, Kingston, Jamaica and Florida Institute of Oceanography, University of South Florida, St. Petersburg Florida, U.S.A.; March 2001.
- Carruthers, T.J.B., van Tussenbroek, B.I., Dennison, W.C., 2005. Influence of submarine springs and wastewater on nutrient dynamics of Caribbean seagrass meadows. *Estuarine Coastal and Shelf Science* 64(2-3), 191–199.
- Chambers, P.A., Prepas, E.E., Hamilton, H.R., Bothwell, M.L., 1991. Current velocity and its effect on aquatic macrophytes in flowing waters. *Ecological Applications* 1, 249–257.
- Chiappa-Carrara, X., Sanvicente-Añorve, L., Monreal-Gomez, A., Salas de Leon, D., 2003. Ichthyoplankton distribution as an indicator of hydrodynamic conditions of a lagoon system in the Mexican Caribbean. *Journal of Plankton Research* 25(7), 687–696.
- CICESE, 2006. Programa de mareas en México; MAR V 0.70 for Windows 95/98/2000/XP.
- Cornelisen, C.D., Thomas, F.I.M., 2004. Ammonium and nitrate uptake by leaves of the seagrass *Thalassia testudinum*: impact of hydrodynamic regime and epiphyte cover on uptake rates. *Journal of Marine Systems* 49, 177-194.
- Costanza, R., d'Arge, R., de Groot, R., Farberk, S., Grasso, M., Hannon, B., Limburg, K., Naeem, S., O'Neill, R.V., Paruelo, J., Raskin, R.G., Sutton, P., van den Belt, M., 1997. The value of the world's ecosystem services and natural capital. *Nature* 387, 253-260.
- Cotton, J.A., Wharton, G., Bass, J.A.B., Heppell, C.M., Heppell, C.M., Wotton, R.S., 2006. The effects of seasonal changes to in-stream vegetation cover on patterns of flow and accumulation of sediment. *Geomorphology* 77, 320-334.
- Cowen, R.K., Paris, C.B., Srinivasan, A., 2006. Scaling of population connectivity in marine populations. *Science* 311, 522–527.
- David, L.T., Kjerfve, B., 1998. Tides and currents in a two-inlet coastal lagoon: Laguna de Terminos, Mexico. *Continental Shelf Research* 18, 1057-1079.
- Dawson, F. H., Robinson, W.N., 1984. Submersed macrophytes and the hydraulic roughness of a lowland chalkstream. *Verh. int. Ver. Limnol.* 22, 1944–1948.
- Delft3D-FLOW: Simulation of multi-dimensional hydrodynamic flows and transport phenomena, including sediments; User Manual. WL|Delft Hydraulics.
- Didger®, Version 3.02. 2001. ©Golden Software, Inc.

- Dronkers, J., Zimmerman, J.T.F., 1982. Some principles of mixing in tidal lagoons. *Oceanologica acta. Proceedings of the International Symposium on Coastal Lagoons, Bordeaux, France, 9–14 September, 1981*, p. 107–117.
- Duarte, C.M., Chiscano, C.L., 1999. Seagrass biomass and production: a reassessment. *Aquatic Botany* 65, 159-174.
- Edwards, F., 1989. Environmentally sound tourism development in the Caribbean. Banff Centre School Management. University of Calgary, 143 pp.
- Eldridge, P.M., Kaldy, J.E., Burd, A.B., 2004. Stress response model for the tropical seagrass *Thalassia testudinum*: The interactions of light temperature, sedimentation, and geochemistry. *Estuaries* 27(6), 923-937.
- Enriquez, C., Mariño-Tapia, I.J., Herrera-Silveira, J.A., 2010. Dispersion in the Yucatan coastal zone: implications for red tide events. *Continental Shelf Research* 30, 127-137.
- Espejel, J.J., 1983. Biología acuática: Descripción general de los recursos bióticos y económicos, pp. 195-214. In: Careaga, A. (Ed.), Sian Ka'an. Estudios preliminares de una zona en Quintana Roo propuesta como reserva de la biosfera. CIQRO-SEDUE.
- Fernandes, E.H.L., Dyer, K.R., Niencheski, L.F.H., 2001. TELEMAC-2D calibration and validation to the hydrodynamics of the Patos Lagoon (Brazil). *Journal of Coastal Research* 34, 470-488.
- Fourqurean, J.W., Zieman, J.C., Powell, G.V.N., 1992. Phosphorus limitation of primary production in Florida Bay: evidence from C:N:P ratios of the dominant seagrass *Thalassia testudinum*. *Limnology and Oceanography* 37, 162-171.
- Fourqurean, J.W., Robblee, M.B., 1999. Florida Bay: a history of recent ecological changes. *Estuaries* 22, 345-357.
- Fourqurean, J.W., Rutten, L.M., 2003. Monitoring of soft-bottom marine habitat on the regional scale: the competing goals of spatial and temporal resolution. In: Busch, D., Trexler, J.C. (Eds.), *Ecological monitoring of ecosystem initiatives*. pp 257-288. Island Press, Washington, DC.
- Franklin, J.L., 2008. Tropical cyclone report: Hurricane Dean. National Hurricane Center. NOAA Technical Report, NWS NHC AL042007, 23pp.
- García, E., 1988. Modificaciones al sistema de clasificación climática de Köppen para adaptarlo a las condiciones particulares de la República Mexicana. Offset Larios. UNAM, Instituto de Geografía. Mexico, D.F.
- Gasca, R., Suarez, E., 1994. Zooplankton biomass fluctuations in a Mexican Caribbean Bay (Bahía de la Ascension) during a year cycle. *Caribbean Journal of Science* 30, 116-123.
- Gayle, P.M.H., Woodley, J.D., 1998. CARICOMP: A Caribbean network of marine laboratories parks, and reserves for coastal monitoring and scientific collaboration. In: Kjerfve, B. (Ed.), *CARICOMP-Caribbean coral reef, seagrass and mangrove sites*. pp 17-33. UNESCO, Paris.
- Gordon, D.C., Boudreau, P.R., Mann, K.H., Ong, J.E., Silvert, W.L., Smith, S.V., Wattayakorn, G., Wulff, F., Yanagi, T., 1996. LOICZ biogeochemical modelling

- guidelines. LOICZ Reports & Studies No. 5, vi +96 pp. LOICZ, Texel, The Netherlands.
- Hall, M.O., Durako, M.J., Fourqurean, F.W., Zieman, J.C., 1999. Decadal changes in seagrass distribution and abundance in Florida Bay. *Estuaries* 22, 445-459.
- Hanshaw, B.B., Back, W., 1980. Chemical mass-wasting of the northern Yucatan Peninsula by groundwater dissolution. *Geology* 8(5), 222-224.
- Hemminga, M.A., Slim, F.J., Kazungu, J., Ganssen, G.M., Nieuwenhuize, J., Kruyt, N.M., 1994. Carbon outwelling from a mangrove forest with adjacent seagrass beds and corals reefs (Gazi Bay, Kenya). *Marine Ecology Progress Series* 106, 291-301.
- Hench, J.L., Leichter, J.J., Monismith, S.G., 2008. Episodic circulation and exchange in a wave-driven coral reef and lagoon system. *Limnology and Oceanography* 53, 2681-2694.
- Herbert, D.A., Fourqurean, J.W., 2009. Phosphorus availability and salinity control productivity and demography of the seagrass *Thalassia testudinum* in Florida Bay. *Estuaries and Coasts* 32, 188-201.
- Herrera-Silveira, J. A., Comin, F.A., 1995. Nutrient fluxes in a tropical coastal lagoon. *Ophelia* 42, 127-146.
- Holland, H.D., 1978. *The chemistry of the atmosphere and the oceans*. John Wiley & Sons, New York.
- Holmer, M., Bachmann-Olsen, A., 2002. Role of decomposition of mangrove and seagrass detritus in sediment carbon and nitrogen cycling in a tropical mangrove forest. *Marine Ecology Progress Series* 230, 87-101.
- INEGI. 2002. Bahía la Ascensión (E16A28) Q. Roo | 1:50,000 | México | INEGI.
- INEGI. 2008. Anuario Estadístico de Quintana Roo, edición 2008. INEGI.
- Irlandi, E., Orlando, B., Macia, S., Biber, P., Jones, T., Kaufman, L., Lirman, D., Patterson, E.T., 2002. The influence of freshwater runoff on biomass, morphometrics, and production of *Thalassia testudinum*. *Aquatic Botany* 72, 67-78.
- Isaaks, E. H., Srivastava, R. M., 1989. *An introduction to applied geostatistics*. Oxford Univ. Press.
- Jackson, I., 1986. Carrying capacity for tourism in small tropical Caribbean islands. *UNEP Industry Environment* 9(1), 7-10.
- Jacobs, S., Struyf, E., Maris, T., Meire, P., 2008. Spatiotemporal aspects of silica buffering in restored tidal marshes. *Estuarine, Coastal and Shelf Science* 80, 42-52.
- Jensen, J.R., 2007. *Remote sensing of the environment*. Prentice-Hall Series in Geographic Information Science. Upper Saddle River, NJ: Prentice Hall, pp. 203-9. ISBN 0-13-188950-8.
- Jickells, T.D., 1998. Nutrient biogeochemistry of the coastal zone. *Science* 281, 217-222.
- Kitheka, J.U., 1996. Water circulation and coastal trapping of brackish water in a tropical mangrove-dominated bay in Kenya. *Limnology and Oceanography* 41, 169-176.
- Kjerfve, B., 1981. Tides of the Caribbean Sea. *Journal of Geophysical Research* 86, 4243-4247.

- Kjerfve, B., 1986. Comparative oceanography of coastal lagoons, pp. 63-81. In: Wolfe, D.A. (Ed.), *Estuarine variability*. Academic Press, San Diego, CA.
- Kjerfve, B., 1990. Manual for investigation of hydrological processes in mangrove ecosystems. Research and its application to the management of the mangroves of Asia and the Pacific (RAS/86/120). UNESCO/UNDP Regional Project, pp. 40-45.
- Kjerfve, B., 1994. Coastal lagoon processes. Elsevier Oceanography Series, Amsterdam.
- Kjerfve, B., Miranda, L.B., Wolanski, E., 1991. Modelling water circulation in an estuary and intertidal salt marsh system. *Netherlands Journal of Sea Research* 28, 141-147.
- Koch, E.W., 1994. Hydrodynamics, diffusion-boundary layers and photosynthesis of the seagrasses *Thalassia testudinum* and *Cymodocea nodosa*. *Marine Biology* 118, 767-776.
- Koltes, K.H., Tschirky, J.J., Feller, I.C., 1998. CARICOMP: A Caribbean network of marine laboratories parks, and reserves for coastal monitoring and scientific collaboration. In: Kjerfve, B. (Ed.), *CARICOMP-Caribbean coral reef, seagrass and mangrove sites*. pp 79-94. UNESCO, Paris.
- Koppen, W., 1936. Climate classification system. In: McKnight, T.L., Hess, D. (Eds.), 2000. *Climate zones and types: the Köppen System, physical geography: A landscape appreciation*. Prentice Hall, Upper Saddle River, NJ. pp. 200-1. ISBN 0-13-020263-0.
- Lee, T.N., Rooth, C., Williams, E., McGowan, M., Szmant, A.F., Clarke, M.E., 1992. Influence of Florida current, gyres and wind-driven circulation on transport of larvae and recruitment in the Florida Keys coral reefs. *Continental Shelf Research* 12, 971-1002.
- Leichter, J.J., Stewart, H.L., Miller, S.L., 2003. Episodic nutrient transport to Florida coral reefs. *Limnology and Oceanography* 48, 1394-1407.
- Littler, D.S., Littler, M.M., 2000. *Caribbean reef plants: an identification guide to the reef plants of the Caribbean, Bahamas, Florida, and Gulf of Mexico*. OffShore Graphics Inc., Washington DC.
- Lipcius, R.N., Eggleston, D.B., Miller, D.L., Luhrs, T.C., 1998. The habitat-survival function for Caribbean spiny lobster: an inverted size effect and non-linearity in mixed algal and seagrass habitats. *Marine and Freshwater Research* 49(8), 807-816.
- Lopez-Ornat, A., 1983. Localizacion y medio fisico, pp. 21-49. In: Careaga, A. (Ed.), *Sian Ka'an. Estudios preliminares de una zona en Quintana Roo propuesta como reserva de la biosfera*. CIQRO-SEDUE.
- Lozano-Alvarez, E., Briones-Fourzan, P., Phillips, B., 1991. Fishery characteristics, growth, and movements of the spiny lobster *Panulirus argus* in Bahia de la Ascension, Mexico. *Fishery Bulletin* 89, 79-89.
- Madden, C., Day, Jr., J.W., 1992. An instrument system for high speed mapping of chlorophyll and physico-chemical parameters. *Estuaries* 15(3), 421-427.
- Madden, C.J., Kemp, W.M., 1996. Ecosystem model of an estuarine submersed plant community: calibration and simulation of eutrophication responses. *Estuaries* 19, 457-474.

- Marin, L.E., 1990. Field investigations and numerical simulation of the karstic aquifer of northwest Yucatan, Mexico. PhD dissertation, Northern Illinois University, 183pp.
- Marin, L.E., Perry, E.C., 1994. The hydrogeology and contamination potential of northwestern Yucatan, Mexico. *Geofísica Internacional* 33(4), 619-623.
- Marshall, T., 2009. On the performance of buildings in hurricanes. A study of the Saffir-Simpson scale committee. Haag Engineering Co. 34 pp.
- Mazzotti, F.J., Fling, H.E., Merediz, G., Lazcano, M., Lasch, C., Barnes, T., 2005. Conceptual model of the Sian Ka'an Biosphere Reserve, Quintana Roo, Mexico. *Wetlands* 25, 980-997.
- Medeiros, C., Kjerfve, B., 1993. Hydrology of a tropical estuarine ecosystem: Itamaracá, Brazil. *Estuarine, Coastal and Shelf Science* 36, 495-515.
- Medina-Gómez, I., Herrera-Silveira, J.A., 2003. Spatial characterization of water quality in a karstic coastal lagoon without anthropogenic disturbance: a multivariate approach. *Estuarine Coastal and Shelf Science* 58(3), 455-465.
- Medina-Gómez, I., Herrera-Silveira, J.A., 2006. Primary production dynamics in a pristine groundwater influenced coastal lagoon of the Yucatan Peninsula. *Continental Shelf Research* 26, 971-986.
- Medina-Gómez, I., Herrera-Silveira, J.A., 2009. Seasonal responses of phytoplankton productivity to water-quality variations in a coastal karst ecosystem of the Yucatan Peninsula. *Gulf of Mexico Science* 27, 39-51.
- Merino, M., Czitrom, S., Jordán, E., Martín, E., Thomé, P., Moreno, O., 1990. Hydrology and rain flushing of the Nichupté Lagoon System, Cancún, México. *Estuarine, Coastal and Shelf Science* 30, 223-237.
- Millero, F.J., Huang, F., Zhu, X., Liu, X., Zhang, J., 2001. Adsorption and desorption of phosphate on calcite and aragonite in seawater. *Aquatic Geochemistry* 7, 33-56.
- Moore, D.R., 1963. Distribution of the sea grass, *Thalassia* in the United States. *Bulletin of Marine Science of the Gulf and Caribbean* 13, 329-342.
- Morin, J., Leclerc, M., Secretan, Y., Boudreau, P., 2000. Integrated two-dimensional macrophytes-hydrodynamic modeling. *Journal of Hydraulic Research* 38, 163-172.
- Mortimer, C.H., 1953. The resonant response of stratified lakes to wind. *Schweizerisches Zeitschrift für Hydrologie* 15, 94-151.
- Mutchler, T., Dunton, K., Townsend-Small, A., Fredriksen, S., Rasser, M.K., 2007. Isotopic and elemental indicators of nutrient sources and status of coastal habitats in the Caribbean Sea, Yucatan Peninsula, Mexico. *Estuarine, Coastal and Shelf Science* 74, 449-457.
- Nixon, S.W., 1988. Physical energy inputs and the comparative ecology of lake and marine ecosystems. *Limnology and Oceanography* 33, 1005-1025.
- Nuttle, W.K., Fourqurean, J.W., Cosby, B.J., Ziemann, J.C., Robblee, M.B., 2000. Influence of net freshwater supply on salinity in Florida Bay. *Water Resources Research* 36, 1805-1822.



- Orellana, R., Nava, F., Espadas-Manrique, C., 2007. El clima de Cozumel y la Riviera maya. In: Mejía-Ortiz, L.M. (Ed.), *Biodiversidad acuática de la Isla de Cozumel*, pp 23-32. Universidad de Quintana Roo-Campus Cozumel, Cozumel Q. Roo, México.
- Orth, R., Carruthers, T.J.B., Dennison, W.C., Duarte, C.M., Fourqurean, J.W., Heck, K., Hughes, R., Kendrick, G.A., Kenworthy, W.J., Olyarnik, S., Short, F.T., Waycott, M., Williams, S.I., 2006. A global crisis for seagrass ecosystems. *BioScience* 56, 987-996.
- Pawlowicz, R., Beardsley, B., Lentz, S., 2002. Classical tidal harmonic analysis including error estimates in MATLAB using T\_TIDE. *Computers and Geosciences* 28, 929-937.
- Pritchard, D.W., 1967. What is an estuary: physical standpoint. In: Lauf, G.H. (Ed.), *Estuaries*. pp 3-5. American Association for the Advancement of Science. Publication 83. Washington, DC.
- Quintal-Lizama, C., Vasquez-Yeomans, L., 2001. Asociaciones de larvas de peces en una bahía del Caribe mexicano. *Revista de Biología Tropical* 49(2), 559-570.
- Redfield, A.C., 1955. The influence of the continental shelf on the tides of the Atlantic Coast of United States. *Journal of Marine Research* 17, 432-448.
- Restrepo, J. D., Kjerfve, B., 2000. Magdalena River: interannual variability (1975–1995) and revised water discharge and sediment load estimates. *Journal of Hydrology* 235, 137-149.
- Reynolds-Fleming, J.V., Luettich, Jr., R.A., 2004. Wind-driven lateral variability in the upper Neuse River Estuary. *Estuarine, Coastal and Shelf Science* 60, 395-407.
- Rivera-Monroy, V.H., Twilley, R.R., Bone, D., Childers, D.L., Coronado-Molina, C., Feller, I.C., Herrerra-Silviera, J.A., Jaffe, R., Mancera, J.E., Rejmankova, E., Salisbury, J.E., 2004. A conceptual framework to develop long-term ecological research and management objectives in the wider Caribbean Region. *BioScience* 54(9), 843-856.
- Robertson, G.P., 2008. *GS+: Geostatistics for the Environmental Sciences*. Gamma Design Software, Plainwell, MI.
- Ruiz-Renteria, F., van Tussenbroek, B., Jordan-Dahlgren, E., 1998. CARICOMP: A Caribbean network of marine laboratories parks, and reserves for coastal monitoring and scientific collaboration. In: Kjerfve, B. (Ed.), *CARICOMP-Caribbean coral reef, seagrass and mangrove sites*. pp 57-66. UNESCO, Paris.
- Rutkowski, C.M., Burnett, W.C., Iverson, R.L., Chanton, J., 1999. The effect of groundwater seepage on nutrient delivery and seagrass distribution in the northeast Gulf of Mexico. *Estuaries* 22(4), 1033-1040.
- Sheng, Y.P., Peene, S., Yassuda, E., 1996. Circulation and transport in Sarasota Bay, Florida: The effect of tidal inlets on estuarine circulation and flushing quality, pp. 184-210. In: Pattiaratchi, C. (Ed.), *Mixing in estuaries and coastal seas*. American Geophysical Union, Washington, DC.
- Smith, N.P., 1977. Meteorological and tidal exchanges between Corpus Christi Bay, Texas, and the northwestern Gulf of Mexico. *Estuarine and Coastal Marine Science* 5, 511-520.

- Smith III, T.J., Robblee, M.B., Wanless, H.R., Doyle, T.W., 1994. Mangroves, hurricanes, and lightning strikes. *Bioscience* 44(4), 256-262.
- SMN 2007. Servicio Meteorológico Nacional de México. Datos históricos EMAs. <http://smn.cna.gob.mx/productos/emas/emas.html>.
- Sousa, M.C., Dias, J.M., 2007. Hydrodynamic model calibration for a mesotidal lagoon: the case of Ria de Aveiro (Portugal). *Journal of Coastal Research* 50, 1075-1080.
- Spalding, M.D., Taylor, M.L., Ravilious, C., Short, F., Green, E., 2003. Global overview. The distribution and status of seagrasses. In: Green E., Short, F.T. (Eds.), *World atlas of seagrasses*, pp. 5-26. University of California Press, Berkeley.
- Staneva, J.V., Stanev, E.V., 1998. Oceanic response to atmospheric forcing derived from different climatic data sets. Intercomparison study for the Black Sea. *Oceanologica Acta* 21, 393-417.
- Thornthwaite, C.W., 1948. An approach toward a rational classification of climate. *Geography Review*. 38, pp. 55-94.
- TNTmips®. 2006. Image classification tutorial. ©MicroImages, Inc. <http://microimages.com>.
- Tomasko, D.A., Dawes, C., Hall, O., 1996. The effects of anthropogenic nutrient enrichment on turtle grass (*Thalassia testudinum*) in Sarasota Bay, Florida. *Estuaries* 19, 448-456.
- Tomasko, D.A., Lapointe, B., 1991. Productivity and biomass of *Thalassia testudinum* as related to water column nutrient availability and epiphyte levels: field observations and experimental studies. *Marine Ecology Progress Series* 75, 9-17.
- Tudela, F., 1989. La modernización forzada del trópico: El caso de Tabasco. El Colegio de México, IFIAS, CINVESTAV, UNRISD, México, 465 pp.
- Umgiesser, G., Neves, R., 2005. Physical processes in coastal lagoons: ecosystem processes and modeling for sustainable use and development, CRC Press, Boca Raton, FL, chap. 3.
- UNAM, 2007. Cambio Climático Global y el Niño: Expectativas para 2007. Centro de Ciencias de la Atmósfera. Universidad Autónoma de México; Press Bulletin: <http://www.atmosfera.unam.mx/cclimatico/boletin/cambio07.pdf>.
- Valdes, A., Cortez, M., Pastrana, J.J., 2005. Un estudio explorativo de los sistemas convectivos de mesoescala de México. *Investigaciones Geográficas* 56, 26-42.
- Valdes, D., Real, E., 1994. Ammonium, nitrite, nitrate and phosphate fluxes across the sediment-water interface in a tropical lagoon. *Ciencias Marinas* 20, 65-80.
- Valdes, D., Real, E., 2004. Nitrogen and phosphorus in water and sediments at Ria Lagartos coastal lagoon, Yucatan, Gulf of Mexico. *Indian Journal of Marine Sciences* 33, 338-345.
- Valiela, I., 1995. Nutrient cycles and ecosystem stoichiometry, in *Marine ecological processes*, 2<sup>nd</sup> ed., Springer-Verlag, New York, chap. 14.
- van Tussenbroek, B.I., 1994. The impact of Hurricane Gilbert on *Thalassia testudinum* in Puerto Morelos reef lagoon, Mexico: a retrospective study. *Botánica Marina* 37, 421-428.

- van Tussenbroek, B.I., Barba-Santos, M.G., van Dijk, J.K., Sanabria-Alcaraz, M., Téllez-Calderón, M.L., 2008. Selective elimination of rooted plants from a tropical seagrass bed in a back-reef lagoon: a hypothesis tested by Hurricane Wilma (2005). *Journal of Coastal Research* 24, 278-281.
- Vidal, L., Basurto, M., 2003. A preliminary trophic model of Ascension Bay, Quintana Roo, Mexico. *Fisheries Centre Research Reports* 11(6), 255-264.
- Walstra, D.J.R., Van Rinj, L.C., Blogg, H., Van Ormondt, M., 2001. Evaluation of a hydrodynamic area model based on the Coast3D Data at Teignmouth 1999. *Proceedings of coastal dynamics 2001 conference*. Lund, pp D4.1-D4.4.
- Wear, D.J., Sullivan, M.J., Moore, A.D., Millie, D.F., 1999. Effects of water-column enrichment on the production dynamics of three seagrass species and their epiphytic algae. *Marine Ecology Progress Series* 179, 201-213.
- Wolanski, E., 1994. *Physical oceanographic processes of the Great Barrier Reef*. CRC Marine Science Series, CRC Press, Boca Raton, FL, 194 pp.
- Wong, K.C., DiLorenzo, J., 1988. The response of Delaware's inland bays to ocean forcing. *Journal of Geophysical Research* 93, 525-535.
- Wong, K.C., Wilson, R.E., 1984. Observations of low-frequency variability in Great South Bay and relations to atmospheric forcing. *Journal of Physical Oceanography* 14, 1893-1900.
- Yáñez-Arancibia, A.C., Lara-Domínguez, A.L., Day, Jr., J.W., 1993. Interactions between mangrove and seagrass habitats mediated by estuarine nekton assemblages: coupling of primary and secondary production. *Hydrobiologia* 264, 1-12.
- Young, M.B., Gonneea, M.E., Fong, D.A., Moore, W.S., Herrera-Silveira, J., Paytan, A., 2008. Characterizing sources of groundwater to a tropical coastal lagoon in a karstic area using radium isotopes and water chemistry. *Marine Chemistry* 109, 377-394.
- Zieman, J.C., 1975. Seasonal variation of turtle grass, *Thalassia testudinum* (König), with reference to temperature and salinity effects. *Aquatic Botany* 1, 107-123.
- Zimmerman, R.C, Kohrs, D.G., Alberte, R.S., 1996. Top-down impact through a bottom-up mechanism: the effect of limpet grazing on growth, productivity and carbon allocation of *Zostera marina* L. (eelgrass). *Oecologia* 107, 560-567.

## VITA

Israel Medina completed his Bachelor of Biology studies in the Universidad Autónoma de Yucatán in 1995. He entered the Master of Science program with a specialty in Marine Biology in Centro de Investigación y de Estudios Avanzados del Instituto Politécnico Nacional in August 1997 and obtained his degree in October 2000.

His research interests include oceanography of coastal ecosystems and the relationship between the physical setting and the variability of their water quality and trophic status, with special emphasis on the functional connectivity along the mangrove-seagrass-reef continuum.

Mr. Medina may be reached at Centro de Investigación y de Estudios Avanzados del Instituto Politécnico Nacional, km 6 Antigua Carretera a Progreso, Cordemex, C.P. 97310, Mérida, Yucatán, México. His e-mail is [imedgomez@gmail.com](mailto:imedgomez@gmail.com).